Technical Report EL-95-21
July 1995

US Army Corps of Engineers
Waterways Experiment Station

Imaging Smolt Behavior on Bypass Screens and a Vertical Barrier Screen at McNary Dam in 1992

by John M. Nestler, Robert A. Davidson

Prepared for U.S. Army Engineer District, Walla Walla

PRINTED ON RECYCLED PAPER

Technical Report EL-95-21
July 1995

Imaging Smolt Behavior on Bypass Screens and a Vertical Barrier Screen at McNary Dam in 1992

by John M. Nestler, Robert A. Davidson

U.S. Army Corps of Engineers
Waterways Experiment Station
3909 Halls Ferry Road
Vicksburg, MS 39180-6199

Final report

Approved for public release; distribution is unlimited

Prepared for U.S. Army Engineer District, Walla Walla
Building 602, City-County Airport
Walla Walla, WA 99362-9265

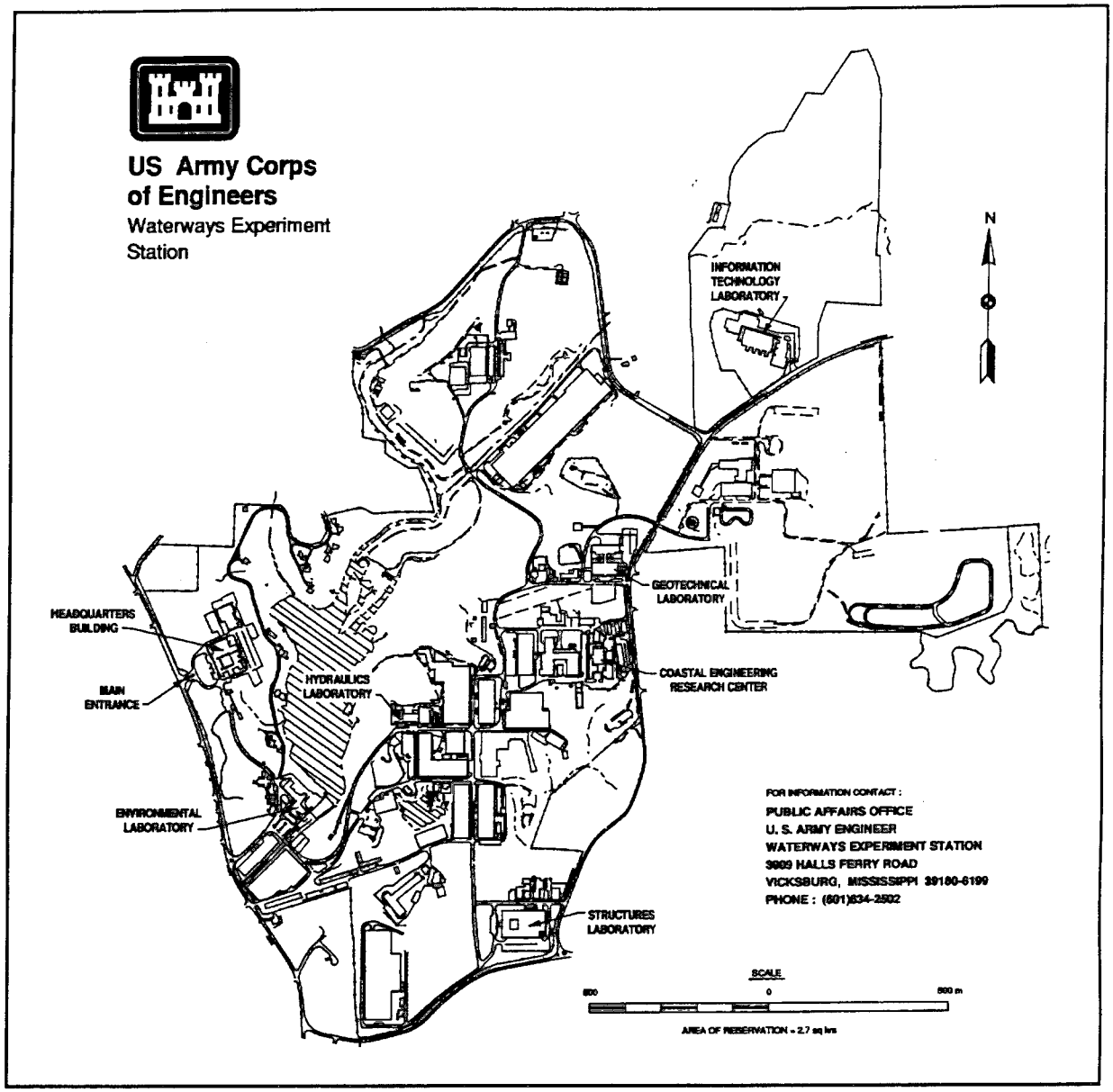

Waterways Experiment Station Cataloging-in-Publication Data

Nestler, John M.

Imaging smolt behavior on bypass screens and a vertical barrier screen at McNary Dam in 1992 / by John M. Nestler, Robert A. Davidson ; prepared for U.S. Army Engineer District, Walla Walla.

175 p. : ill. ; 28 cm. — (Technical report ; EL-95-21)

Includes bibliographic references.

1. Fish screens — Evaluation. 2. Dams — Columbia River (Or. and Wash.) —Environmental aspects. 3. Underwater imaging systems. 4. Fishes — Migration. I. Davidson, Robert A. II. United States. Army. Corps of Engineers. Walla Walla District. III. U.S. Army Engineer Waterways Experiment Station. IV. Environmental Laboratory (U.S. Army Engineer Waterways Experiment Station) V. Title. VI. Series: Technical report (U.S. Army Engineer Waterways Experiment Station) ; EL-95-21.

TA7 W34 no.EL-95-21

Contents

SF 298

List of Figures

List of Tables

Preface

This report presents findings of video imaging studies of smolt behavior and impingement on a standard-length submerged traveling screen, an extended-length submerged bar screen, and a modified balanced flow vertical barrier screen at McNary Dam during FY92. This report was prepared in the Environmental Laboratory (EL) and Hydraulic Laboratory (HL), U.S. Army Engineer Waterways Experiment Station (WES), Vicksburg, MS. The study was sponsored by the U.S. Army Engineer District, Walla Walla, and was funded under the Intra-Army order for Reimbursable Services No. E86920081 dated 24 Feb 1992.

The Principal Investigators of this study were Dr. John M. Nestler, Water Quality and Contaminant Modeling Branch (WQCMB), Environmental Processes and Effects Division (EPED), EL, and Mr. Robert Davidson, Locks and Conduits Branch, HL. This report was prepared by Dr. Nestler and Mr. Davidson under the direct supervision of Dr. Mark Dortch, Chief, WQCMB, and under the general supervision of Mr. Donald L. Robey, Chief, EPED, and Dr. John W. Keeley, Director, EL. This report was also prepared under the direct supervision of Mr. John George, Chief, Locks and Conduits Branch, and under the general supervision of Mr. Glenn Pickering, Chief, Hydraulic Structures Division, and Mr. Frank Herrmann, Director, HL. The assistance of Ms. Dottie Hamlin-Tillman, WQCMB, in the collation of data and editing of the report is gratefully acknowledged. Video imaging data were collected and processed by Messrs. Ahmed Darwish, University of Maryland Eastern Shore, Robert Jenkins, Jackson State University, and Jace Pugh, Millsaps College. Technical reviews by Messrs. Gene Ploskey and Tom Cole and Ms. L. Toni Schneider, WQCMB, are gratefully acknowledged.

At the time of publication of this report, Director of WES was Dr. Robert W. Whalin. Commander of WES was COL Bruce K. Howard, EN.

This report should be cited as follows:

Nestler, J. M., and Davidson, R. A. (1995). "Imaging smolt behavior on bypass screens and a vertical barrier screen at McNary Dam in 1992," Technical Report EL-95-21, U.S. Army Engineer Waterways Experiment Station, Vicksburg, MS.

Summary

During the spring and summer of 1992, video imaging of smolt bypass systems at McNary Dam on the Columbia River was conducted using low-light sensitive underwater video cameras to record smolt behavior and impingement characteristics on a modified balanced flow vertical barrier screen (MBFVBS), a standard-length submerged traveling screen (SSTS), and an extended-length submerged bar screen (ESBS). Video images of the screen surface were obtained from five to six cameras located on the screen centerline from the top (nearest the deck or intake) to the bottom of each screen. Cameras imaged laterally across the screen at locations 2, 13, 21, 26, 31, and 38 ft from the top of the ESBS and at locations 6, 10, 12, 15, and 18 ft from the top of the SSTS. The cameras on the ESBS recorded smolt behavior to three closure gate settings, two screen positions, three discharges, two screen angles, and presence/absence of a fyke net. The cameras on the SSTS recorded smolt behavior only at the standard deployment settings. A total of 3,684 smolts (imaging rate of about 0.14 smolt/min) representing 458 conditions was imaged, processed, and analyzed. Five cameras were located on the MBFVBS and imaged the passage of smolts up the gate slot. During imaging of the MBFVBS, one additional camera was located on top of the bypass screen to document gap loss and smolt passage over the top of the bypass screen. The cameras on the MBFVBS recorded smolt behavior to four unit-loads (12,000, 13,000, 14,000, and 16,000 cfs) and three closure gate settings (normal gate setting, partial gate setting, and no gate).

A variety of hydraulic and behavioral data were collected from each recorded image for the bypass screens. Data from physical model studies were used to supplement imaging data for some design or deployment configurations. For the bypass screens, hydraulic data included direct measurements of water approach angle relative to the screen surface. Behavioral data collected included descriptions of the approach of the smolt to the screen (i.e., angle of approach, angle of retreat after a strike, orientation of the fish in the water) and descriptions of entrainment and impingement of smolts on the screen (e.g., entrainment without strike or impingement, strike with escape, impingement without escape, head-first approach without strike or impingement, and head-first approach with impingement).

For the MBFVBS, hydraulic data collected included multiple measurements of the angle of flow relative to the screen surface. Behavioral variables

included estimates of the proportions of smolts moving towards the screen, the proportions of smolts moving towards the camera, the proportion of smolts entrained in or moving with the flow, the proportion having no control over their orientation in the flow field, the proportion of smolts exhibiting severe contact with the screen, and the proportion of smolts lost between the top of the bypass screen and the bottom of the vertical barrier screen (gap loss).

Results from the video imaging are summarized in the following tabulation. Spring testing showed that the fyke net has a large, significant effect on almost all behavioral variables and some hydraulic variables. The fyke net was present for much of the summer tests, and it is reasonable to expect the summer tests to be biased by the presence of the fyke net.

The video imaging demonstrated that direct imaging of smolt behavior in the different parts of a bypass system can provide valuable information on the effects of different screen design or deployment configurations. Video imaging within the bypass screen system should be used to supplement fish guidance efficiency (FGE) studies to determine localized effects of the bypass system.

Gap loss is a significant component of fall chinook passage. Approximately 37 percent of the smolts imaged by the gap loss cameras passed through the gap. It is estimated that between 12 and 37 percent of the smolts initially guided by the ESBS are lost between the MBFVBS and the bypass screen. Many of the smolts passing through the gap appear to be injured or stunned. It is speculated that many smolts that impinge or are injured on the ESBS may be lost through the gap and are, therefore, not assessed during descaling studies. Loss of smolts through the gap and under the toe of bypass screens is a significant effect of different screen designs and deployment alternatives presently not assessed during FGE studies. It is recommended that FGE studies be modified to better assess this aspect of smolt-screen interaction.

Results indicate that more smolts impinged on the ESBS than on the SSTS. However, there are insufficient data to conclusively relate these findings to differences in screen type only. Differences in impingement characteristics of screens may also be affected by differences in screen length (40 ft versus 20 ft) which substantially alter the percentage of the intake that is blocked (22 versus 47 percent). Additionally, individual and synergistic effects mediated by the deployment or configuration of the screen, slot, and VBS may influence the results. Recent improvements to certain design details of bar screens may reduce the impingement rates from those observed in this study. A more complete understanding of hydraulic patterns and associated response of smolts will require additional testing, particularly to describe effects on impingement rates resulting from alterations in bar screen design from those investigated in this study.

Season	Screen	Test	Impingement Rate	Impingement Index	Passage Index	Comments
Spring	ESBS	Fyke Net	g[1]d[2]	gd	gi[3]	Fyke net introduced significant bias to imaging results
Spring	ESBS	Lowered Screen	l[4]d	ns[5]	ns	Smolts probably farther above screen surface towards top of screen
Spring	ESBS	62° Screen Angle	gi	gi	gd	Impingement decreased lower on screen, but large increases higher on screen
Spring	ESBS	Increase Unitload	ns	ns	ns	No patterns observed
Spring	ESBS	"No Gate" Setting	li	li	ld	No gate setting compared to partial gate, affected camera location 2 only
Spring	ESBS	"Partial Gate"	ld	ld	li	Partial gate setting compared to no gate, affected camera location 2 only
Spring	ESBS	Compare to SSTS	gi	gi	gd	ESBS had increased impingement
Spring	ESBS	Increase Velocity	gi	gi	gd	Increase velocity resulted in increased impingement, occurred as threshold
Spring	ESBS	Current Angle[6]	gi	gi	gi	More perpendicular flow to screen increased impingement
Summer	ESBS	No Gate Setting	ns	ns	ns	No patterns observed
Summer	ESBS	Partial Gate	ns	ns	ns	No patterns observed
Summer	ESBS	Increase Unitload	ns	ns	ns	No patterns observed
Summer	ESBS	Increase Velocity	na[7]	na	na	No velocity information available
Summer	ESBS	Increase Angle[6]	gi	gi	ns	Opposite of spring pattern
Summer	MBFVBS	Increase Unitload	li	li	ns	Results not conclusive
Summer	MBFVBS	No Gate Setting	gi	gi	gd	Compared to normal gate position
Summer	MBFVBS	Partial Gate	gi	gi	gd	Compared to normal position, less impingement than no gate
Summer	GAPLOSS	Increase Unitload	ns	ns	ns	No pattern observed
Summer	GAPLOSS	No Gate Setting	gd	gd	na	Compared to normal gate position
Summer	GAPLOSS	Partial Gate	gd	gd	na	Same effect as partial gate position
Spring Summer	ESBS	Seasonal Comparison	gi	gi	gd	Spring compared to summer

[1] g = Global.
[2] d = Decrease.
[3] i = Increase.
[4] l = Local.
[5] ns = Not significant.
[6] Flow more perpendicular to screen.
[7] na = Not available.

Conversion Factors, Non-SI to SI Units of Measurement

Non-SI units of measurement used in this report can be converted to SI units as follows:

Multiply	By	To Obtain
cubic feet	0.02831685	cubic meters
inches	2.54	centimeters
pounds (mass)	0.4535924	kilograms

1 Introduction

Background

The Corps of Engineers operates hydropower dams on rivers that support valuable anadromous fisheries. Extensive bypass facilities have been installed at these dams to intercept out-migrating salmon smolts before they enter turbines. The first component of a bypass facility encountered by smolts is a submerged screen of relatively fine mesh or small bar spacing (the bypass screen). The bypass screen intercepts and guides smolts to the gatewell where another screen, the vertical barrier screen, guides the smolts up the gatewell to a transport system that passes them around the dam and into the tailrace either for immediate release or for holding until later transport. Several screen designs and deployment configurations are being considered by the U.S. Army Engineer District, Walla Walla (CENPW) to increase guidance efficiency.

CENPW sponsored pilot studies at McNary Dam in FY 91 to evaluate extended-length (40-ft long) fish screens using the most recent advances in underwater imaging systems to detect and describe differential impingement rates associated with alternative prototype screen designs (Nestler and Davidson 1993). Before this study, real-time imaging of entrainment and impingement of smolts on prototype screens under operational conditions had rarely been performed. Pilot study results demonstrated that smolts could be successfully imaged, using existing technology, as they approach and are intercepted by bypass screens and that flow patterns on the screen surface vary considerably from the top (nearest the slot) to the bottom of the screen. The proportion of smolts impinged on the screen depends on localized hydraulic conditions where the smolt is intercepted by the screen. Consequently, determining the effectiveness of a screen design (e.g., a mesh traveling screen or a stationary bar screen) or impact of a deployment configuration (e.g., screen angle or gate setting) requires that the hydraulic patterns on the screen surface be integrated with the depth distribution of the smolts.

Promising results obtained from pilot studies suggested that guidance performance of different screen designs and deployment configurations could be systematically investigated using video imaging. Results of such studies could be used to answer questions regarding detailed response of out-migrating

smolts to bypass screen and modified balance flow vertical barrier screen (MBFVBS) design features and deployment configurations. CENPW can use this information to optimally design and operate fish protection systems at McNary Dam and other dams where bypass screens and VBS's are used to bypass fishes.

Objectives

After mobilizing at McNary Dam, WES staff were directed by CENPW to modify the study objectives as listed in the Scope of Work. The following revised general and seasonal objectives associated with fish passage efficiency and impingement were addressed.

Spring objectives

For an ESBS, the effects of the following conditions and deployment configurations on passage and impingement behavior and hydraulic patterns were determined.

a. Presence/absence of the fyke net (used by the National Marine Fisheries Service (NMFS) to estimate the number of smolts entering the turbines and not guided by the screens into the fish bypass system: the fyke nets are not required for imaging).

b. Screen position (standard screen position compared to lowering the screen by 24 in.

c. Screen angle (the angle of the screen relative to the vertical, 55 deg or 62 deg).

d. Closure gate position (no closure gate, partial closure gate (closure gate is raised 7.5 ft from its normal storage position), and normal closure gate position (closure gate is in its normal storage position)).

e. Different unit loadings (12,000, 14,000, and 16,000 cfs) on impingement behavior (defined as the response of smolts to the presence of the screen which may include behaviors ranging from complete avoidance of the screen to impingement) and hydraulic patterns on the screen surface.

f. Passage efficiency and impingement characteristics of an extended-length submerged bar screen (ESBS) compared to a standard-length submerged traveling screen (SSTS) both under their standard deployment configurations.

g. Effects of localized hydraulic conditions related to smolt impingement behavior.

For a SSTS, the effects of different unitloadings (12,000, 14,000, and 16,000 cfs) on impingement behavior and hydraulic patterns on the screen surface were determined.

Summer objectives

For an ESBS, the effects of the following deployment configurations on passage and impingement behavior and hydraulic patterns were determined:

a. Closure gate position (no closure gate, partial closure gate, and normal closure gate position).

b. Different unitloads (12,000, 15,000, and 16,000 cfs).

c. For an ESBS, the effects of localized hydraulic conditions on smolt impingement behavior were related.

For a MBFVBS, the effects of the following deployment configurations on smolt passage, smolt impingement, smolt "scraping" behavior (smolts scraping on MBFVBS on their way up the gate slot), and hydraulic variables were determined.

a. Unitload (12,000, 13,000, 14,000, and 16,000 cfs).

b. Closure gate position (same as for ESBS).

For a MBFVBS-ESBS combination, gap loss was determined and related to two items:

a. Unitload (12,000, 13,000, 14,000, and 16,000 cfs).

b. Closure gate position (gate positions same as for ESBS).

General objectives

This study had the following general objectives.

a. For the ESBS, spring and summer passage and impingement for similar deployment configurations were compared.

b. Whether video imaging could be used to determine descaling or to estimate fish guidance efficiency (FGE) was determined.

c. Imaging system bias, caused by both the presence of the camera and associated mounting hardware and the illumination system, was determined.

2 Materials and Methods

Site Description

McNary Dam is a multipurpose Corps of Engineers (CE) project located in south central Washington State on the Columbia River at river mile 292 (Figure 1) which was completed in 1954. Presently, McNary Dam consists of two small house units (oriented from south to north) to provide internal power requirements, a powerhouse with 14 Kaplan turbines (numbered 1 to 14, south to north), a spillway structure with 22 gates, and a navigation lock (Figure 2). Power generation releases from McNary Dam (Lake Wallula) are on a run-of-the-river basis and are closely governed by releases from the dams upstream and the flow requirements of the power projects downstream.

McNary Dam has extensive facilities to aid in the collection and transportation of both adult and juvenile migrating fishes. Adult fish are provided passage by a fish ladder located by each shore. Downstream migrating fingerlings are collected by bypass screens located in the turbine penstocks and vertical barrier screen (VBS) in the gatewells (Figure 3). These screens divert juvenile fish away from the turbines and into a flume which carries them to a holding area where they await transportation downstream or are released back into the river.

Screen Descriptions

Two different bypass screen designs (ESBS and SSTS) and one type of VBS (MBFVBS) were evaluated at McNary Dam.

SSTS

The SSTS is the standard screen utilized at CE dams on the Columbia River. The SSTS is 20 ft long and of sufficient width to completely span the width of the intake. The SSTS assembly consists of two frames: an outer support frame designed to slide in the gate slots for screen deployment and

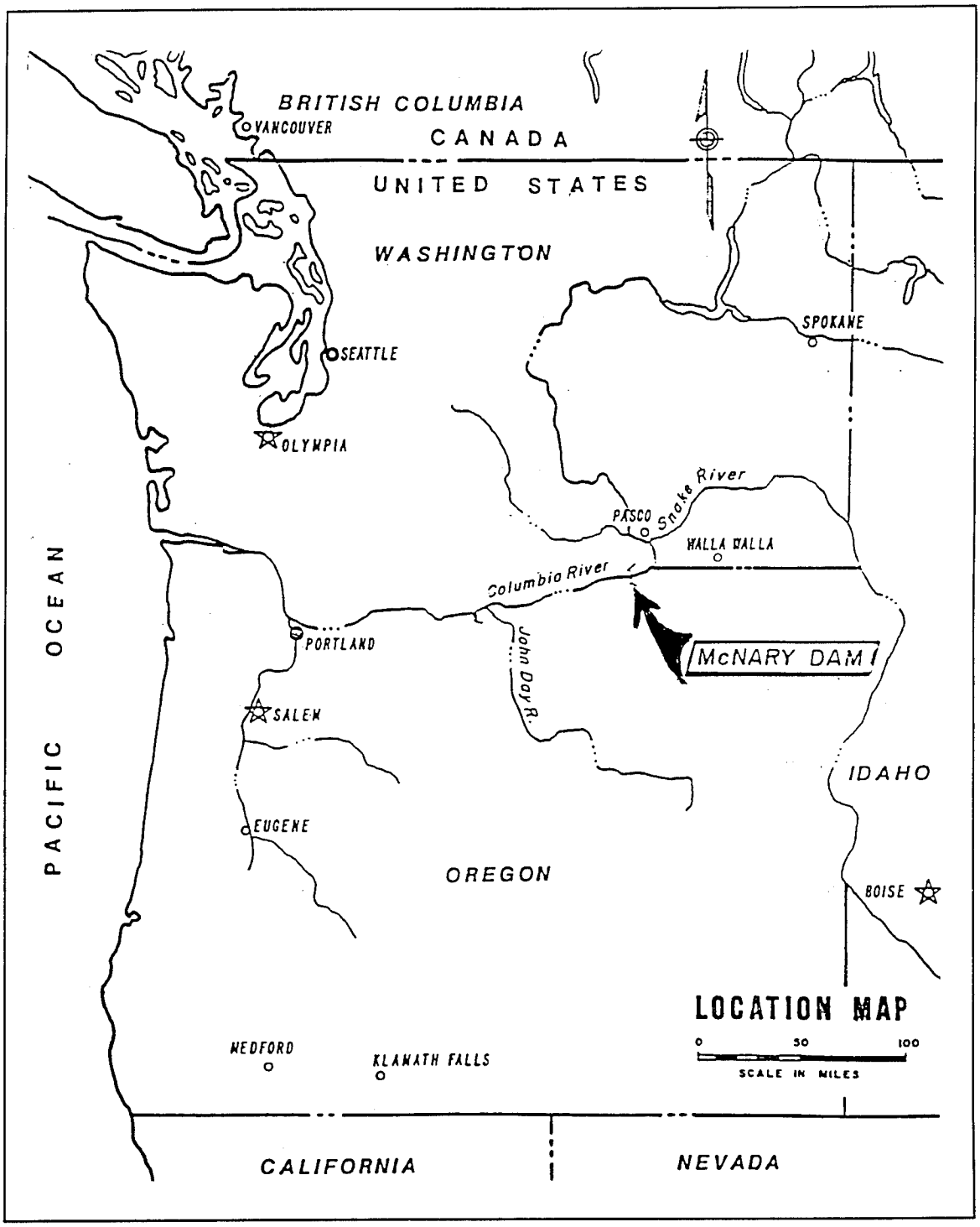

Figure 1. Site map showing location of McNary Dam on the Columbia River

retrieval and an inner frame (attached to the outer frame) providing the structural support for the screen mesh (Figure 4). The outer frame is made up of two support beams and two connecting tube beams. The inner frame is made

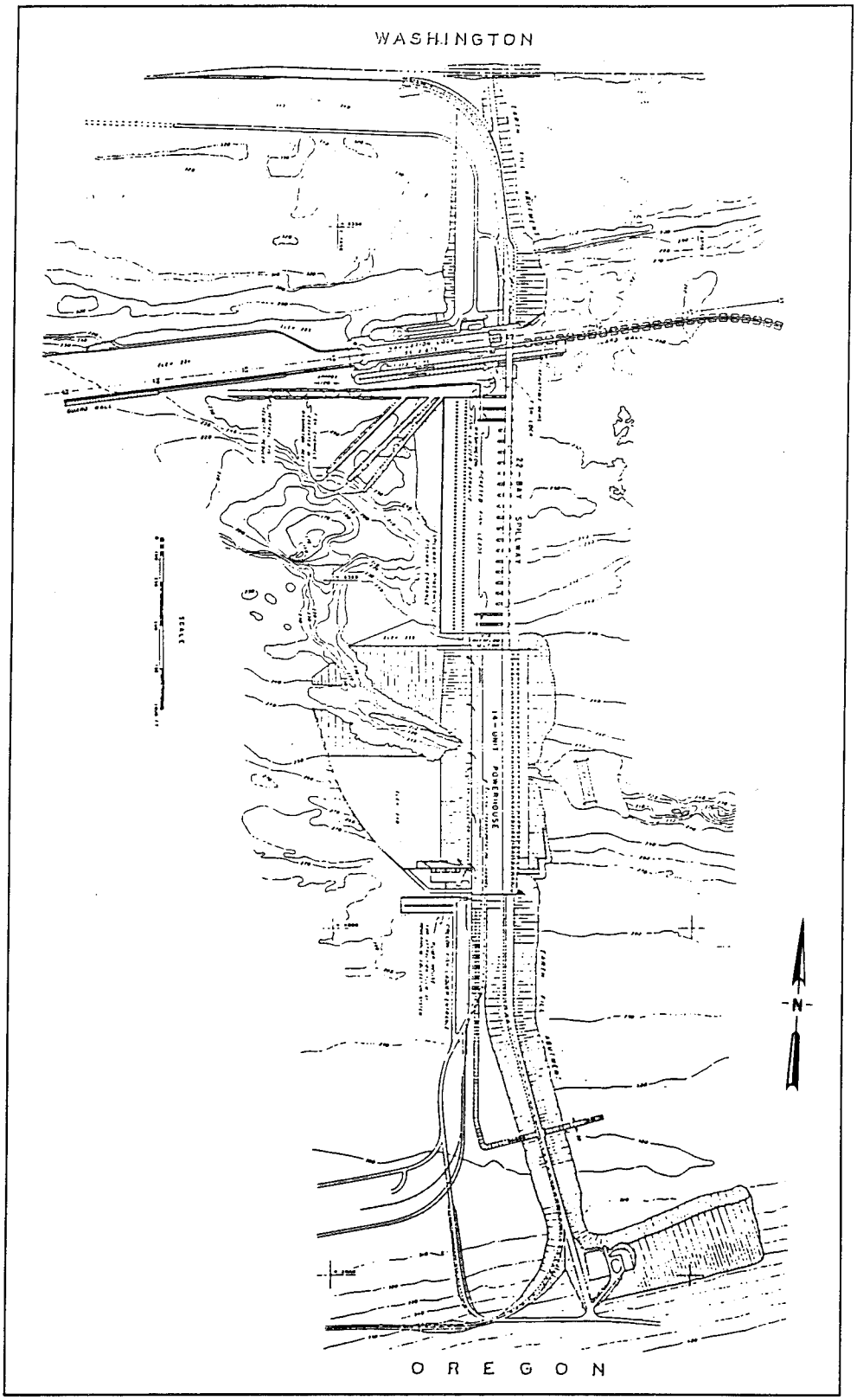

Figure 2. Plan view showing approach channel and location of the powerhouse and spillway

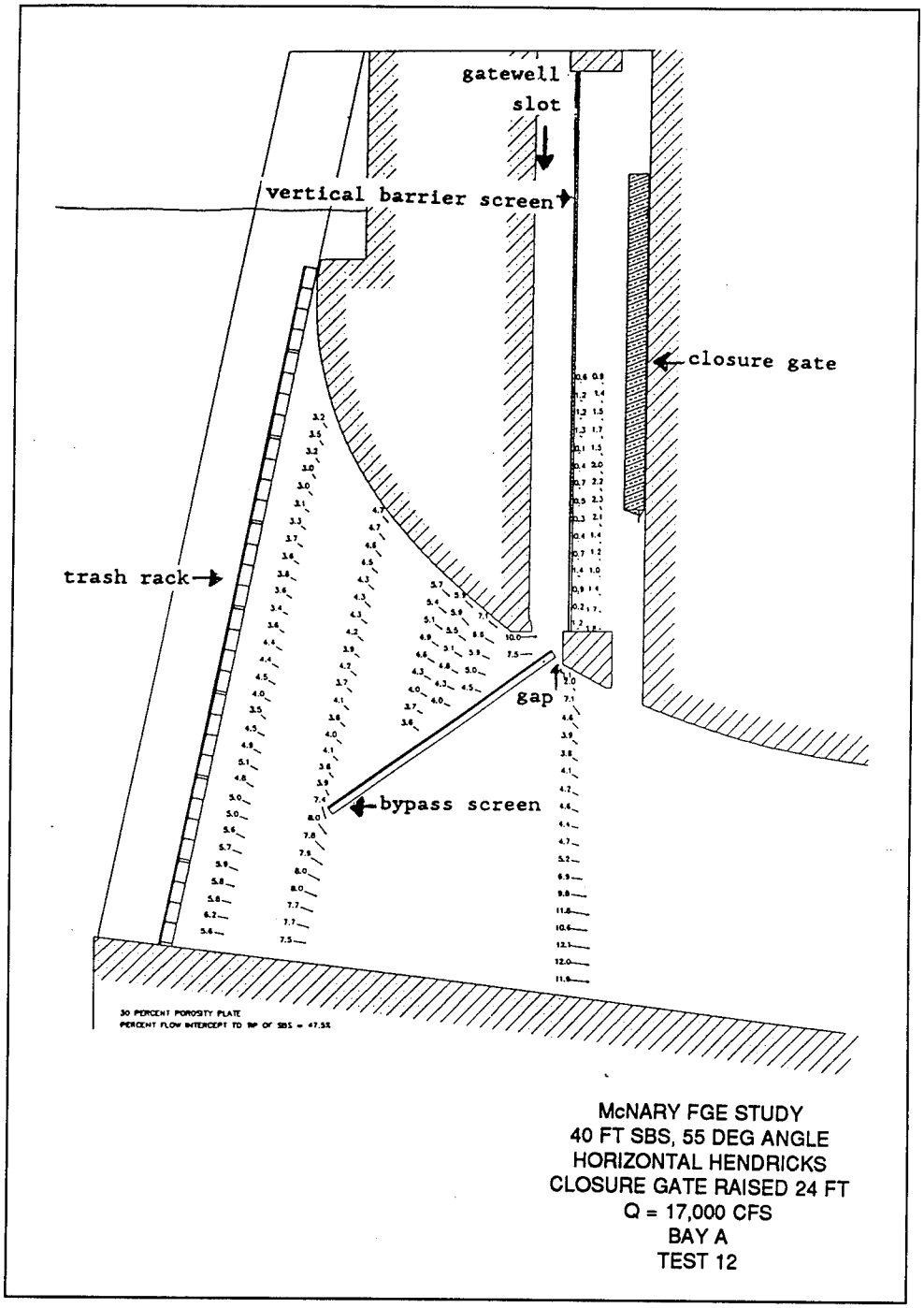

Figure 3. Profile view through an intake showing location of trashracks, SSTS, MBFVBS, and gatewell (slot in which VBS is stored). Velocity vectors were obtained from physical hydraulic model studies of this screen design and deployment configuration

up of two outer support beams, one center support beam, and several connecting box beams. Porosity plates span the space between the outer support beams of the inner frame. They are bolted from each outer support beam to

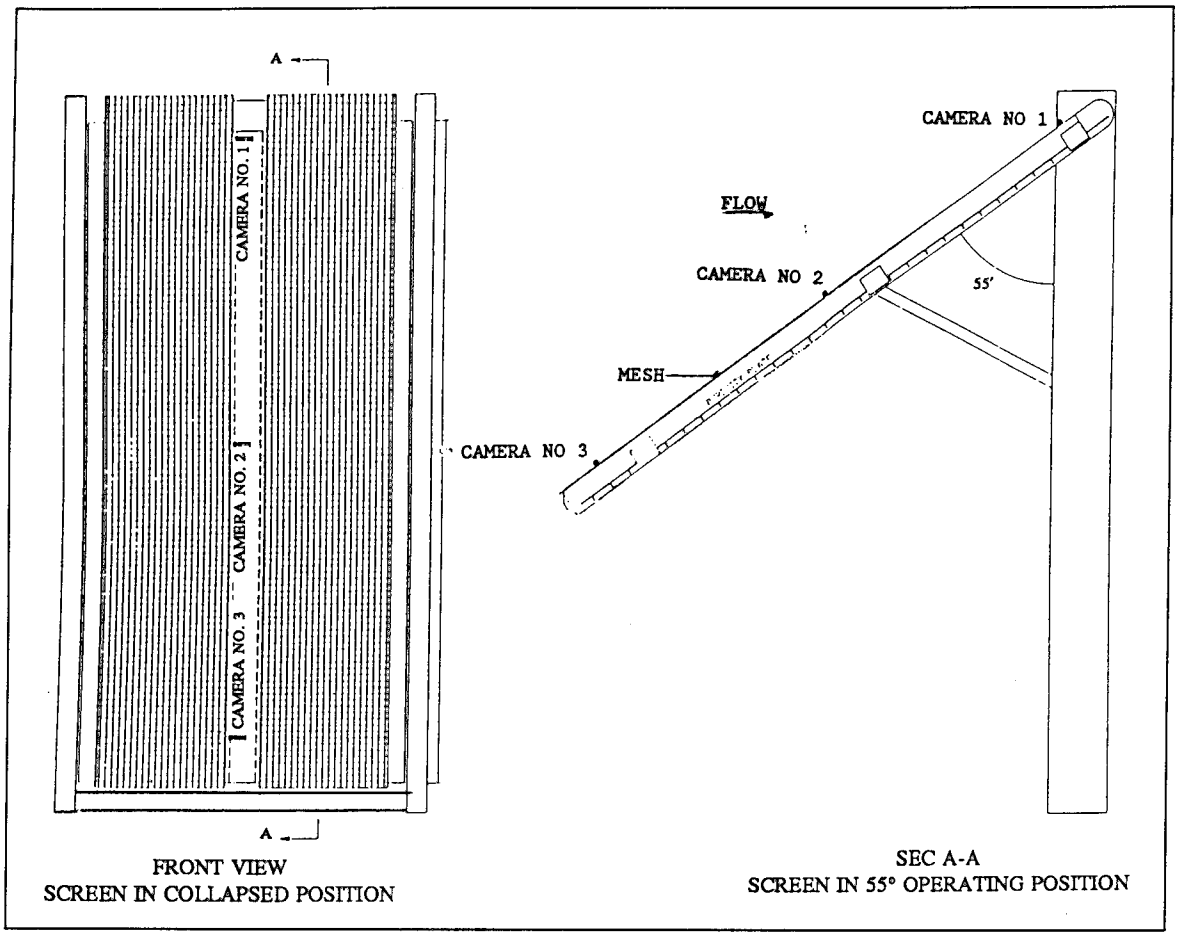

Figure 4. General configuration of a SSTS with approximate locations of video cameras indicated

the intermediate support beam. Porosity plates are used to control water velocity through the screen. Plates having different porosities can be used to manipulate water velocities through the screen. Nylon mesh screen is wrapped around the perimeter of the inner frame on each side of the center support beam to form two separate screen surfaces. The mesh from each screen surface extends from the center support beam to the outer support beam. The screens are rotated periodically to remove debris from the screen surface.

The inner frame is pinned to the outer frame at a pivot point near the top of the screen assembly, and the inner frame is supported by two strut arms deployed from the bottom of the screen assembly. The SSTS is deployed by lowering the screen assembly down a bulkhead slot in a collapsed (vertical) position. Once it reaches the desired elevation, the strut arms are extended which causes the inner frame to rotate about the pivot point. Deployment elevation can be varied, but usually the screen is deployed so that the top of the screen is near the base of the MBFVBS that concentrates and guides smolts up the gate slots. The strut arms are extended until the inner frame

has been rotated to its desired operating angle, usually about 55 deg as measured from the vertical.

ESBS

The ESBS (Figure 5) is one of two new screen designs that is being considered as a replacement for the SSTS. The ESBS is 40 ft long and of a width sufficient to span the width of the intake. The ESBS assembly consists of three frames: an outer support frame designed to slide in the gate slot for screen deployment and retrieval; an inner frame made up of two outer support beams; two inner beams which support the tracks for the brush cleaning system and a series of horizontal connecting box beams; and an intermediate frame which connects the inner and outer frames and is used to set the deployment angle of the screen. Porosity plates span the space between the outer support beams of the inner frame. They are bolted from each outer support beam to the intermediate support beams. Porosity plates are used to control water velocity through the screen. The flat screen surface is comprised of 1/8-in. wedge wire with a 1/8-in. clear space running parallel to the centerline of the screen reinforced on the underside at 6-in. intervals by U-bars. The screen is supported by the perimeter of the inner frame on each side and the inner vertical members and the connecting horizontal box beams.

The screen surface presented to the approaching flow is completely flat and uninterrupted by fasteners, tie-down bars, or other support members. The screen surface is swept by an automatic cleaning brush to prevent build-up of debris. The brush is stored at the toe of the screen when not in use. The presence of the cameras prevented the automatic cleaning brush from operating during imaging. The inner frame of the ESBS is pinned to the outer-frame at a pivot point near the top of the screen assembly, and the inner frame is supported by the intermediate beams deployed from the bottom of the screen assembly. The ESBS is deployed and retrieved in a manner similar to the SSTS. The ESBS can have different porosity plates or alternative deployment configurations similar to the SSTS.

MBFVBS

The MBFVBS (Figure 6) extends vertically up the gatewell from a position approximately 2.5 ft above the top of the ESBS to the water surface of the gatewell. As flow moves along the roof of the intake and along the surface of the top portion of the ESBS, a portion of the water is forced up the screen slot. The majority of this screen slot flow will be drawn off through the VBS and will re-enter the penstock through the closure gate slot. The fish pass from the area between the ESBS and the roof of the intake into the screen slot where the VBS acts as a barrier to keep the fish from re-entering the penstock and as a guiding device, guiding the fish to the orifice area. The fish will eventually find the orifice and will either be drawn into it or trapped by the velocities entering the orifice. Once the fish pass through the orifice, they

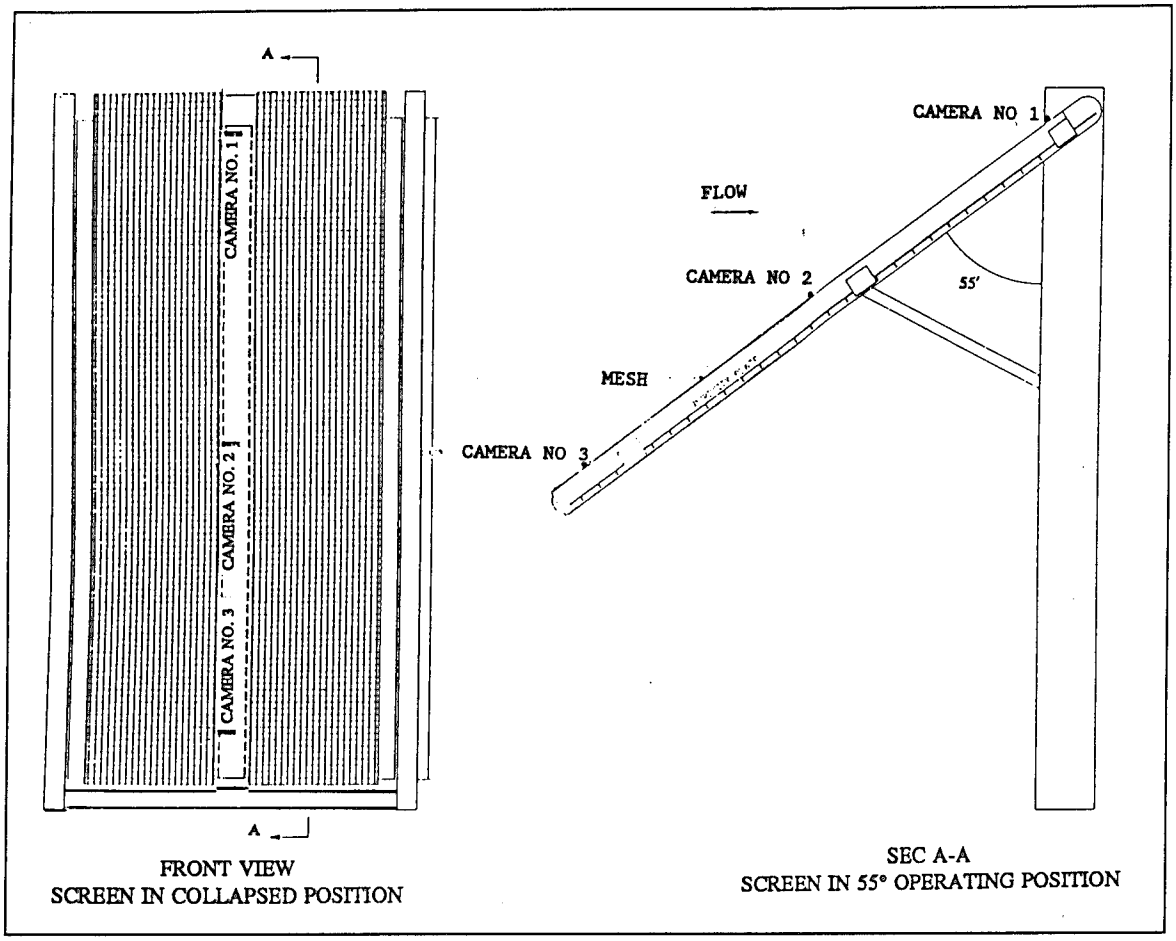

Figure 5. General configuration of an ESBS with approximate locations of video cameras indicated

will enter a collection channel which transports them to an area downstream of the structure. The deployment configurations of the MBFVBS are more limited than the deployment configurations of the bypass screens. However, the porosity plate arrangement on the back of the VBS can be changed to distribute the flow evenly through the VBS. The absence or storage position of the closure gate in the gate slot can have a significant effect on hydraulic conditions within the gate slot.

Camera and Illumination System

The camera and illumination system were changed from the Outland Technology UWC-160 underwater color TV system used in FY 91 to three different camera and illumination systems to improve image quality. Three cameras were selected for use based on economics and availability. The first camera selected was the SL-99 Silicon-Intensified-Target (SIT) TV camera

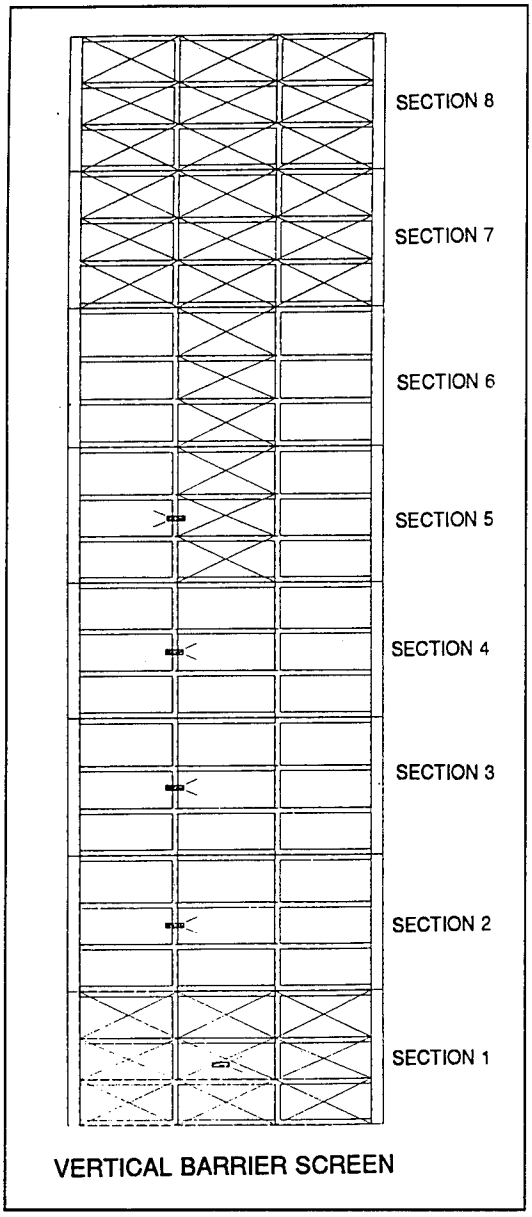

Figure 6. General configuration of a MBFVBS with approximate locations of video cameras indicated

which is highly suited for conditions ranging from very low light to daylight conditions. Two less expensive cameras, the OE 1359 underwater solid state television camera and the DeepSea Power & Light Micro-SeaCam underwater video camera were chosen to monitor the rest of the ESBS and used exclusively on the MBFVBS. High leasing or purchasing costs generally limit the use of the SIT camera. The Micro-SeaCam was chosen because only two OE 1359 cameras were available. Both cameras produced comparable imaging quality and had high definition and sensitivity. Two cameras of each type were used in the study for a total of six cameras. Camera specifications for each type of camera are listed in Appendix A.

Sampling Period and Conditions

FY 92 studies were performed between 2000 to 0200 hr at McNary Dam between 6 to 26 May and 8 to 16 July on days concurrent with FGE testing conducted by NMFS. In some cases, imaging occurred in bays used for FGE testing but at a time when NMFS staff had completed FGE testing. At other times, imaging occurred simultaneously to FGE testing but in units not used for FGE testing. Consequently, imaging performed in neighboring units should not be effected by the presence of the fyke net used during FGE testing. Storm events or freshets which increased turbidity and reduced imaging quality in FY pilot studies did not occur during these tests. Consequently, imaging quality in FY92 was generally superior to that observed in FY91.

Bypass System Configuration

Intake configuration

The top of each bellmouth intake at McNary Dam is located at el 329.5, a depth of 10.5 ft at normal pool. The bottom of the intake is located at el 233.6. Each intake is guarded by steel trashracks located approximately 20 ft upstream from the toe end of the ESBS and 35 ft upstream from the toe end of the SSTS.

Screen surface and gatewell

Findings by the WES Hydraulics Laboratory indicate that diversion screens generate complex hydraulic patterns that vary across the surface of the screen and change as screen design, angle, position, closure gate position, or unit loading is altered (e.g., compare hydraulic patterns in Figures 7 and 8. In addition, center, side, and cross supports of the screen produce local flow anomalies. The ability and propensity of fishes to respond to local flow conditions in rivers are well-known. Not surprisingly, the complex hydraulic field on the screen surface results in localized differences in smolt behavior and impingement (Nestler and Davidson 1993).

Imaging was performed at multiple points to insure that screen contact and impingement behavior of smolts is adequately quantified across the range of hydraulic conditions observed on the screen surface. As a general guide, the screen surface for both the ESBS and SSTS can be separated into three different zones: upper third (nearest the gatewell), middle half, and lower sixth (nearest the toe). The three zones are defined by the angle of flow and water velocity. In the upper third of the screen, the flow lines become increasingly parallel to the surface of the screen. A passive object caught in this flow feature would be either entrained into the gatewell, pushed towards the gatewell on the screen surface, or slip through the gap between the MBFVBS and bypass screen. In the middle zone, flow lines are approximately perpendicular to the surface of the screen and the flow passes directly through the screen. A passive object caught in this flow may be impinged and pressed onto the screen surface. In the bottom zone, the flow lines deviate from perpendicular to the screen surface and, at least at highest discharges, the flows lines begin to move towards the toe of the screen. A passive object caught in the lower zone of the screen would either be pressed into the screen surface or pushed towards the toe of the screen, under the bottom edge of the screen, and then into the turbine (Figure 9).

Imaging System Deployment

The camera mounting system used at McNary Dam had to allow for normal deployment of the SSTS, ESBS, and MBFVBS through the gate slots and

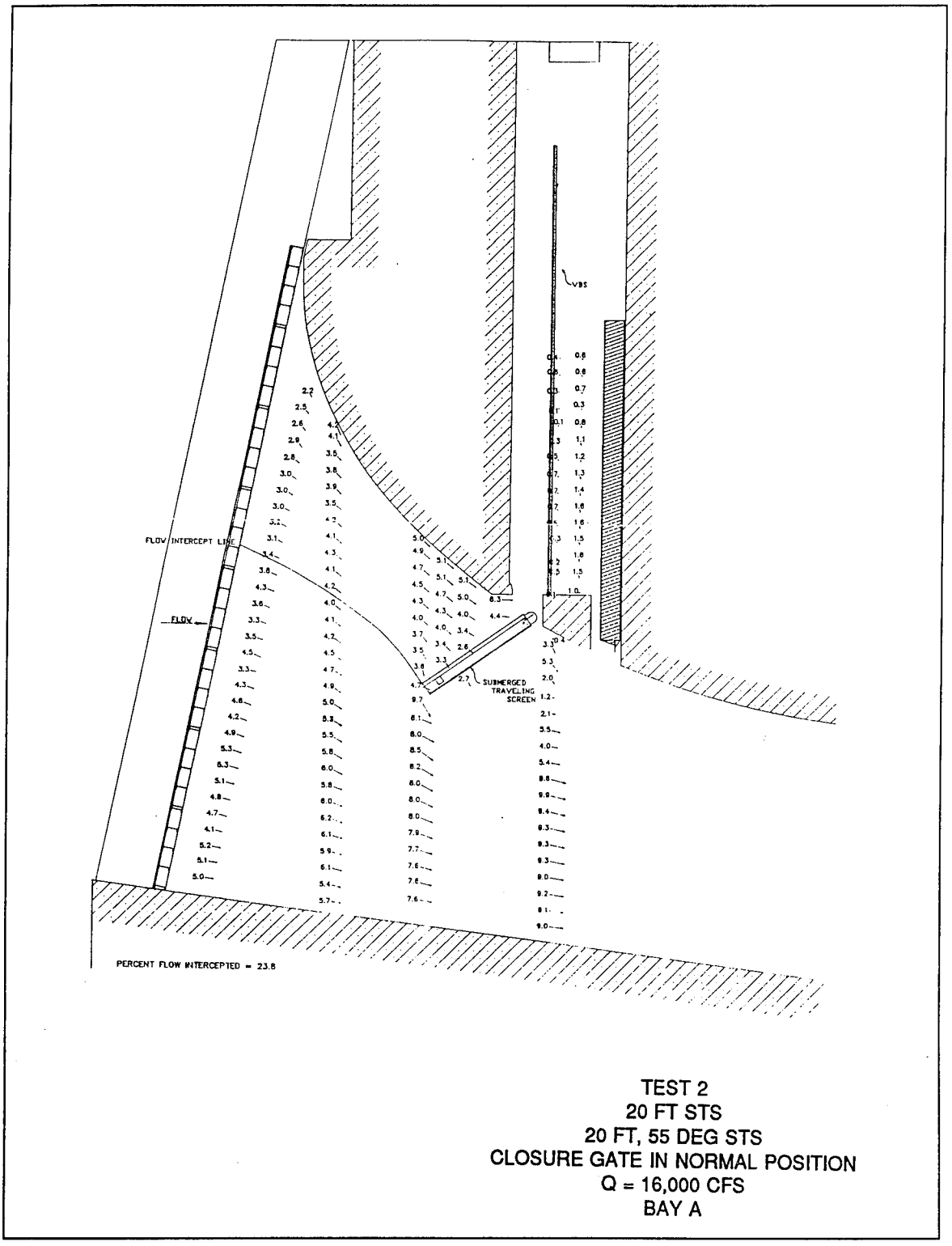

Figure 7. Side view of velocity distribution on surface of SSTS (Note how the direction and velocity of flow vectors change from the toe to the top of the screen.)

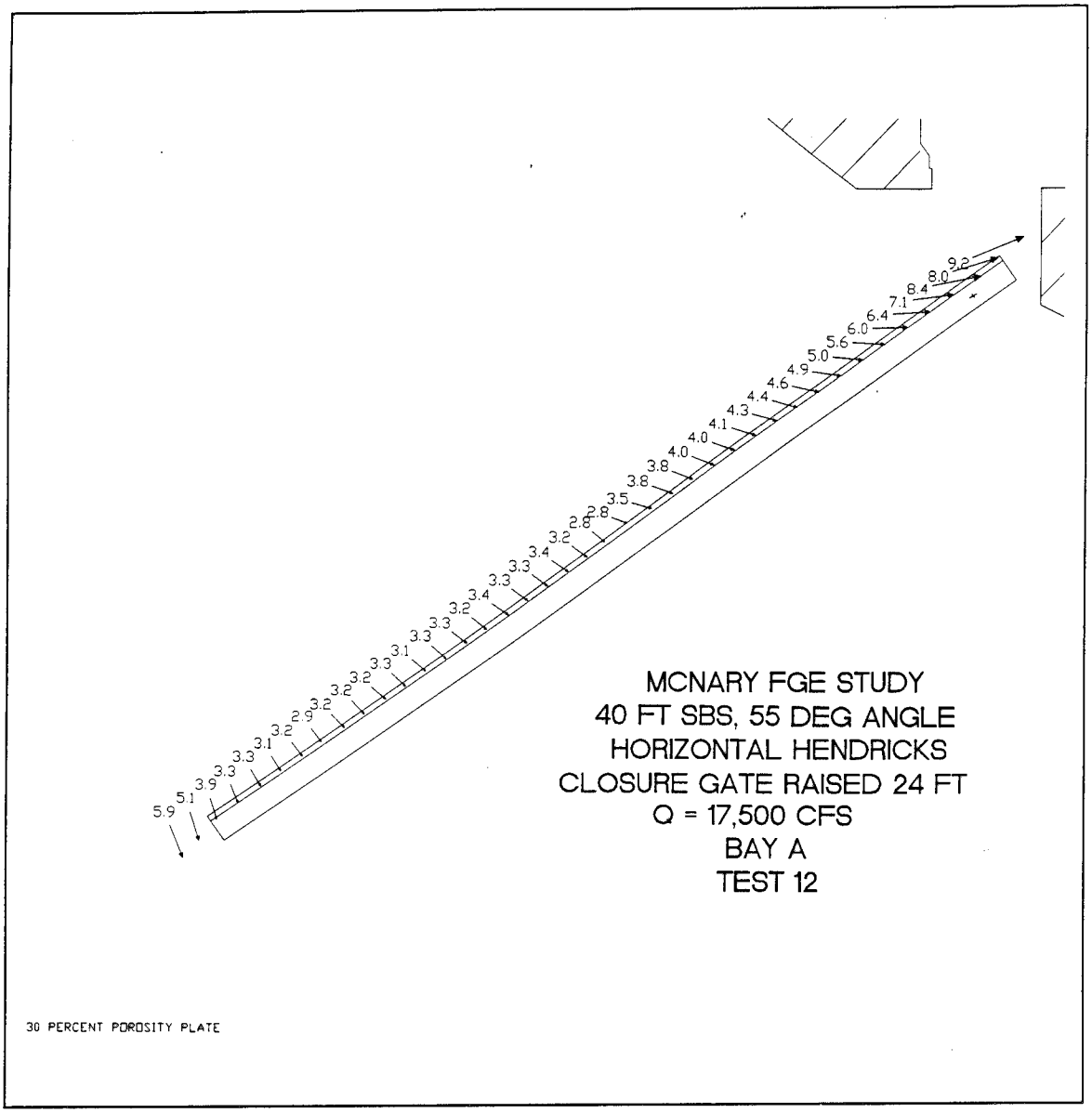

Figure 8. Side view of velocity distribution on surface of ESBS (Note how the direction and velocity of flow vectors change from the toe to the top of the screen.)

without a need for divers for attachment and inspection. WES staff, with assistance from McNary Dam project personnel, attached the light and camera system to the screen, secured cables, and performed other tasks necessary to complete attachment and installation of imaging equipment.

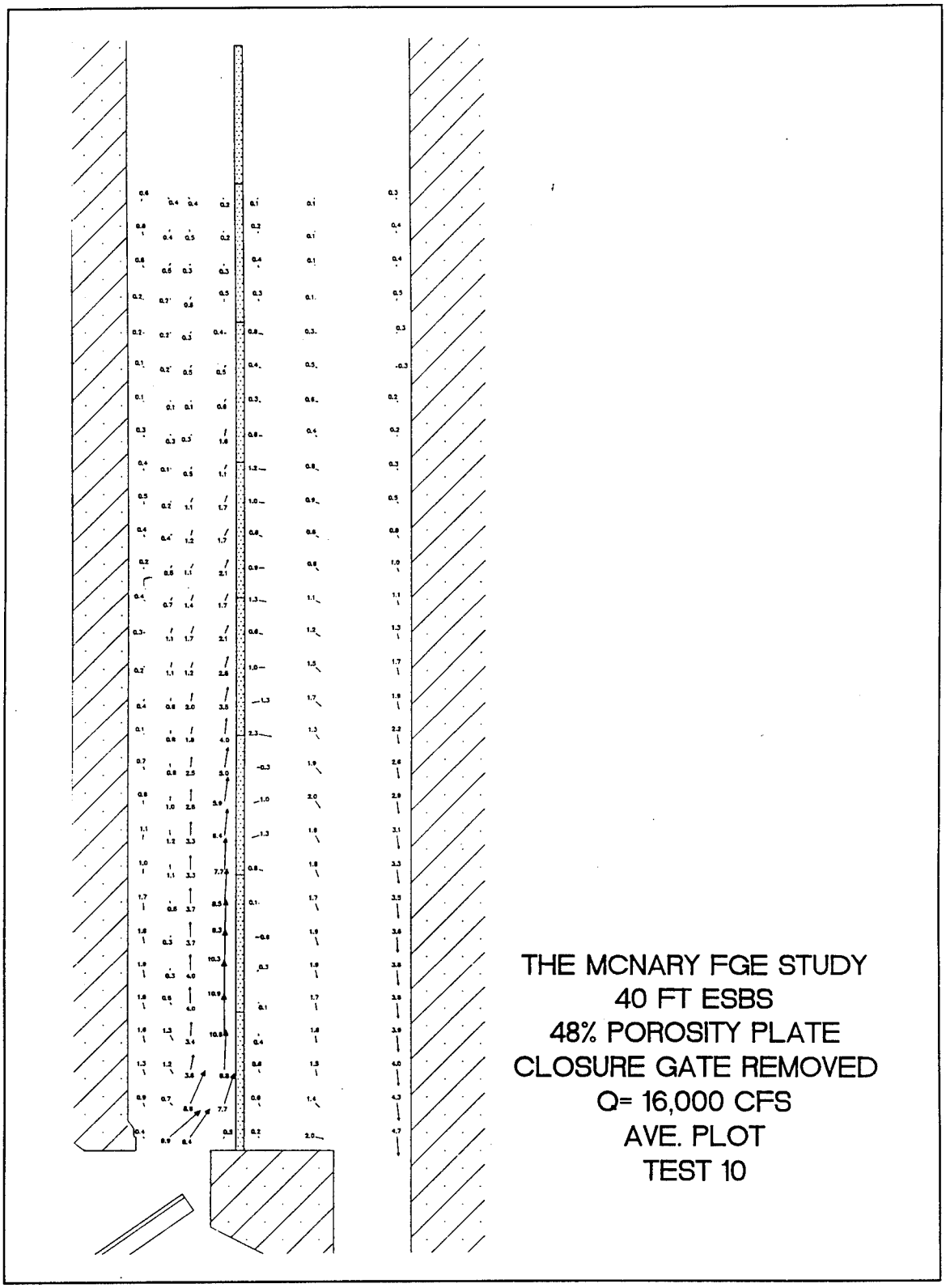

Figure 9. Side view of velocity distribution next to the surface of a MBFVBS (Note the extreme change in direction and velocity of flow vectors as the flow moves up the gatewell.)

Camera mounting system

Cameras were inserted into a sleeve of 4.0, 2.0, or 1.58 in. inside diameter steel or aluminum pipe, as dictated by the diameter of the camera, and secured to the sleeve with set screws. The pipe was welded to a flat plate (Figure 10). The flat plate was bolted onto the nonmoving center support of the SSTS. For the ESBS, the flat plate was banded to the bar screen material using a stainless steel 0.5-in. banding material. On the MBFVBS, camera mounts were bolted to the support members of the screen using all-thread clamps. On all screen types, cameras were aimed laterally looking across the surface of the screens except for the gap loss camera.

Camera depth-of-view, based on our ability to identify structural features (bolt heads on the tie down bar), was about 24 to 36 in. However, smolts are so highly reflective when illuminated from the side that they could be detected at distances estimated to be about 48 in.

Camera locations

Screen contact, impingement, and behavior of the smolts as they were intercepted by a SSTS or an ESBS were imaged by six video cameras mounted along the centerline of the SSTS and alongside the ESBS. Each camera imaged an area of the screen that had been previously identified through physical model studies as having hydraulic features that could affect impingement characteristics of smolts. Cameras imaged laterally across the screen at locations 2, 13, 21, 26, 31, and 38 ft from the top of the ESBS and at locations 6, 10, 12, 15, and 18 ft from the top of the SSTS (Figures 4 and 5). In all cases the cameras on the bypass screen imaged from screen right to screen left (from the observer's point of view facing the camera). Five cameras used on the MBFVBS were located on the midsection of the bottom five of the eight panels that comprise the bypass screen (Figure 6). The sixth camera (gap loss camera) was located on the top of the bypass screen and aimed parallel to the surface of the screen pointing towards the gap. An incandescent light source with a maximum intensity of 120 W was either strapped to the pipe sleeve or bolted to the flat plate and aimed parallel to the aim of the camera. The third camera on the SSTS stopped operating shortly after the study began.

During imaging, each camera was connected to a video cassette recorder (VCR) and a television monitor. Field personnel constantly observed each of the monitors and recorded the time that a smolt was observed on each tape in a log book that also contained screen design, deployment configuration, and related information. Usually two video cassettes per camera were used nightly with each cassette covering 2 hr of video imaging. In the spring, images were recorded on 176 video tapes with 148 documenting the ESBS and 28 documenting the SSTS. In the summer, imaging data were recorded on 184 video tapes with 109 documenting the ESBS and 75 documenting the MBFVBS and gap loss. Each tape associated with bypass screens contained

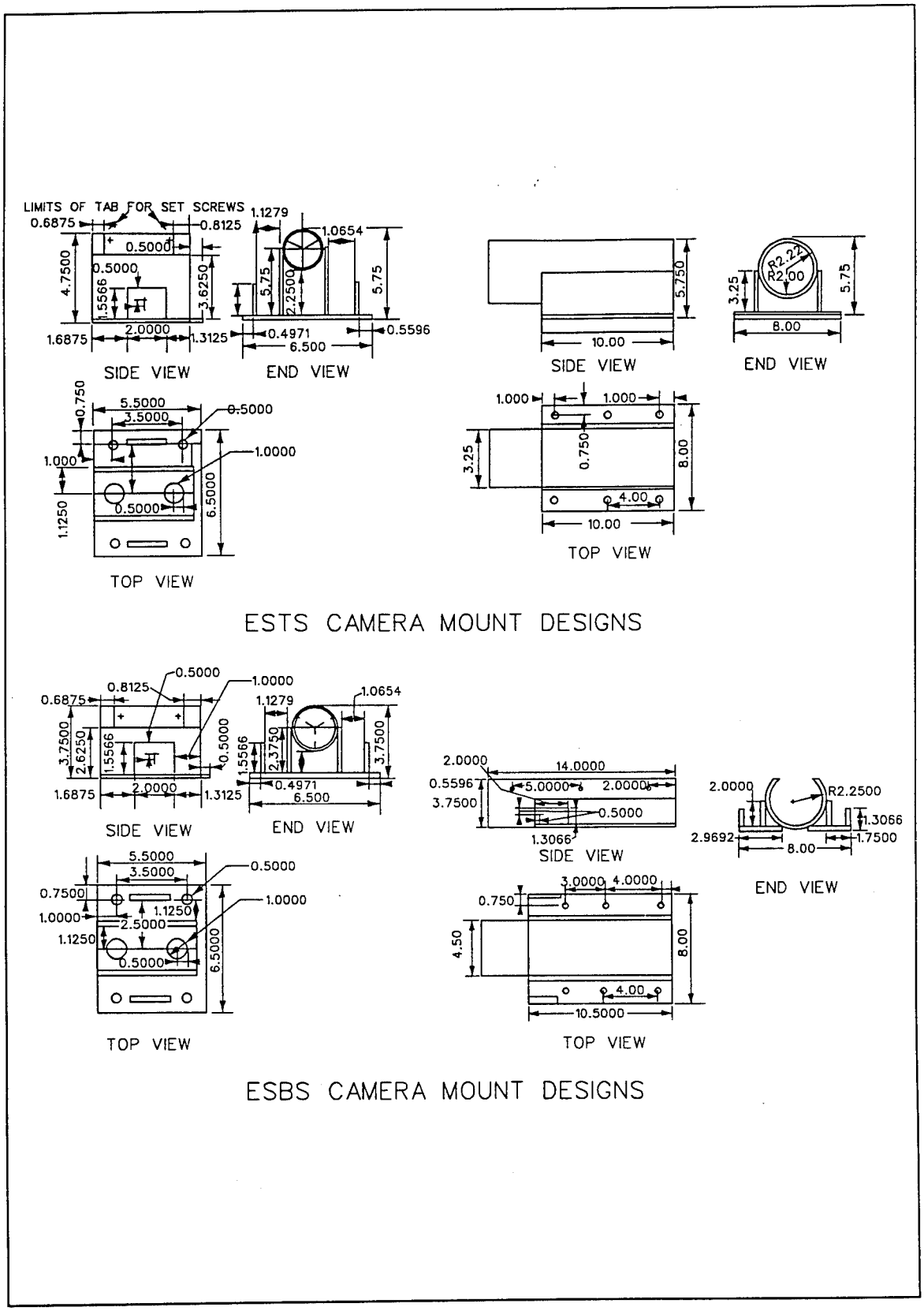

Figure 10. Camera mount designs used to image smolts on SSTS and ESBS

images of approximately 15 to 20 smolts although some tapes recorded no events. Tapes associated with the MBFVBS imaging generally contained numerous images of smolts.

Imaging System Bias Evaluation

Describing impingement on and smolt behavior to bypass and vertical barrier screens using video imaging must address two potential experimental biases. First, the presence of the camera, illumination system, and mounting hardware will produce a significant hydraulic anomaly on an otherwise flat screen surface that may potentially influence fish response if the anomaly is large enough to be detected by and thus influence approaching smolts. Second, the illumination field required for camera imaging may also cause smolts to be attracted or repelled from the immediate vicinity of the camera and thus also bias fish responses to bypass or vertical barrier screens.

Camera body bias

Potential sampling biases resulting from the presence of the camera, illumination system, and mounting hardware on the flat screen surfaces were minimized in several ways. First, the cameras employed at McNary Dam were generally small (2.0 in. outside diameter by 6.0 in. length) as were the mounting and attachment hardware (Figure 10). The relatively small size of the camera body and mounting system should minimize the size of the associated hydraulic anomalies. Second, flow lines over most of the screen are nearly perpendicular to the screen surface. Consequently, the pressure waves associated with the camera mounting system would attenuate quickly because they would propagate directly into the flow lines. Those screen locations where the flow lines were beginning to parallel the screen (upper third of the screen) were characterized by water velocities from 5.0 to 10 fps (Figure 8) that would minimize the time that smolts had to respond to the camera mounting system. Studies to determine the effect of a camera and mounting system bias are described in Chapter 3.

Light bias

The illumination system used to provide light for the cameras could bias the findings by either attracting or repelling smolts. The effects of the illumination system on smolt behavior were probably minimal for several reasons. First, the cameras used at McNary Dam could provide adequate images under relatively low-light conditions. The illumination fields for the tests at McNary Dam were generated at a setting of the illumination control dial that corresponded to about a 125 to 150 W light source. The intensity and spectral characteristics of the light source were not measured and are unknown. Based on the extent of the field of vision using low light cameras, it is estimated that

the light field extended about 4 to 5 ft from the camera. Second, our experience with lights suggests that the effects of an illumination zone are highly localized. Fish outside an illuminated area are unaware that it exists because of the rapid attenuation of light in turbid water. Consequently, fish should enter the illumination field at the same rate and orientation as if the field did not exist. Third, nearly identical lighting (50 percent setting) was used for all cameras so that the effect of the lighting system on smolt behavior or impingement rate estimation would be a constant bias in the analysis as opposed to a random or fluctuating bias. Thus, while it is possible for the light system to influence the behavior of the fish or impingement rate once the fish have entered into the illumination zone, this bias should have the same effect across all treatments. Fourth, a rationale for the direction of the bias can be provided based on a "worst case" estimation of the effects of the bias introduced by lights. Without light the smolts can use only the octavo-lateralis system to sense the presence and location of the screen. With light available, the smolts can also use vision to locate the screen. Consequently, if there is a light bias, it is speculated the bias should function to reduce impingement rate, all other factors being equal.

Information on fish behavior also can provide some insight into the direction of bias introduced by the presence of the light system. The response of fish to light is partially determined by antecedent illumination conditions because fish acclimate to ambient light conditions. If fish are removed from ambient light conditions they will attempt to return to those conditions, if ambient conditions are available. Thus, fish held under daylight conditions and then quickly introduced into a test chamber under low light conditions will not respond the same as fish held in low light and then introduced into a low light environment. Similarly, fish held under low light conditions will not respond to daytime light conditions the same as fish held under daytime light conditions and introduced into high light conditions. If active, fish held in low light conditions will tend to seek low light conditions (Pucket and Anderson 1987). In nighttime tests of different lighting systems at Richard B. Russell Dam (on the Savannah River at the border of Georgia and South Carolina), a time duration of approximately 45 min must pass before large numbers of blueback herring respond to underwater lights. It seems doubtful that the few seconds of illumination available to smolts as they are intercepted by the screens are adequate to modify their behavior substantially from their behavior under no light or low-light conditions. Studies to quantify the effects of the light bias are described in Chapter 3.

3 Data Analysis

Experimental Design

Bypass screen imaging

The cameras on the ESBS recorded smolt behavior to three closure gate settings, two screen elevations, three discharges, two screen angles, and presence/absence of a fyke net (referred to as different deployment configurations). The cameras on the SSTS recorded smolt behavior at the standard deployment settings (no gate, 48 percent porosity, 55 deg screen angle, standard screen position) and operated at three different discharges. For each deployment configuration, video imaging was used to collect multiple impingement events. The screen designs and deployment configuration evaluated are depicted in Figure 11 and summarized in Table 1. In Figure 11, the statistical analysis for effects of design or deployment alternatives were restricted to data blocks in which only the effect being evaluated was allowed to vary, and other variables were held constant. For example, effects of the Fyke net were determined using the data blocks within the barred boxes, and effects of closure gate position were evaluated using data blocks within the shaded box. MBFVBS deployment configurations and gap loss determination conditions are detailed in Figure 12.

Smolt impingement characteristics associated with different screen designs or deployment configurations were evaluated by determining the proportion of smolts exhibiting different impingement responses during discrete blocks of time. Each of these time blocks was treated as a replication. A minimum of three smolts had to be imaged during each replication. In some cases, when a particular condition was evaluated during a time period of reduced smolt passage, this relatively low number of smolts in a replication influenced the results. These situations were identified in the results section. The sample was replicated to 15 smolts per sample when more than 30 smolts were observed for a specific deployment configuration. Replications were obtained sequentially, not randomly, because it was logistically impossible to randomize the independent variables. However, this should not present a major problem for two reasons. First, the imaging rate was sufficiently low that the behavior of each smolt should not be influenced by the behavior of previous smolts, (i.e., the sequential nature of the data should not produce

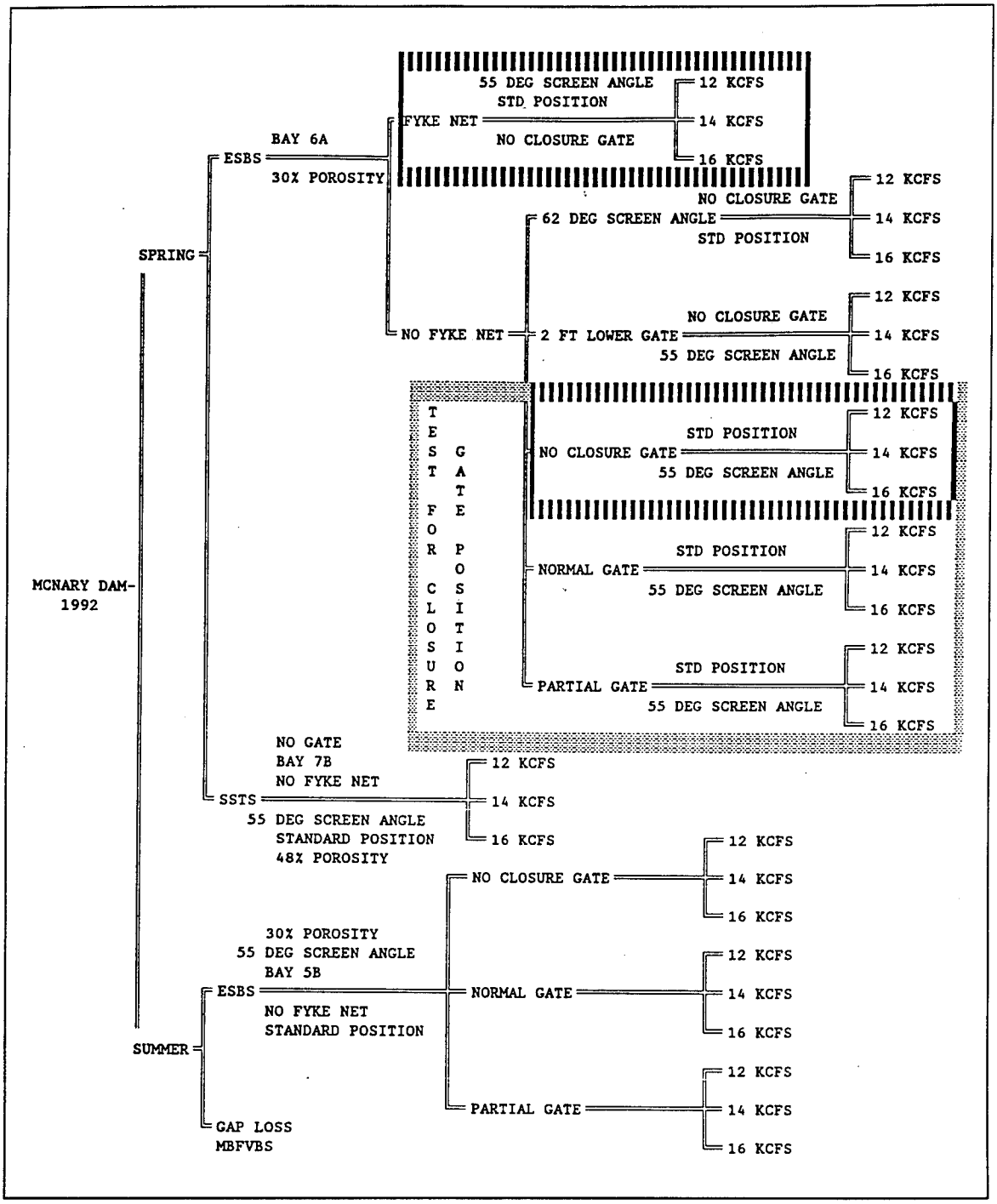

Figure 11. Summary of screen design and deployment configurations evaluated during 1992 imaging studies at McNary Dam

autocorrelation problems). The mean time between smolts was 13 min in the spring and 1.6 min in the summer. Second, the significance levels produced by statistical analysis were viewed as indices and not as statistically rigorous significance levels. Significant results had to be supported by patterns of

Table 1
Summary of Tests at McNary Dam in 1992

Month/Screen	Test	Unit	Bay	Pore	Angle	EL	Gate Position	Fyke Net	Unitloads
M[1] ESBS	Fyke Net	6	A	30%	55°	STD[2]	NO GATE	P[3] & A[4]	12, 14, 16 KCFS
M ESBS	Screen Position	6	A	30%	55°	STD/L24[5]	NO GATE	A	12, 14, 16 KCFS
M ESBS	Screen Angle	6	A	30%	55°/ 62°	STD	NO GATE	A	12, 14, 16 KCFS
M ESBS	Unit-Load	6	A	30%	55°	STD	ALL POS[6]	A	12, 14, 16 KCFS
M ESBS	Gate Setting	6	A	30%	55°	STD	ALL POS	A	12, 14, 16 KCFS
M ESBS /SSTS	Screen Type	6 7	A B	30% 48%	55°	STD	NO GATE	A	12, 14, 16 KCFS
M & J[7] ESBS	Month	6 5	A B	30%	55°	STD	ALL POS	P (J)[8] A (M)[9]	12, 14, 16 KCFS
J ESBS	Unit-Load	5	B	30%	55°	STD	ALL POS	P	12, 14, 16 KCFS
J ESBS	Gate Setting	5	B	30%	55°	STD	ALL POS	P	12, 14, 16 KCFS
J MBFVBS	Gate Setting	5	B	20%	Vertical	STD	ALL POS	P	12, 13, 14, 16 KCFS
J MBFVBS	Unit-Load	5	B	20%	Vertical	STD	ALL POS	P	12, 13, 14, 16 KCFS
J GAP LOSS	Gate Setting	5	B	30%	55°	STD	ALL POS	P	12, 13, 14, 16 KCFS
J GAP LOSS	Unit-Load	5	B	30%	55°	STD	ALL POS	P	12, 13, 14, 16 KCFS
M SSTS	Light Bias	7	B	48%	55°	STD	NO GATE	A	16 KCFS
M SSTS	Body Bias	7	B	48%	55°	STD	NO GATE	A	16 KCFS

[1] May.
[2] Standard position.
[3] Present.
[4] Absent.
[5] Lowered 24 in.
[6] Normal gate, partial gate, and no gate.
[7] July.
[8] July tests performed with the Fyke net.
[9] May tests performed without the Fyke net.

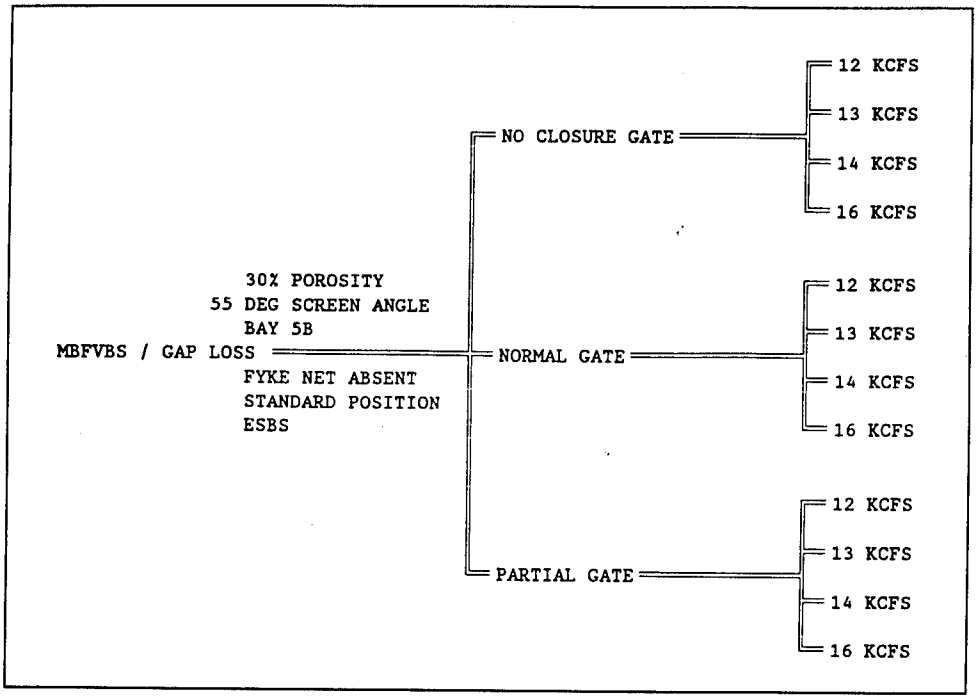

Figure 12. MBFVBS deployment configurations and gap loss determination conditions for 1992 imaging studies at McNary Dam

results across cameras and discharges and had to be consistent with hydraulic patterns either determined from physical models or observed through the video cameras.

Estimates of the approach angle of the flow to the screen were also based on a minimum of three observations. In cases where fewer than three smolts were observed, additional observations of only hydraulic conditions were added. In cases where the water angle varied substantially over time and three or more smolts were observed, water angle was determined either when the smolt was observed or when screen strike occurred. When three or fewer smolts were observed, water angle was estimated from portions of the videotape that corresponded to the maximum, minimum, and average excursion of the flow angle on the screen surface to insure that the range of possible flow angles on the screen was bracketed. Variability in flow conditions (turbulence) on the screen surface was approximated by using the standard deviation of the multiple water angle estimates obtained for each replicate.

MBFVBS and gap loss imaging

The MBFVBS that was video monitored had a porosity of 20 percent, was operated in a partially raised normal storage position under incremental unit-loads of 12,000, 13,000, 14,000, and 16,000 cfs and with the closure gate absent. The orifice connecting the gatewell to the fish channel was closed during imaging so that smolts could not exit from the gatewell. Consequently,

smolts would concentrate in higher numbers in the gatewell than they would with an open orifice. The effect of the orifice being closed on imaging results is unknown. A typical hydraulic field for the MBFVBS is depicted in Figure 9.

Imaging on the MBFVBS was separated into 2.5 min replicate time blocks for each camera. The behavior of individual smolts was generally not recorded for the MBFVBS analysis because of the large numbers of smolts that were observed. Multiple estimates of instantaneous water angle to the screen were recorded at each camera on the MBFVBS as well as on the camera used for gap loss determination. In cases where large numbers of smolts were observed within each 2.5-min time block, 30-sec time periods at the beginning and end of each time block were evaluated.

Collection of Data from Video Tapes

Bypass screens

Video camera images of smolts being intercepted by the ESBS and SSTS were consolidated onto eight VHS video tapes (four for each season sampled) by selectively copying segments of the original video tapes that contained footage of fish onto a new tape using a second VCR. An additional leading and trailing 5 sec were also copied so that each fish-screen interaction on the consolidation tape was separated by approximately 10 sec. Log-book entries made in the field were used to locate each image on the original videotapes. Use of consolidation tapes simplified the process of recording data onto code forms and was particularly useful when preliminary analyses of the data require that certain variables or conditions be recoded or re-evaluated. The consolidation process took 6 weeks to complete.

The consolidation tapes were played back in slow motion, and values for variables describing screen hydraulics and smolt interception behavior (passage, screen contact, or impingement-hereafter collectively termed impingement behavior) were recorded by a technician. Data encoding procedures and variable definitions for the bypass screens are presented in Appendix B. There were 2,896 fish observed in the summer data collection and 968 fish in the spring; totaling 3,864 fish interception events representing 458 different design or deployment configurations. Encoder bias was evaluated by having one of the two encoders analyze 100 impingement events of the other encoder. Slight differences in encoding procedures were identified and reconciled. Examples of smolt impingement events on an ESBS and on an SSTS are depicted in Figure 13.

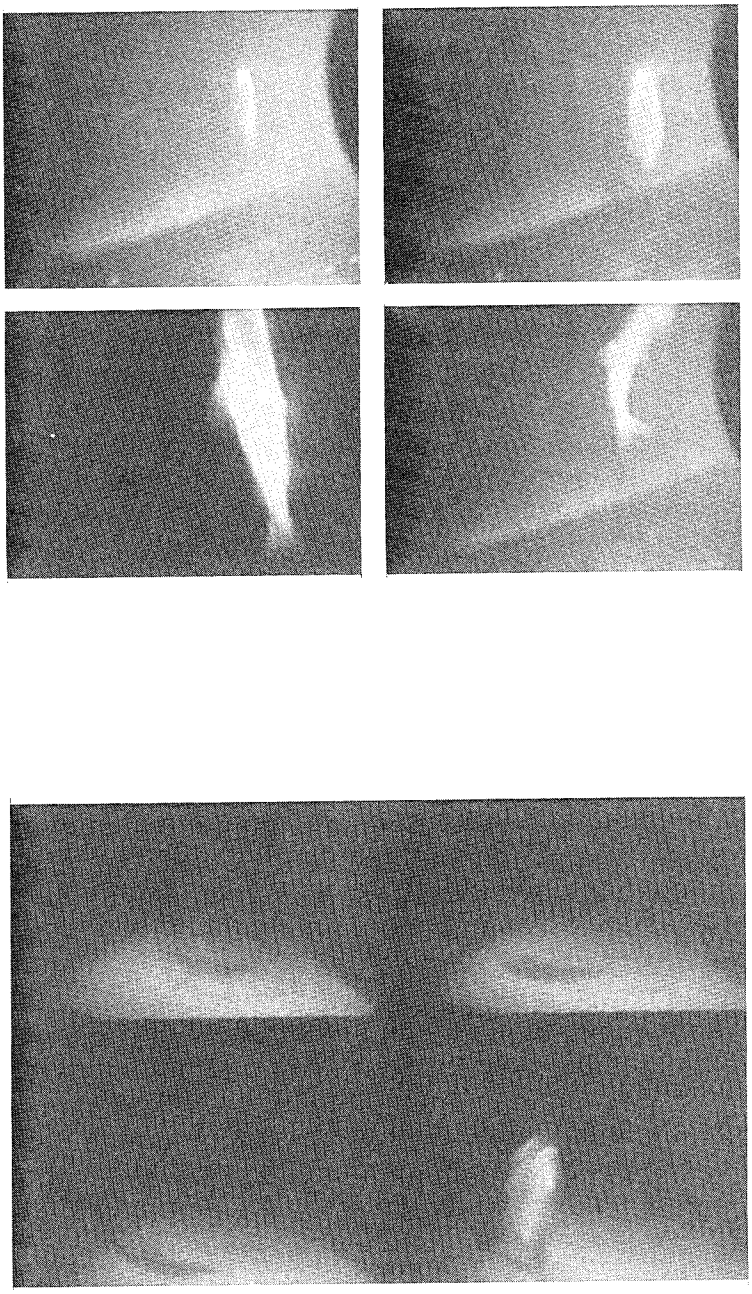

Figure 13. Examples of smolt impingement behavior on an ESBS (top block) and SSTS (bottom block). The mesh construction of the SSTS and the bar construction of the ESBS can be observed from the images. For the top set of images, the dark crescent on the right is the edge of the body of the light source. The bar screen is located on the bottom of the image and the line located at an angle to the bottom of the image is the horizon of the bar screen. The smolt imaged on the ESBS is exhibiting "tail walking" and would be entered into the data as "contact with escape" with multiple screen contacts. The bottom block shows a smolt escaping from the screen and would also be described as contact with escape.

MBFVBS and gap loss

The large numbers of fishes imaged during the MBFVBS monitoring eliminated the need for consolidation tapes. Tallies of smolts exhibiting different categories of behavior were made for each time block using a laboratory counter. At the conclusion of each time block, a technician recorded the tallies for different impingement behaviors obtained from the original video tapes onto code sheets along with estimates of water-flow angle at the beginning and end of each time block. Examples of different smolt impingement behavior during passage along the MBFVBS are depicted in Figure 14. At times, highly turbulent flow patterns were observed near the MBFVBS. Turbulent flow patterns in the MBFVBS appeared to behave as a threshold process. It seemed prudent to not extrapolate physical model predictions of average flow patterns to the potentially turbulent environment of the prototype MBFVBS. More detailed model studies will be performed in FY93, but the results will be unavailable for inclusion in this report. Consequently, only general flow patterns from the model could be extrapolated to the prototype screen.

Examples of gap loss imaged by the video cameras are presented in Figure 15. Gap loss is easily discerned and not hindered by observer subjectivity as are bypass screen evaluations and MBFVBS assessments. Detailed data encoding procedures and variable definitions for the MBFVBS and gap loss determination are presented in Appendix C. There were 33,842 smolts observed and evaluated for the MBFVBS imaging and 508 smolts (of which 188 were observed entering the gap) observed for gap loss determination.

Complex Variables

The data recorded by technicians describing smolt-screen interaction and the hydraulic environment were combined into complex variables, or indices, that could be used to describe and summarize the impingement characteristics of different screen designs and deployment configurations. The following variable and index abbreviations are used throughout the text.

Bypass screens

For each impingement or passage index, except the impingement index, a smolt meeting the index requirement receives a weighting of 1.0; whereas a smolt not meeting the index requirement receives a weighting of 0.0. The impingement index had a "touch or strike with escape" category that received an intermediate weighting of 0.5. The 0.5 value was used because a touch or strike was assumed to be intermediate in its potential negative impact on the smolts between entrainment (without screen contact) and impingement.

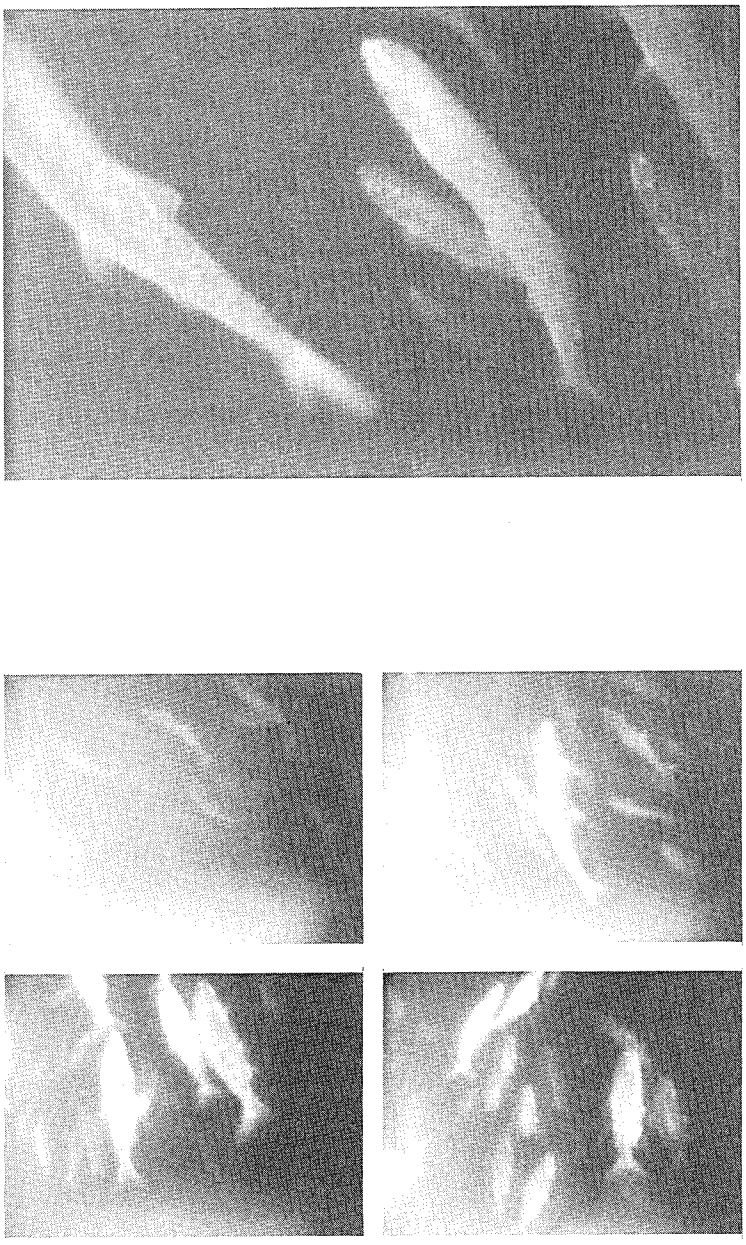

Figure 14. Examples of video imaging of the MBFVBS. Note the large numbers of smolts in the images (top image) compared to Figure 13 indicating the much higher imaging rate associated with the VBS. For each image, the MBFVBS is located at the bottom of the image, and the top of the MBFVBS is located to the reader's right. The top two images of the four-panel images depict smolts in a turbulent environment. Note the random distribution of the smolts relative to the screen surface and the apparent trajectory of some of the smolts towards the screen surface. The bottom two images represent the behavior of smolts to laminar flow conditions. Note that the smolts are oriented parallel to the MBFVBS and are swimming perpendicular to the screen surface and directly into the flow.

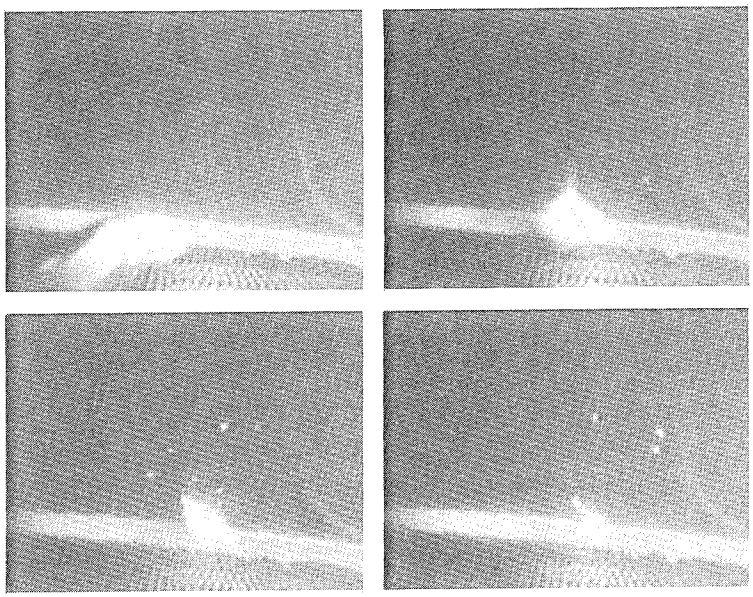

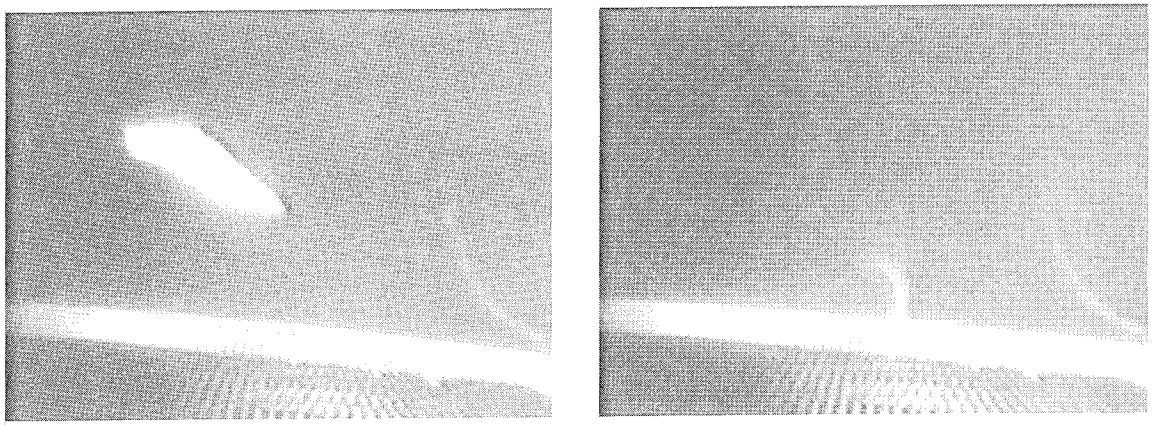

Figure 15. Example images of gap-loss obtained video imaging. The camera is aimed parallel to the screen and pointing towards the gap between the bypass and vertical barrier screens (the top of the bypass screen can be seen in the foreground and the barrier screen cannot be seen). A smolt disappearing below the horizon formed by the top of the screen is passing through the gap. The "rope" on the right side of each image is the power supply and fiber optic cable servicing the camera. Note the halo of scales surrounding the smolt, particularly in the lower half of the top group of four images, just as the smolt is passing into the gap indicating the possible severe impact of screen contact on scale loss.

a. *R_PERMIN.* The imaging rate is the rate at which smolts are imaged as the number observed divided by the duration of imaging. This index can exhibit complex behavior because of its sensitivity to unit-load. Increased unitload while smolt density (smolts/m^3) remains constant will result in an increase in the number of smolts moving past a fixed point (imaging rate). In addition, increased unitload also increases water velocity through the screen so that smolts are more likely to be forced closer to the screen by the current and thus increase their probability of being imaged. Imaging rate should be evaluated with care because of the complex effects of several of the independent variables.

b. *R_IMPNEN.* The entrainment proportion is the number of smolts entrained that do not strike or touch the screen divided by the number of smolts observed.

c. *R_IMPNES.* The strike proportion is the number of smolts that touch or strike the screen and escape divided by the number of smolts observed.

d. *R_IMPNGD.* The impingement proportion is the number of smolts that impinge on the screen and do not escape divided by the number observed.

e. *R_IMPNGI.* The impingement index is the number of smolts that either touch, strike, or impinge on the screen divided by the number observed (For this index a smolt that touches or strikes the screen but does not impinge receives a weighting of 0.5).

f. *R_IMPNGN.* The entrained headfirst is the number of smolts entrained headfirst that do not touch or strike the screen. Although speculative, it seems reasonable that optimum guidance occurs when the smolt is moving headfirst parallel to the direction of flow without striking the screen. This orientation implies that the smolt is being guided efficiently and has not touched or struck the screen. Smolts that strike the screen often reorient and move headfirst into the flow with their tails striking the surface of the screen (e.g., Figure 13, panels 1-4).

g. *R_IMPNGH.* The headfirst strike is the number of smolts that are entrained headfirst and are observed to touch or strike the screen and impinge.

h. *MN_CRANG.* The mean current angle 0 to 180 deg is the mean water current angle ranging from 0 to 180 deg with 0 deg representing water flow moving parallel to the screen away from the gateslot and 180 deg representing water flow moving parallel to the screen surface towards the gate slot.

i. *MN_CRAN9*. The mean current angle 0 to 90 deg is the mean water current angle ranging from 0 to 90 deg calculated as the absolute value of the current angle with 0 deg representing flow perpendicular to the screen and 90 deg representing water flow moving parallel to the screen in either direction.

j. *MN_CRCV*. The variance in current angle is the variance in current angle over time used as a surrogate for turbulence. More turbulent flow conditions on the screen will produce a greater variance.

k. *MN_CR9CV*. The current angle plus variance is the mean current angle plus the variance in mean current angle. This variable attempts to integrate both variation in flow and flow angle.

l. *CR_ANGRD*. The physical model current angle is the mean current angle determined from physical hydraulic model studies rounded to the nearest 10 deg.

m. *CR_VELRD*. The physical model current velocity is the mean current velocity determined from physical hydraulic model studies rounded to the nearest foot per second.

The above indices were selected not only because they characterize different entrainment behaviors but also because they vary in their data requirements. The impingement index provides only very general information but, in compensation, is not data intensive because a number of different impingement categories will produce an increase in this index. This index is most likely to provide useful information for those conditions where few smolts are available for analysis. The indices requiring more observations, such as the two headfirst indices, can provide detailed information for those conditions having many images but are of limited usefulness when the passage rate of smolts is low because relatively few smolts meet the requirements of this index. Consequently, the headfirst indices must be used with caution because their values may be determined by only 1 or 2 smolts. Two measures of current angle were used to insure that the reference system for current angle did not unduly influence the analysis. Variance in current angle is used as a surrogate for turbulence.

MBFVBS and gap loss

The following indices were employed for each MBFVBS condition or replicate. Each of the complex variables represents the proportion of smolts exhibiting a behavior associated with potential screen contact or consequences of screen contact. Data were encoded as the proportion of smolts in the following different categories for each condition based on total tallies within each time block for each index:

a. *R_TSCRN.* The proportion moving toward screen is the number of smolts moving toward the screen divided by the total number observed in that replicate.

b. *R_TCAMR.* The proportion moving toward camera is the number of smolts distinctly moving towards the camera as opposed to just moving towards the screen divided by the total number observed in that replicate.

c. *R_WFLOW.* The proportion of entrained smolts is the number of smolts entrained in or moving with the flow not contacting or impinging on the screen divided by the total number observed.

d. *R_NOCONT.* The proportion of smolts unable to swim is the number of smolts having no control over their orientation in the flow field divided by the total number observed.

e. *R_CONTCT.* The proportion contacting screen is the number of smolts exhibiting severe contact with the screen whether they escape or not divided by the total number observed.

f. *R_CONTES.* The contact with escape is the number of smolts contacting the MBFVBS and escape divided by the total number observed.

g. *R_CONTNO.* The contact with no escape is the number of smolts contacting the MBFVBS and unable to escape from the screen surface divided by the total number observed.

h. *MN_ANGL.* The mean water angle is the mean of multiple direct measurements of the angle of flow relative to the screen surface. The screen angle for each replicate is based on the mean of the water angle at the beginning of the time block and end of the time block.

i. *VR_ANGL.* The variance in water angle is the variance in current angle obtained from multiple measurements of screen angle. The variance in screen angle for each replicate is a surrogate for turbulence.

The R_TCAMR index can be used to evaluate the degree of bias introduced by the presence of the camera. This index will be large if the camera is having a large influence on smolt behavior. The R_NOCONT index is designed to identify smolts that entered the camera field of vision but were injured elsewhere in the system.

Study Biases

Camera mounting system bias

Camera body bias was evaluated in the spring of 1992 at McNary Dam on an SSTS. Camera body bias testing was conducted for the worst case scenario, that is, when the camera body was in a flow field that was nearly parallel to the screen. In this setting, the size and persistence of the hydraulic anomaly caused by the camera mounting system should be maximized. Two cameras were mounted on the center support of the SSTS. One camera was mounted in the normal configuration, that is, aimed laterally across the mesh fabric. The second camera was located in the wake of the first camera and was used to determine if smolts were responding to or concentrating in the small hydraulic refuge or disturbance of the hydraulic field associated with the first camera.

Light bias

It was not possible to directly quantify the bias introduced by the lighting system because the ambient light levels were too low to image without supplemental lighting. Thus, it was not possible to perform light on/off tests to quantify bias. However, the light bias was evaluated indirectly by performing imaging at four different light settings that bracketed the light settings routinely used for imaging. Thus, if there was a light bias caused by the size of the illumination field, then that bias should increase as light intensity increased because the size of the illumination field would increase. The light bias can take one of two forms: the characteristics of the light field can influence the behavior of the smolts, or the efficiency of imaging can be affected.

Light bias field testing was conducted at McNary Dam with a SSTS on 8-10 May of 1992 between 2000 hr to 0100 hr of the next day in unit 7B at a unitload of 16 kcfs. Imaging was performed with four different illumination settings corresponding to approximately 63, 125, 188, and 250 W (maximum setting) of power to the lights. The sequence of light intensity settings were randomly selected. Field experience has indicated that an intermediate light setting of 125 to 150 W is optimal because it provides sufficient light for imaging and minimizes light reflection from particles entrained in the flow.

The effect of illumination system intensity setting on several indices was tested. The influence of the light intensity setting of the illumination system on R_PERMIN (rate at which smolts were observed), R_IMPNGI (proportion of smolts that touch or impinge on the screen), TOT_IMP (total number of smolts that touch or impinge on the screen for each time block), and TOT_SEEN (total number of smolts observed within each time block) was evaluated using correlation analysis and analysis of variance (ANOVA). The TOT_SEEN variable was used to evaluate the denominator of the impingement proportion variable (i.e., Was there a bias in illumination setting that

would affect the rate at which smolts were being imaged?) and the TOT_IMP variable was used to evaluate the numerator of the impingement index. The R_IMPNGI index was evaluated to determine if light setting affects the impingement characteristics of smolts. R_IMPNGI was selected because a large proportion of smolts usually touch or impinge on the screen. Consequently, this index is less sensitive to a smaller sample size than most of the other candidate indices. The R_IMPNGI index is also highly correlated to most of the other indices used to evaluate screen design or deployment configurations. Thus, if R_IMPNGI is affected by light intensity setting of the illumination system, then other of the indices also will be affected.

In addition to light setting, CAMLOC (camera location) was also used as a treatment because it was a variable known to significantly affect both indices. The effect of light setting could be compared to the effect of CAMLOC as an additional qualitative comparison. The analysis was restricted to time blocks in which at least five smolts were observed (i.e., the denominator of R_IMPNGI was at least 5). Unfortunately, too few observations were available to restrict the analysis to time blocks in which more smolts were observed. If more than five smolts were used, the number of replicates drops too low for ANOVA.

Data Analysis

Data analysis for the bypass screens, vertical barrier screens, and gap loss determinations was performed using the Statistical Analysis System (SAS Institute 1988).

Bypass screens

Data analyses were performed at two levels. First, general analyses were performed to determine the effects of water velocity and water approach angle predicted by physical hydraulic models on the impingement variables defined earlier but without consideration of screen deployment configuration or camera location. Second, detailed analyses were performed to determine the effects of specific screen design or deployment configurations on impingement variables.

Statistical power analysis (Peterman 1990) was considered but not performed. Statistical power analysis would provide information on the probability of rejecting a null hypothesis when it is false. However, the major data inadequacy occurred in the formation of proportions based on relatively few fish (This problem was most severe in the spring.). Statistical power analysis would not address this problem. In lieu of statistical power analysis, included is the number of observations upon which the proportions are based for all summary tables so that those analyses based on relatively few observations can be readily identified.

a. *General analyses*. The general analyses were performed to determine the response of smolts to hydraulic conditions at the point where they are intercepted by the screen. The results of the general analyses can be used to develop design guidelines or optimize deployment configurations. The general analyses were performed separately for the spring and summer months and were comprised of the following four steps.

(1) Summary tables were constructed providing means of variables for each screen design or deployment configuration. These tables provide expanded information that can be used to interpret results of the ANOVA.

(2) Correlation analysis (PROC CORR) was used to determine general relationships among independent and dependent variables. In particular, relationships between independent variables were explored to determine possible confounding effects among independent variables. For some cases, either because of logistical restraints or dam operator convenience, application of the treatments was not random but occurred in a set pattern over time. The confounding effects of correlated independent variables must be considered in interpreting the results of the analysis. Correlation analysis was also used to examine patterns of response among the dependent variables, particularly for the spring analysis. In cases where the number of smolts was limited, effects of a particular independent variable were inferred based on observing a consistent pattern across several correlated dependent variables.

(3) ANOVA using the General Linear Models Procedure (PROC GLM of SAS) was used to test for the effects of different treatments on dependent variables describing smolt impingement behavior or hydraulic patterns on the bypass screen. Analyses were considered to be significant at $\alpha = 0.05$. However, analyses significant at up to $\alpha = 0.20$ (and highlighted by bolding) were evaluated, but were considered only when they fell within consistent patterns across treatments or replicates. The rigor at which significance was accepted was relaxed because there was doubt regarding whether the imaging data consistently met the assumptions for ANOVA. Therefore, significance levels generated by ANOVA were utilized as a relative index to rank effects rather than in the normal context of statistical analysis. In many cases, hindered by small sample size, it seemed prudent to lessen the rigor of the criteria used to determine significance to reduce the probability of accepting a false hypothesis. The null hypothesis that sample means were identical was tested. The long time intervals (usually minutes) separating the occurrence of smolts on the tapes suggest that autocorrelation should not be a problem and that the behavior of each successive smolt should not be influenced by its predecessors on the tape.

(4) Regression analysis using backward elimination (PROC REG) was used to build statistical models to predict impingement behavior variables using hydraulic variables as independent variables. Backward elimination was employed so that quadratic effects could be evaluated. If successful, the regression equations could be used to infer the impingement characteristics across a screen surface if the hydraulic patterns across the screen could be determined from physical hydraulic model studies or from video imaging analysis of prototype screens during time periods when smolts were not passing.

b. Detailed analyses. Detailed analyses were performed using ANOVA to determine the effect of different screen designs, screen angles, unitloading, closure gate positions, presence/absence of the fyke net, month of sampling, and vertical screen position on hydraulic conditions and impingement characteristics. Separate analyses were performed for each condition except for closure gate position and unitload where sufficient data were available to do a two-way analysis of variance. Only main effects were evaluated because too few observations were available to evaluate interaction effects. Statistical analysis for effects of design or deployment alternatives were restricted to data blocks in which only the effect being evaluated was allowed to vary and other variables were held constant. For example, effects of the presence of the Fyke net were determined using the data blocks in which closure gate position, gate elevation, and deployment angle were held constant ("barred" boxes, Figure 11). Similarly, the effects of closure gate position were evaluated using data blocks in which the presence of the Fyke net, gate elevation, and deployment angle were held constant ("shaded" box, Figure 11).

The detailed analyses were performed in two phases. In the first phase, imaging results of all cameras except ESBS camera location two were combined to provide information on the overall impact of a particular screen design or deployment configuration on hydraulic variables and impingement characteristics. Camera location two was eliminated from the combined analyses because of the flow characteristics of the ESBS at this location. Generally, flow lines were parallel or nearly parallel to the screen surface and moved towards the gatewell. Consequently, smolts imaged by camera number two were moving parallel to the screen, and any screen interaction they may have had will have occurred lower on the screen.

Phase two analyses were performed using the imaging results for each camera separately allowing the effects of different deployment configurations to be related to specific positions on the screens. The experimental design is summarized in Table 1 and Figures 11 and 12, unless otherwise stated.

c. Descaling analysis. Descaling data collected by NMFS were provided to WES to determine if video imaging could be used to estimate descaling rates in lieu of determining descaling during FGE studies by

physical examination of smolts recovered by gatewell dipping. Summary video imaging data and descaling data that were collected under the same experimental conditions and deployment conditions, except for unit and bay number, were merged into one data set. Stepwise multiple regression using backward elimination was used to determine if the descaling rate could be predicted from video imaging data.

MBFVBS and gap loss

Data analyses were performed at two levels. General analyses were performed to determine the effects of the water approach angle on the impingement variables defined earlier but without consideration of screen deployment configuration or unit operation. Unitload was included in the general analysis as a surrogate for water velocity since water velocity predictions or measurements were unavailable for the MBFVBS. Detailed analyses were performed to identify the effects of unitload and closure gate position on MBFVBS impingement variables. The Fyke net was present during the MBFVBS and gap loss determinations and probably affected the results of the analysis.

The general analyses were performed to determine the response of smolts to hydraulic conditions on the MBFVBS. The results of the general analyses can be used to develop design guidelines or optimal deployment configurations for VBS. The general analyses comprised the same basic steps of summary tables, correlation analysis, ANOVA, and regression analysis as were employed for the analysis of the bypass screens. Detailed analyses were performed using ANOVA to determine the effect of closure gate position and unitload on impingement behavior and hydraulic patterns. Sufficient numbers of observations were available to test effects of both unitload and closure gate position. The MBFVBS assessment was performed separately for each camera; however, some camera locations were characterized by having only one or two observations for certain treatments.

4 Results

This chapter contains results of statistical analyses for the bypass screen evaluations, MBFVBS assessment, and gap loss determinations. Organization of this chapter generally follows Table 1 and Figure 11 except where noted.

The bypass screen evaluations were separated into three sections. Results for the spring objectives are presented first; the summer results are presented second, and results for the general objectives are presented third. Results for the general objectives are presented at the end of the bypass screen evaluation section because complete interpretation requires an understanding of the relationships among variables within each of the seasons. Separate analyses were performed for spring and fall chinook. FGE studies conducted over a number of years indicate major differences between the races of chinook, and it seemed reasonable that their impingement behavior would also differ.

Spring Bypass Screen Analysis

The bypass screen evaluation for the spring was separated into eight sections. The first section presents summary statistics to describe general patterns between and within the variables. The first section also includes correlation analysis of the dependent and independent variables. The second section describes the results of studies to determine the response of smolts to localized hydraulic conditions (immediate velocity and current angle) on the screen surface 13, 21, 26, 31, and 38 ft from the top of the screen. It includes summary tables and ANOVA to determine the effects of hydraulic variables on impingement behavior. Regression analysis was used to determine if local hydraulic variables can be used to predict impingement behavior. The next six sections present tabular summaries and results from ANOVA of different bypass screen design and deployment configurations including screen type, presence of the fyke net, screen angle, screen position, closure gate position, and unitload (gate position and unitload are blocked). Tables of results from each of the last six sections are presented in similar order by content type to enhance comparability between sections. This may cause some of the tables within a section to be referenced out of sequence.

Summary statistics

a. Summary tabulations. Table 2 presents summary data and simple statistics for the dependent and independent variables used in analyses. Hydraulic data from physical model studies of the ESBS were available for the spring for those configurations in which the fyke net was not deployed. It was possible to extrapolate both water velocity and water angle results from the model studies to the prototype screen. Physical model data, when available, were used in lieu of observed hydraulic data obtained from the video cameras.

Table 2
Simple Statistics for Analysis of Localized Hydraulic Conditions in the Spring

Variable	N	Mean	Std Dev	Sum	Minimum	Maximum
R_PERMIN	32	0.079687	0.050569	2.549973	0.025000	0.283333
R_IMPNEN	32	0.250740	0.250510	8.023670	0	1.000000
R_IMPNES	32	0.492402	0.235041	15.756878	0	1.000000
R_IMPNGI	32	0.435972	0.175064	13.951094	0	0.833333
R_IMPNGD	32	0.126155	0.173254	4.036969	0	0.666667
R_IMPNGN	32	0.030276	0.079139	0.968838	0	0.333333
R_SDEAD	32	0.023251	0.069619	0.744048	0	0.333333
HOURBEG	32	21.812500	1.856766	698.000000	20.000000	26.000000
CURR_ANG	32	122.906819	20.983450	933.018195	75.000000	150.000000
CR_ANGRD	32	30.625000	15.644746	980.000000	10.000000	50.000000
CR_VELRD	32	2.906250	0.640533	93.000000	2.000000	4.000000

Note: Results combined for all cameras except camera two. Variables defined on pp 29 and 30 of the text.

The number of observations in the spring is reduced relative to the number of summer samples because hydraulic modeling study results were not available for all combinations of screen deployment configurations and because springtime imaging rates are low. Reduced imaging rate means a higher proportion of imaged fish must be deleted because of inadequate sample size (less than three smolts) in the replicates.

b. Correlation analysis. Correlation analysis (Table 3) of the impingement/entrainment (dependent) variables for the spring identified the following relations:

Table 3
Pearson Correlation Coefficients for the Spring Analysis of Localized Hydraulic Effects

	R_PERMIN	R_IMPNEN	R_IMPNES	R_IMPNGI	R_IMPNGD	R_IMPNGN	R_SDEAD	HOURBEG	CURR_ANG	CR_ANGRD	CR_VELRD
R_PERMIN	1.00000 0.0	0.30476 **.0899**	-0.17574 0.3360	-0.32324 **0.0711**	-0.20427 0.2621	0.11968 0.5141	-0.13094 0.4750	0.15061 0.4106	0.35503 0.0462	0.26918 **0.1363**	-0.13837 0.4501
R_IMPEN	0.30476 **0.0899**	1.00000 0.0	-0.58590 **0.0004**	-0.87810 **0.0001**	-0.33100 **0.0642**	0.46954 **0.0067**	-0.23183 **0.2017**	0.02253 0.9026	0.39296 **0.0261**	0.43064 **0.0139**	-0.26231 **0.1470**
R_IMPNES	-0.17574 0.3360	-0.58590 **0.0004**	1.00000 0.0	0.27975 **0.1210**	-0.28603 **0.1125**	-0.17937 0.3260	-0.22850 0.2084	0.26608 **0.1410**	0.01248 0.9459	-0.03018 0.8697	0.00393 0.9830
R_IMPNGI	-0.32324 **0.0711**	-0.87810 **0.0001**	0.27975 0.1210	1.00000 0.0	0.73911 **0.0001**	-0.43445 **0.0130**	0.46786 **0.0069**	-0.15813 0.3874	-0.43236 **0.0135**	-0.50482 **0.0032**	0.29801 **0.0976**
R_IMPNGD	-0.20427 0.2621	-0.33100 **0.0642**	-0.28603 **0.1125**	0.73911 **0.0001**	1.00000 0.0	-0.20698 0.2557	0.60338 **0.0003**	-0.26261 **0.1465**	-0.31336 **0.0807**	-0.39834 **0.0239**	0.22600 0.2136
R_IMPNGN	0.11968 0.5141	0.46954 **0.0067**	-0.17937 0.3260	-0.43445 **0.0130**	-0.20698 0.2557	1.00000 0.0	-0.13189 0.4718	0.02481 0.8928	0.28427 **0.1148**	0.34949 0.0499	-0.30873 **0.0856**
R_SDEAD	-0.13094 0.4750	-0.23183 0.2017	-0.22850 0.2084	0.46786 **0.0069**	0.60338 **0.0003**	-0.13189 0.4718	1.00000 0.0	-0.26524 **0.1423**	-0.18896 0.3003	-0.29584 **0.1002**	0.05046 0.7839
HOURSBEG	0.15061 0.4106	0.02253 0.9026	0.26608 **0.1410**	-0.15813 0.3874	-0.26261 **0.1465**	0.02481 0.8928	-0.26524 **0.1423**	1.00000 0.0	0.13127 0.4739	0.09300 0.6127	-0.39498 **0.0253**
CURR_ANG	0.35503 **0.0462**	0.39296 **0.0261**	0.01248 0.9459	-0.43236 **0.0135**	-0.31336 **0.0807**	0.28427 **0.1148**	-0.18896 0.3003	0.13127 0.4739	1.00000 0.0	0.82769 **0.0001**	-0.09467 0.6063
CR_ANGRD	0.26918 **0.1363**	0.43064 **0.0139**	-0.03018 0.8697	-0.50482 **0.0032**	-0.39834 **0.0239**	0.34949 **0.0499**	-0.29584 **0.1002**	0.09300 0.6127	0.82769 **0.0001**	1.00000 0.0	-0.31587 **0.0782**
CR_VELRD	-0.13837 0.4501	-0.26231 **0.1470**	0.00393 0.9830	0.29801 **0.0976**	0.22600 0.2136	-0.30873 **0.0856**	0.05046 0.7839	-0.39498 **0.0253**	-0.09467 0.6063	-0.31587 **0.0782**	1.00000 0.0

Note: Variables are defined on pages 29 and 30. For each block of numbers, the top number is the correlation coefficient and the second number is the probability of obtaining the test statistic (F-value) for the listed correlation coefficient if the null hypothesis (slope = 0.0) is true. Each correlation coefficient is based on 32 observations.

(1) The passage variables (no impingement or screen contact - R_IMPNEN and R_IMPNGN) were negatively correlated to the impingement variables (impingement or screen contact - R_IMPNGI, R_IMPNGD, R_IMPNES). The headfirst impingement without escape index (R_IMPNGH) was dropped from the analysis because too few non-zero observations occurred.

(2) Increasing current velocity increased the impingement indices and decreased the passage indices.

(3) Increasing water angle decreased the impingement indices and increased the passage indices.

(4) Current angle and velocity were inversely correlated because water velocity tended to increase near the top of the screen where the angle of the flow tended to more closely parallel the surface of the screen.

(5) The effects of changing current angle were more significant than the effects of changing water velocity over the range of values available for this analysis.

(6) The effects of beginning time (HOURBEG) appeared to have some effect on several behavioral variables and water velocity. Further inspection (detailed in a later section) indicated that changes in unitload (and hence corresponding changes in water velocity) were not random but appeared to decrease with time. Consequently, HOURBEG and UNITLOAD are confounded variables. The effects on impingement/passage variables attributed to HOURBEG are probably associated with decreases in UNITLOAD although it was unable to quantify the interaction.

(7) R_IMPNGI and R_IMPNGD were correlated ($r = 0.74$, $P = 0.0001$) suggesting that when observations were sparse R_IMPNGI (which has reduced data requirements) was a good surrogate for R_IMPNGD.

(8) The rate at which fish were imaged (R_PERMIN) appeared to be related to current angle; however, this relationship may be spurious since water angle increased significantly towards the top of the screen. Consequently, more fish should be seen at the top-most camera (at location 13 because camera 2 was not used in the correlation analysis) because most of the fishes intercepted by the screen would have to pass this camera.

(9) The current angle obtained from the hydraulic model studies was highly correlated (R=0.82769, P=0.0001) to the current angles obtained by observation through the video cameras suggesting that results from the hydraulic modeling could be applied to understand the impingement behavior of smolts to the prototype. However, the discrepancy between the two methods of determining values for the hydraulic variables needs to be reconciled in future studies. Hydraulic measurements were made with the cameras when available.

The results of correlation analysis of independent variables for the spring is found in Table 4. For the spring analysis, there were a number of highly significant correlation coefficients ($p < 0.01$) among the independent variables, but none of the correlation coefficients were greater than 0.42 (i.e., presence of the fyke net times gate setting - correlation coefficient of 0.42 means that 0.18 percent of the variance in one variable is explained by the other), and few were greater than 0.20 suggesting that generally, confounding effects were minimal, at least compared to the summer analysis. However, greater effort must be made in future video imaging studies to randomize the independent variables.

Table 4
Correlation Matrix for Independent Variables for Spring

Pearson Correlation Coefficients/Prob > |R| under Ho: Rho=0/N = 189

	UNITLOAD	FIKN_NET	HOURBEG	CAMLOC	GATSET	SCRN_PSN	SCRNANGL
UNITLOAD	1.00000 0.0	-0.02773 0.7048	-0.28486 **0.0001**	-0.02502 0.7325	0.03934 0.5909	0.13711 **0.0599**	0.05004 0.4941
FIKN_NET	-0.02773 0.7048	1.00000 0.0	0.79818 **0.142**	-0.03471 0.6354	-0.41942 **0.0001**	-0.22563 **0.0018**	-0.16079 **0.0271**
HOURBEG	-0.28486 **0.0001**	0.17818 **0.0142**	1.00000 0.0	0.00133 0.9855	-0.20798 **0.0041**	-0.06068 0.4068	-0.02079 0.7764
CAMLOC	-0.02502 0.7325	-0.03471 0.6354	0.00133 0.9855	1.00000 0.0	0.04666 0.5238	0.01672 0.8193	-0.09692 0.1846
GATSET	0.03934 0.5909	-0.41942 **0.0001**	-0.20798 **0.0041**	0.04666 0.5238	1.00000 0.0	-0.27038 **0.0002**	-0.19268 **0.0079**
SCRN_PSN	0.13711 **0.0599**	-0.22563 **0.0018**	-0.06068 0.4068	0.01672 0.8193	-0.27038 **0.0002**	1.00000 0.0	-0.10365 **0.1558**
SCRNANGL	0.05004 0.4941	-0.16079 **0.0271**	-0.02079 0.7764	-0.09692 **0.1846**	-0.19268 **0.0079**	-0.10365 **0.1558**	1.00000 0.0

Note: The non-numeric variables FIKN_NET (presence/absence of the fyke net), GATSET (closure gate setting), and SCRN_PSN (screen position) were converted to numeric variables by replacing alphameric configuration descriptions with 0, 1, or 2. For example, FIKN_NET has a value of 0 if the fyke net is absent and value of 1 if the fyke net is present.

Effects of local hydraulic conditions

a. *Data tabulation and analysis of variance.* Summaries of different impingement/entrainment variables by camera location, current angle, velocity, and beginning time are presented in Table 4 with associated statistics in Table 5 for the spring analysis. Note the pattern of increase in the R_IMPNGD and R_IMPNGI indices and decrease in R_IMPNES at camera location 31. The highest values of R_IMPNGD (Table 5) are associated with water approach angles nearly perpendicular (10 deg) to the screen surface (The ratio of impinged to observed is 0.25 contrasted to about 0.075 for the shallower approach angles). The effect of water velocity appears as a threshold effect. That is, a velocity of 2 fps results in decreases in impingement indices and increases in passage indices whereas no difference could be discerned between water velocities of 3 and 4 fps. However, velocity and angle are negatively correlated with increased flows near the top of the screen, where flow lines tend to be more parallel to the screen surface. There appear to be effects of beginning time on the values of some of the indices; however, beginning time and unitload are confounded, and it is not possible to separate the effects of these two variables. Note that two frequencies are reported in Table 5 and similar tables presented later. The first frequency, immediately following the CAMLOC variable represents the number of proportions that was based on a minimum of three smolts. The second frequency immediately following the R_IMPNES variable represents the number of all proportions (including those having 0, 1, or 2 smolts). The R_PERMIN variable is based on the second frequency to avoid biasing imaging rate by omitting those replicates when few or no smolts were observed.

ANOVA results generally follow the trends identified by direct inspection of the data. For the spring analysis, the R_IMPNGI and R_IMPNGD indices were significantly affected by local hydraulic conditions (six significant entries - Table 6). However, the passage indices were less affected by local hydraulic conditions as indicated by the reduced number of significant entries in Table 6 under the passage variables R_IMPNEN and R_IMPNGN (two significant entries).

b. *Regression analysis.* Multiple regression equations predicting the impingement behavior of smolts are presented in Table 7 for the spring period. In the spring, predictive equations having a R^2 of approximately 0.30 were found for the two impingement indices (R_IMPNGI and R_IMPGD). While these values are probably too low for use in design studies, they are high enough to suggest that more refined studies may be possible to develop equations having design value. Development of improved methods for assessing hydraulic variables using video imaging would probably lead to increased R^2 values.

Table 5
Proportions of Smolts Responding to Different Localized Hydraulic Conditions for Springtime Using Velocities and Angles Extrapolated from Physical Models

Summary Proportions by Camera Location

CAMLOC	FREQ	R_IMPNGH	R_IMPNGI	R_IMPNGD	R_IMPNGN	R_IMPNEN	R_IMPNES	FREQ	R_PERMIN
13	15	0	0.34035	0.06408	0.05507	0.38338	0.48380	20	0.07838
21	7	0	0.48308	0.11582	0.02041	0.13379	0.55006	8	0.07678
26	4	0	0.51786	0.10495	0.00000	0.06923	0.58498	5	0.03605
31	4	0	0.61905	0.37798	0.00000	0.13988	0.28571	7	0.03605
38	2	0	0.45833	0.16667	0.00000	0.25000	0.58333	5	0.03172

Summary Proportions by Angle

CR_ANGRD	FREQ	R_IMPNGH	R_IMPNGI	R_IMPNGD	R_IMPNGN	R_IMPNEN	R_IMPNES	FREQ	R_PERMIN
10	9	0	0.55159	0.25167	0.00000	0.14849	0.47957	15	0.04256
30	13	0	0.44074	0.08110	0.02060	0.19108	0.52341	15	0.08117
50	10	0	0.32572	0.07176	0.07010	0.42032	0.46365	15	0.06838

Summary Proportions by Velocity Categories

CR_VELRD	FREQ	R_IMPNGH	R_IMPNGI	R_IMPNGD	R_IMPNGN	R_IMPNEN	R_IMPNES	FREQ	R_PERMIN
2	8	0	0.30923	0.04596	0.08762	0.42749	0.48685	12	0.07642
3	19	0	0.48817	0.15277	0.00752	0.17057	0.79611	27	0.05515
4	5	0	0.44038	0.15333	0.02500	0.27258	0.48719	6	0.07924

Summary Proportions by Hourbegin

HOURBEG	FREQ	R_IMPNGH	R_IMPNGI	R_IMPNGD	R_IMPNGN	R_IMPNEN	R_IMPNES	FREQ	R_PERMIN
20	13	0	0.46068	0.79037	0.2828	0.24901	0.43199	15	0.06468
22	11	0	0.45254	0.11775	0.02435	0.21266	0.52749	14	0.06985
24	6	0	0.34737	0.08782	0.05556	0.37455	0.45643	12	0.05606
26	2	0	0.45000	0.00000	0.00000	0.10000	0.80000	4	0.06528

Note: Hydraulic variables had to be rounded to the nearest fps for velocity and to the nearest 20 deg for the angle of the flow to the screen to minimize the degrees of freedom of the analysis.

Screen type

Tables 8 through 11 summarize the effects of screen type on impingement/passage characteristics and hydraulic variables. Table 8 (top block) provides summaries by camera location for all screen types, unitloads, and beginning times combined. Results for camera locations 10 and 20 ft

Table 6
Summary of Probabilities (P ≤ 0.20 are in bold) From Analysis of Variance for Springtime for Effects of Localized Hydraulic Variables on Smolt Entrainment and Impingement Behavior

Combined Analysis							
SOURCE	R_PERMIN	R_IMPNEN	R_IMPNES	R_IMPNGI	R_IMPNGH	R_IMPNGN	R_IMPNGD
COMBINED	**0.1774**	**0.0873**	0.4292	**0.0557**	0	0.5461	**0.0428**
CR_ANGRD	**0.0233**	0.9358	0.3617	0.5667	0	0.9983	**0.0848**
CR_VELRD	**0.1021**	0.3566	0.9307	**0.1075**	0	0.2051	**0.0489**
HOURBEG	0.9925	**0.0823**	0.2416	0.2959	0	0.3308	0.8961
CAMLOC	**0.1046**	0.4689	0.2766	0.2078	0	0.9920	**0.0574**
UNITLOAD	**0.1810**	•	•	•	•	•	•
N	45	32	32	32	32	32	32

ENTRAINMENT SAMPLES - DURATION = 3,020 MIN : TOT_SEEN = 223 SMOLTS :
RATE_SEEN = 0.073841 SMOLTS/MIN

Note: Summaries at the bottom of the table provide sampling information including the number of replicates and smolts, the duration of sampling, and the imaging rate of smolts.

Table 7
Summary of Multiple Regression Analysis Using Backward Elimination of Spring Entrainment Impingement Variables Against Select Hydraulic Variables

Dependent Variable	R-square	DF reg/err/tot	Equation Prob > F	Independent Variables	Parameter Estimates	Individual Probabilities
R_PERMIN	0.253	3/28/31	0.0403	INTERCEP CR_ANGSQ CR_VELRD CAMLOC	0.3167416 -0.0000328 -0.0299295 -0.0055261	0.0037 0.0902 0.0909 0.0112
R_IMPNEN	0.211	1/31/31	0.0081	INTERCEP CR_ANGSQ	0.1106862 0.0001192	0.0918 0.0081
R_IMPNGI	0.3170	2/29/31	0.0040	INTERCEP CR_VELRD CAMLOC	-0.0016495 0.0785442 0.0103704	0.9907 0.0713 0.0041
R_IMPNGH	- ALL VALUES FOR R_IMPNGH ARE 0.0'S -					
R_IMPNGN	0.1779	2/29/31	0.0584	INTERCEP CR_VELRD CAMLOC	0.1957671 -0.0373547 -0.0028200	0.0088 0.0830 0.0986
R_IMPNGD	0.2889	3/28/31	0.0212	INTERCEP CR_ANGRD CR_ANGSQ CR_VELRD	0.1924616 -0.0247866 0.0003573 0.0939270	0.2459 0.0170 0.0390 0.0938

Table 8
Summary Proportions of Springtime Smolts Exhibiting Different Impingement Behaviors

Summary Proportions by Camloc - All Cameras Combined Except Camera Location 2

CAMLOC	FREQ	R_IMPNGH	R_IMPNGI	R_IMPNGD	R_IMPNGN	R_IMPNEN	R_IMPNES	FREQ	R_PERMIN	MN_CRANG	MN_CRAN9	MN_CR9CV	MN_CRCV
10	21	0	0.33904	0.03560	0.06519	0.35751	0.43401	24	0.087130	143.704	53.7037	45.5556	8.1481
20	13	0	0.43797	0.07143	0.16667	0.18694	0.51502	19	0.065622	110.000	26.3636	-11.3636	37.7273
30	6	0	0.53571	0.21084	0.00000	0.13941	0.46935	9	0.050539	101.538	11.5385	3.8462	7.6923
40	2	0	0.45833	0.16667	0.00000	0.25000	0.58333	5	0.031717	80.000	10.0000	2.8571	7.1429

Summary Proportions by Unitload - All Cameras Combined Except Camera Location 2

UNITLOAD	FREQ	R_IMPNGH	R_IMPNGI	R_IMPNGD	R_IMPNGN	R_IMPNEN	R_IMPNES	FREQ	R_PERMIN	MN_CRANG	MN_CRAN9	MN_CR9CV	MN_CRCV
12	10	0	0.41378	0.10626	0.13095	0.26759	0.43695	18	0.050842	116.818	31.3636	10.4545	20.9091
14	10	0	0.46664	0.12261	0.00667	0.18934	0.51870	12	0.084722	117.222	29.4444	-3.3333	32.7778
16	22	0	0.37001	0.04481	0.09816	0.30478	0.46526	27	0.074798	120.690	35.5172	30.3448	5.1724

Summary Proportions by Unitload - Camera Location 10 Only

12	5	0	0.36566	0.065385	0.061905	0.33407	0.40311	6	0.072559	145.000	55.0000	47.5000	7.5000
14	4	0	0.36421	0.063492	0.000000	0.33506	0.48795	5	0.091667	143.333	53.3333	38.3333	15.0000
15	12	0	0.31956	0.013889	0.088294	0.37477	0.42890	13	0.092110	143.077	53.0769	47.6923	5.3846

Summary Proportions by Unitload - Camera Location 20 Only

12	3	0	0.43651	0.095238	0.33333	0.18519	0.41799	6	0.045707	111.429	27.1429	-21.4286	48.5714
14	3	0	0.46667	0.044444	0.02222	0.11111	0.57778	3	0.108333	112.000	26.0000	-64.0000	90.0000
16	7	0	0.42630	0.072789	0.15714	0.22018	0.52971	10	0.064758	108.000	26.0000	22.0000	4.0000

Note: The top block (Summary Proportions by Camloc) provides proportions of springtime smolts exhibiting different impingement behaviors by camera location for all screen types, beginning times, and unitloads combined. The other blocks (Summary Proportions by Unitload) provide proportions of springtime smolts exhibiting different impingement behaviors by unitload separated out by camera location for screen type and beginning times combined. Camera location was rounded to the nearest 10 ft because camera locations were not consistent between the SSTS and ESBS and to minimize degrees of freedom in the analysis because of the relatively small numbers of smolts that were observed. A total of 69 measurements of the hydraulic variables was made.

Table 9
Proportions of Springtime Smolts Exhibiting Different Impingement Behaviors by Screen Type (SSTS and ESBS) and Camera Location for all Discharges and Beginning Times Combined

SCRN-TYPE	FREQ	R_IMPNGH	R_IMPNGI	R_IMPNGD	R_IMPNGN	R_IMPNEN	R_IMPNES	FREQ	R_PERMIN	MN_CRANG	MN_CRAN9	MN_CR9CV	MN_CRCV
All Cameras Combined Except Camera Location 2													
T	24	0	0.36033	0.03522	0.13934	0.31455	0.45298	32	0.066359	128.182	42.4242	35.1515	7.2727
X	18	0	0.46091	0.13496	0.01065	0.20696	0.49560	25	0.073115	109.722	23.6111	-3.0556	26.6667
Camera Location 10 Only													
T	16	0	0.32717	0.020677	0.065476	0.36633	0.42490	19	0.079785	144.211	54.2105	46.8421	7.3684
X	5	0	0.38072	0.070940	0.025000	0.30950	0.50824	5	0.115040	142.500	52.5000	42.5000	10.0000
Camera Location 20 Only													
T	8	0	0.37937	0.034799	0.200000	0.27607	0.52295	13	0.046737	106.429	26.4286	19.2857	7.1429
X	5	0	0.41865	0.079365	0.011110	0.22354	0.48280	6	0.106540	116.250	26.2500	-65.0000	91.2500

Note: Camera locations are rounded to the nearest 10 ft. The top block includes all camera locations for both screen types. T = standard-length submerged traveling screen and X = extended-length submerged bar screen.

Table 10
Proportions of Springtime Smolts Exhibiting Different Impingement Behaviors by Beginning Time for Both Screen Types and for All Discharges and Beginning Times Combined

HOURBEG	FREQ	R_IMPNGH	R_IMPNGI	R_IMPNGD	R_IMPNGN	R_IMPNEN	R_IMPNES	FREQ	R_PERMIN
All Cameras Combined Except Camera Location 2									
20	13	0	0.37064	0.03888	0.087912	0.29760	0.50162	16	0.066146
22	17	0	0.43713	0.12208	0.079902	0.24783	0.42937	20	0.075485
24	12	0	0.39125	0.05780	0.086210	0.26605	0.49766	19	0.069298
Camera Location 10 Only									
20	7	0	0.29095	0.00000	0.11565	0.41811	0.45196	7	0.090476
22	7	0	0.36261	0.09581	0.04167	0.37058	0.35567	8	0.080833
24	7	0	0.36357	0.01099	0.03827	0.28386	0.49440	9	0.090124
Camera Location 20 Only									
20	4	0	0.40972	0.00000	0.08333	0.18056	0.63056	6	0.040278
22	6	0	0.48413	0.12698	0.17778	0.15873	0.46032	6	0.103636
24	3	0	0.38333	0.05556	0.25556	0.25185	0.47037	7	0.054762

Note: The hydraulic variables are not included in this analysis as dependent variables because beginning time should have no effect on their values.

from the top of the screen are from both screen types. Camera locations 30 and 40 ft from the top of the screen are for the ESBS only (The ESBS is 40 ft long, and the SSTS is 20 ft long). Note that the two impingement variables nearly quadruple from the top of the screen to the bottom of the screen (e.g., R_IMPNGD increases from about 0.05 to about 0.19, P = 0.0482, Table 11). The increase is probably associated with the flow lines becoming nearly perpendicular to the screen surface at the lower end of the ESBS and because the ESBS appears to impinge more smolts than the SSTS. However, the increase in impingement on the lower screen is partially offset by the decreased imaging rate observed lower on the lower half of the ESBS. The rate at which smolts are imaged (R_PERMIN) drops by about one third from the top of the screen to the bottom of the screen (about 0.09 to nearly 0.03 smolts per min (P = 0.0015, Table 11)). Although the proportion of smolts impinged is greater on the lower part of the screen than on the upper part, fewer smolts are observed low on the screen.

The second block of Table 8 presents summaries by unitload for all camera locations combined, except camera location two, including the cameras at locations 30 and 40 on the ESBS. The rest of Table 8 presents summaries by unitload for the camera locations 10 ft and 20 ft from the top of the screen. No statistically significant effects of unitload were observed on any of the

Table 11
Summary of Probabilities (P ≤ 0.20 are in bold) from Analysis of Variance for Effects of Unitload, Screen Type, Beginning Time, and Camera Location on Entrainment and Hydraulic Variables

SOURCE	R_PERMIN	R_IMPNNEN	R_IMPNES	R_IMPNGI	R_IMPNGH	R_IMPNGN	R_IMPNGD	CURR_ANG	CUR_ANG9	CUR_ANCV	CURR_CV
Combined Analysis											
COMBINED	**0.0075**	0.3855	0.7683	**0.0969**	0.0000	0.3369	**0.0087**	**0.0087**	**0.0001**	**0.0033**	**0.0962**
SCRNTYPE	**0.0025**	0.8235	0.6343	0.8189[1]	0.0000	**0.1054**	0.6428[2]	0.4948	0.7668	**0.0407**	**0.0530**
UNITLOAD	**0.1390**	0.5625	0.6896	0.4950	0.0000	0.5197	0.4821	0.9029	0.9995	0.4709	0.4884
HOURBEG	0.7006	0.7900	0.2764	0.6431	0.0000	0.8397	0.2073	•	•	•	•
CAMLOC	**0.0015**	**0.1787**	0.5622	**0.586**	0.0000	0.3964	**0.0482**	**0.0001**	**0.0001**	**0.0102**	**0.0628**
N	57	42					69				
ENTRAINMENT SAMPLES - DURATION = 3,950 MINUTES : TOT_SEEN = 320 SMOLTS : RATE_SEEN = 0.081013 SMOLTS/MINUTE HYDRAULIC SAMPLES - DURATION = 5,558 MINUTES : MEASUREMENTS = 408											
Camera Location 10 Only											
COMBINED	**0.0911**	0.5827	0.3701	0.4631	0.0000	0.3530	0.2138	0.6178	0.6178	0.3363	0.4648
SCRNTYPE	**0.0911**	0.5827	0.3701	0.4631	0.0000	0.3530	0.2138	0.6178	0.6178	0.3363	0.4648
N	24	21					27				
ENTRAINMENT SAMPLES - DURATION = 1,900 MINUTES : TOT_SEEN = 176 SMOLTS : RATE_SEEN = 0.092632 HYDRAULIC SAMPLES - DURATION = 2,230 MINUTES : MEASUREMENTS = 194											
Camera Location 20 Only											
COMBINED	**0.0272**	0.7698	0.6614	0.7238	0.0000	**0.1653**	0.5234	0.6178	0.6789	**0.0523**	**0.0610**
SCRNTYPE	**0.0272**	0.7698	0.6614	0.7238	0.0000	**0.1653**	0.5234	0.6178	0.9789	**0.0523**	**0.0610**
N	19	13					22				
ENTRAINMENT SAMPLES - DURATION = 1,240 MINUTES : TOT_SEEN = 956 | RATE_SEEN = 0.076613 HYDRAULIC SAMPLES - DURATION = 1,774 MINUTES : MEASUREMENTS = 125											

[1] Type I SS P = 0.0215.
[2] Type I SS P = 0.0017.
Note: For each variable there were three classes of unitload (12, 14, and 16 kcfs), two screen types (SSTS and ESBS), three beginning (2000, 2200, and 2400 hr), and two camera locations (10 and 20 ft from the top of the screen).

passage/entrainment variables, although imaging rate generally increased with discharge (P = 0.1390, Table 11) a finding common to almost all tests.

Table 9 summarizes the effects of screen type on impingement behavior and hydraulic variables. The first block of Table 9 combines all camera locations except camera location 2. Note that the combined model is statistically significant for impingement index (P = 0.0969) and impingement rate (0.0087) with CAMLOC being the dominant variable in the analysis. Screen type apparently does not contribute to the significance of the combined model (P = 0.8189 and P = 0.6428) for probabilities based on Type III sum of squares. However, screen type is significant at P = 0.0215 for impingement index and P = 0.0017 for impingement rate for Type I sum of squares (Table 11). The passage variable R_IMPNGN (P = 0.10, Table 11) decreases on the ESBS relative to the SSTS (Table 9). The same pattern of increased impingement index and impingement rate also occurs for camera locations 10 and 20 on the ESBS although the differences are not statistically significant. Examination of the data indicates that the SSTS data set was characterized by low numbers of smolts (3 to 4) per replicate. Consequently, the SSTS data set was more variable than the ESBS data set which was characterized by more smolts. However, because the impingement variables increased on the bar screen and the passage variables decreased, it seems reasonable to conclude that the bar screen results in increased impingement of smolts even though the Type III Sum of Squares is inconclusive. The relative performance of the two screen types needs to be reevaluated in future studies.

No significant trends were observed between beginning time and any of the impingement/passage variables for the screen type analysis (Table 10).

Note the significant increase in variance (P = 0.0530, Table 11) of water angle (MN_CRCV) for the cameras 20 ft from the top of the screen even though the mean angle (MN_CRANG) ranges only from 108 deg to 111 deg suggesting that a flow instability probably sets up (i.e., the water angle changes as the flow lines sweep across the surface of the ESBS whereas for the SSTS the flow lines do not deviate significantly over time) at this location under some conditions. The cause of this instability is unclear but may be associated with the percent of the intake blocked by each screen type. The ESBS covers a larger portion of the intake which causes a headloss and a greater magnitude of flow separation at the toe of the screen. These two factors may result in a greater instability in flow conditions along the surface of the ESBS. Alternatively, the instability may be related to the unit in which the ESBS was tested. The ESBS and SSTS were tested in different units.

Fyke net

Tables 12 through 15 summarize the effects of the presence of the fyke net used to determine FGE on impingement/passage characteristics and hydraulic variables. This analysis was affected by relatively low numbers of observations, particularly for camera location 38. Low numbers of observations will

Table 12
Proportions of Springtime Smolts Exhibiting Different Impingement Behaviors by Camera Location and Unitload for Presence/Absence of the Fyke Net and Beginning Times Combined

Summary Proportions by Camloc

CAMLOC	FREQ	R_IMPNGH	R_IMPNGI	R_IMPNGD	R_IMPNGN	R_IMPNEN	R_IMPNES	FREQ	R_PERMIN	MN_CRANG	MN_CRAN9	MN_CR9CV	MN_CRCV
13	12	0	0.32550	0.03936	0.06883	0.38835	0.49229	14	0.10302	142.632	52.6316	-7.8947	60.5263
21	13	0	0.41255	0.06227	0.04176	0.22863	0.54976	16	0.08426	113.684	23.6842	-17.3684	41.0526
26	6	0	0.42857	0.06996	0.03333	0.21282	0.52610	10	0.05475	106.250	16.2500	7.5000	8.7500
31	6	0	0.49603	0.17421	0.05556	0.18214	0.34603	12	0.04978	94.444	4.4444	-6.1111	10.5556
38	3	0	0.41667	0.11111	0.00000	0.27778	0.50000	9	0.02830	80.769	9.2308	-4.6154	13.8462

Summary Proportions by Unitload - All Cameras Combined Except Camera Location 2

UNITLOAD	FREQ	R_IMPNGH	R_IMPNGI	R_IMPNGD	R_IMPNGN	R_IMPNEN	R_IMPNES	FREQ	R_PERMIN	MN_CRANG	MN_CRAN9	MN_CR9CV	MN_CRCV
12	9	0	0.39865	0.05855	0.09630	0.24891	0.54212	18	0.04759	110.714	23.5714	3.2143	20.3571
14	13	0	0.43075	0.08333	0.03077	0.22183	0.54460	20	0.07417	110.000	22.0000	-18.0000	40.0000
16	18	0	0.38218	0.08167	0.03531	0.31731	0.43490	23	0.08044	108.148	21.8519	-2.9630	24.8148

Summary Proportions by Unitload - Camera Location 2 Only

12	3	0	0.38889	0.00000	0.00000	0.22222	0.61111	5	0.06400	151.667	61.6667	55	6.6667
14	5	0	0.26833	0.04000	0.10667	0.50333	0.40333	5	0.13000	150.000	60.0000	42	18.0000
16	5	0	0.2959	0.10606	0.01667	0.51422	0.30373	5	0.18118	152.000	62.0000	56	6.0000

(Continued)

Note: The ESBS was in unit/bay 6A. For both presence and absence of the fyke net, the screen was deployed with no closure gate, had a screen angle of 55 deg, was in the standard position, and had a screen porosity of 30 percent. Two frequencies are reported. A total of 120 measurements were made of the hydraulic variables.

Table 12 (Concluded)

UNITLOAD	FREQ	R_IMPNGH	R_IMPNGI	R_IMPNGD	R_IMPNGN	R_IMPNEN	R_IMPNES	FREQ	R_PERMIN	MN_CRANG	MN_CRAN9	MN_CR9CV	MN_CRCV
Summary Proportions by Unitload - Camera Location 13 Only													
12	2	0	0.36058	0.03846	0.00000	0.31731	0.56731	3	0.07539	146.667	56.6667	50.0000	6.6667
14	5	0	0.41540	0.02778	0.08333	0.19697	0.74747	5	0.08167	140.000	50.0000	-37.1429	87.1429
16	6	0	0.25388	0.04739	0.08211	0.53962	0.29715	6	0.13436	141.667	51.6667	-31.6667	83.3333
Summary Proportions by Unitload - Camera Location 21 Only													
12	3	0	0.44444	0.00000	0.11111	0.07407	0.70370	5	0.05000	117.143	27.1429	-15.7143	42.8571
14	4	0	0.33214	0.03333	0.01667	0.36905	0.40952	5	0.09833	113.333	23.3333	-55.0000	78.3333
16	6	0	0.45020	0.11270	0.02381	0.21230	0.56627	6	0.10109	110.000	20.0000	18.3333	1.6667
Summary Proportions by Unitload - Camera Location 26 Only													
12	2	0	0.35000	0.10000	0.1	0.40000	0.40000	3	0.05296	106.000	16.0000	6.0000	10.0
14	3	0	0.43333	0.02564	0.0	0.15897	0.54744	4	0.07292	106.667	16.6667	11.6667	5.0
16	1	0	0.57143	0.14286	0.0	0.00000	0.71429	3	0.03232	106.000	16.0000	4.0000	12.0
Summary Proportions by Unitload - Camera Location 31 Only													
12	2	0	0.41667	0.12500	0.16667	0.29167	0.41667	4	0.03694	92.0000	2.00000	-8.0000	10.0000
14	1	0	0.64286	0.42857	0.00000	0.14286	0.14286	3	0.06944	95.7143	5.71429	-2.8571	8.5714
16	3	0	0.50000	0.12222	0.00000	0.12222	0.36667	5	0.04824	95.0000	5.00000	-8.3333	13.3333
Summary Proportions by Unitload - Camera Location 38 Only													
12	•	0	•	•	•	•	•	3	0.02407	•	•	•	•
14	1	0	0.66667	0.33333	0	0.00000	0.66667	3	0.02778	82.5000	7.50000	0.0000	7.50000
16	2	0	0.29167	0.00000	0	0.41667	0.41667	3	0.03306	82.0000	8.00000	-18.0000	26.0000

Table 13
Proportions of Smolts Exhibiting Different Impingement Behaviors by Presence/Absence of the Fyke Net for All Discharges and Beginning Times Combined

FYKE_NET	FREQ	R_IMPNGH	R_IMPNGI	R_IMPNGD	R_IMPNGN	R_IMPNEN	R_IMPNES	FREQ	R_PERMIN	MN_CRANG	MN_CRAN9	MN_CR9CV	MN_CRCV
Summary Proportions by Unitload - All Cameras Combined Except Camera Location 2													
FK	22	0	0.35320	0.02959	0.07775	0.32320	0.49392	36	0.06562	109.592	21.6327	-8.57143	30.2041
NF	18	0	0.46091	0.13496	0.01065	0.20696	0.49560	25	0.07312	109.722	23.6111	-3.05556	26.6667
Summary Proportions by Unitload - Camera Location 2 Only													
FK	10	0	0.33667	0.04652	0.02000	0.37317	0.39520	10	0.12559	151.000	61.0000	53.0000	8.0000
NF	5	0	0.32424	0.05303	0.08333	0.40455	0.48333	5	0.12400	151.667	61.6667	48.3333	13.3333
Summary Proportions by Unitload - Camera Location 13 Only													
FK	9	0	0.22249	0.01307	0.07789	0.56808	0.37403	9	0.09634	142.727	52.7273	-44.5455	97.2727
NF	5	0	0.38072	0.07094	0.02500	0.30950	0.50824	5	0.11504	142.500	52.5000	42.5000	10.0000
Summary Proportions by Unitload - Camera Location 21 Only													
FK	8	0	0.38765	0.04167	0.05952	0.26637	0.59375	10	0.07090	111.818	21.8182	17.2727	4.5455
NF	5	0	0.45238	0.09524	0.01333	0.16825	0.47937	6	0.10654	116.250	26.2500	-65.0000	91.2500
Summary Proportions by Unitload - Camera Location 26 Only													
FK	3	0	0.33333	0.00000	0.06667	0.33333	0.38333	7	0.04571	105.455	15.4545	6.3636	9.09091
NF	3	0	0.52381	0.13993	0.00000	0.09231	0.66886	3	0.07584	108.00	18.0000	10.0000	8.00000
Summary Proportions by Unitload - Camera Location 31 Only													
FK	3	0	0.44444	0.06667	0.11111	0.17778	0.42222	6	0.06167	92.0	2.0	-11	13.0
NF	3	0	0.54762	0.28175	0.00000	0.18651	0.26984	6	0.03789	97.5	7.5	0	7.5
Summary Proportions by Unitload - Camera Location 38 Only													
FK	1	0	0.33333	0.00000	0	0.33333	0.33333	6	0.059359	81.6667	8.3333	-13.3333	21.6667
NF	2	0	0.45833	0.16667	0	0.25000	0.58333	7	0.060671	80.0000	10.0000	2.857	7.1429

Note: The ESBS was in unit/bay 6A, the screen was deployed with no closure gate, had a screen angle of 55 deg, was in the standard position, and had a screen porosity of 30 percent. Abbreviations for impingement variables and hydraulic variables have been previously identified in the text.

Table 14
Proportions of Springtime Smolts Exhibiting Different Impingement Behaviors by Beginning Time for Presence/Absence of the Fyke Net and All Discharges Combined

HOURBEG	FREQ	R_IMPNGH	R_IMPNGI	R_IMPNGD	R_IMPNGN	R_IMPNEN	R_IMPNES	FREQ	R_PERMIN
All Cameras Combined Except Camera Location 2									
20	10	0	0.39240	0.11565	0.05105	0.33085	0.41445	13	0.07949
22	15	0	0.44065	0.09312	0.07056	0.21183	0.52630	21	0.06832
24	11	0	0.37314	0.04790	0.03030	0.29153	0.53121	19	0.06491
26	4	0	0.35714	0.00000	0.00000	0.28571	0.47619	8	0.06111
Camera Location 2 Only									
20	2	0	0.31061	0.09091	0.04167	0.46970	0.31061	2	0.13461
22	5	0	0.34924	0.05303	0.01667	0.35455	0.46667	6	0.10111
24	5	0	0.24410	0.01667	0.09000	0.52846	0.40282	5	0.17667
26	1	0	0.40000	0.20000	0.00000	0.40000	0.40000	2	0.05833
Camera Location 13 Only									
20	3	0	0.18895	0.03922	0.12255	0.66132	0.26025	3	0.14551
22	4	0	0.41493	0.6944	0.03125	0.22958	0.59028	5	0.08448
24	3	0	0.25031	0.02564	0.11111	0.52503	0.39805	4	0.08611
26	2	0	0.46429	0.00000	0.00000	0.07143	0.78571	2	0.11944
Camera Location 21 Only									
20	3	0	0.46032	0.11111	0.04762	0.19048	0.53175	4	0.06683
22	5	0	0.48571	0.09524	0.08000	0.12381	0.59048	6	0.09960
24	4	0	0.38839	0.00000	0.00000	0.19544	0.64980	5	0.08333
26	1	0	0.00000	0.00000	0.00000	1.00000	0.00000	1	0.66667
Camera Location 26 Only									
20	1	0	0.50000	0.07692	0.0	0.7692	0.69231	2	0.6250
22	2	0	0.38571	0.07143	0.1	0.30000	0.45714	3	0.05566
24	3	0	0.43333	0.06667	0.0	0.20000	0.51667	4	0.05556
26	0	0	•	•	•	•	•	1	0.03333
Camera Location 31 Only									
20	2	0	0.57143	0.31429	0.00000	0.17143	0.37143	2	0.07083
22	2	0	0.41667	0.08333	0.16667	0.25000	0.25000	5	0.03224
24	1	0	0.50000	0.25000	0.00000	0.25000	0.50000	3	0.06484
26	1	0	0.50000	0.00000	0.00000	0.00000	0.33333	2	0.05000
Camera Location 38 Only									
20	1	0	0.33333	0.00000	0	0.33333	0.33333	2	0.03141
22	2	0	0.45833	0.16667	0	0.25000	0.58333	2	0.04318

Note: The hydraulic variables are not included in this analysis because beginning time should have no effect on their values.

Table 15
Summary of Probabilities from Analysis of Variance (P ≤ 0.20 are in bold) for Effects of Presence/Absence of the Fyke Net, Unitload, Beginning Time, and Camera Location on Entrainment and Hydraulic Variables

SOURCE	R_PERMIN	R_IMPNNEN	R_IMPNES	R_IMPNGI	R_IMPNGH	R_IMPNGN	R_IMPNGD	CURR_ANG	CUR_ANG9	CUR_ANCV	CURR_CV
All Cameras Combined Except Camera Location 2											
COMBINED	**0.0262**	0.7605	0.8991	0.4410	0	**0.1253**	**0.0752**	**0.0001**	**0.0001**	0.9787	0.6433
FYKE_NET	**0.2012**	0.3897	0.8547	**0.1543**	0	**0.0045**	**0.0176**	**0.1308**	**0.0522**	0.7508	0.8516
UNITLOAD	**0.1685**	0.7063	0.5511	0.6848	0	0.3348	0.8153	0.2907	0.6375	0.6571	0.6812
HOURBEG	0.9850	0.8055	0.8810	0.8862	0	**0.0780**	0.6172	--	--	--	--
CAMLOC	**0.0051**	0.5183	0.7603	0.3130	0	0.6547	0.2098	**0.0001**	**0.0001**	0.9493	0.3635
N	61	40					85				
ENTRAINMENT SAMPLES - DURATION = 3,075 MIN : TOT_SEEN = 268 SMOLTS : RATE_SEEN = 0.0871 SMOLTS/MIN HYDRAULIC SAMPLES - DURATION = 5,583 MIN : MEASUREMENTS = 423											
Camera Location 2 Only											
FYKE_NET	0.9647	0.8027	0.6073	0.6540	0	**0.1120**	0.7788	0.7192	0.7192	0.3963	0.2620
N	15	13					16				
ENTRAINMENT SAMPLES - DURATION = 889 MIN : TOT_SEEN = 124 SMOLTS : RATE_SEEN = 0.13948 HYDRAULIC SAMPLES - DURATION = 1,069 MIN : MEASUREMENTS = 134											
Camera Location 13 Only											
FYKE_NET	0.6370	0.4716	0.8801	0.3339	0	0.2862	**0.1372**				
N	13	12					19	0.9536	0.9536	0.2634	0.2424
ENTRAINMENT SAMPLES - DURATION = 890 MIN : TOT_SEEN = 100 | RATE_SEEN = 0.11236 HYDRAULIC SAMPLES - DURATION = 1,235 MIN : MEASUREMENTS = 125											

(Continued)

Note: For each variable there were three classes of unitload (12, 14, and 16 kcfs), two fyke net conditions (presence and absence), four beginning times (2000, 2200, 2400, and 2600 hr), and five camera locations (13, 21, 26, 31, and 38 ft from the top of the screen). Probabilities based on Type III sum of squares to reduce confounding effects of other variables. The analysis tests the hypothesis that the means of the different entrainment/impingement and hydraulic variables are not different by the treatment variables. Probabilities less than 0.20 are in bold print.

Table 15 (Concluded)

SOURCE	R_PERMIN	R_IMPNNEN	R_IMPNES	R_IMPNGI	R_IMPNGH	R_IMPNGN	R_IMPNGD	CURR_ANG	CUR_ANG9	CUR_ANCV	CURR_CV
Camera Location 21 Only											
FYKE_NET	0.2423	0.5739	0.4543	0.5241	0	0.4282	0.4059	**0.1695**	**0.1695**	**0.0901**	**0.0892**
N	16	13					19				
ENTRAINMENT SAMPLES - DURATION = 965 MIN | TOT_SEEN = 91 | RATE_SEEN = 0.09430 HYDRAULIC SAMPLES - DURATION = 1,249 MIN : MEASUREMENTS = 112											
Camera Location 26 Only											
FYKE_NET	**0.1887**	0.2642	**0.2008**	**0.1054**	0.0000	0.3739	**0.0170**	0.3630	0.3630	0.5191	0.8116
N	10	6					16				
ENTRAINMENT SAMPLES - DURATION = 1,675 MIN | TOT_SEEN = 467 | RATE_SEEN=0.27881 HYDRAULIC SAMPLES - DURATION = 1,135 MIN : MEASUREMENTS = 75											
Camera Location 31 Only											
FYKE_NET	0.2438	0.9360	0.3543	0.2313	0.0000	0.3739	**0.0028**	**0.0567**	**0.0567**	**0.200**	**0.1119**
N	12	6					18				
ENTRAINMENT SAMPLES - DURATION = 1,318 MIN | TOT_SEEN=451 | RATE_SEEN=0.34219 HYDRAULIC SAMPLING - DURATION = 1,135 : MEASUREMENTS = 68											
Camera Location 38 Only											
FYKE_NET	0.4322	0.8790	0.3333	0.7877	0.0000	0.0000	0.6667	0.5669	0.5569	0.289	0.2808
N	9	3					13				
ENTRAINMENT SAMPLES - DURATION = 2,079 : TOT_SEEN = 322 : RATE_SEEN = 0.15488 HYDRAULIC SAMPLES - DURATION = 829 MIN : MEASUREMENTS = 43											

influence those variables that are most data intensive (e.g., impingement index, R_IMPNGD).

Table 12 (top block) provides summaries by camera location for the presence of the fyke net, unitloads, and beginning times combined. Significant relationships between camera location, imaging rate, (R_PERMIN, P = 0.0050 Table 15) and water angle (CURR_ANG, P = 0.0001, Table 15) were observed. Significantly more smolts were observed near the top of the screen (0.10 smolts/min) than at the bottom (0.03 smolts/min). Note that mean water angle at location 38 was past vertical (i.e., the flow lines were moving towards the bottom of the screen). No other effects of camera location were noted.

The second block of Table 12 presents summaries by unitload for all camera locations combined except camera location two. Note the increase in imaging rate (R_PERMIN) as unitload increases (P = 0.1685) - a finding common to many of the analyses. No other significant effects of unitload were observed. The rest of Table 12 presents summaries by unitload for the different camera locations on the ESBS.

Table 13 summarizes the effects of the presence of the fyke net. For the combined analysis (all camera locations combined except location 2) note the significant increase in the impingement variables when the fyke net is not present (R_IMPNGD P = 0.0176, R_IMPNGI P = 0.1543) suggesting that the presence of the fyke net significantly alters the impingement characteristics of bypass screens. The change in the impingement index is completely accounted for by the impingement rate variable (impingement index includes impingement rate). Impingement rate on the screen increases by nearly a factor of 5 when the fyke net is absent. While the effect of the fyke net on R_IMPNGD may be exaggerated because of low numbers, it is difficult to ignore this large a difference between treatments. Consistent with an increase in impingement variables associated with the fyke net is a concurrent decrease in passage variables R_IMPNGN (P = 0.0045) and R_IMPNEN (P = 0.3897). However, like the impingement variables, these two variables are also affected by low numbers, particularly for camera location 38. This finding suggests that screen evaluations using fyke nets must be interpreted with caution because the fyke net significantly alters impingement characteristics of the screens evaluated.

Evaluating impingement variables at specific locations on the screen indicates that the absence of the fyke net results in an increase in these variables at every camera location except camera location 2. Of 10 possible ANOVAs for the impingement variables (5 camera locations by 2 variables) 4 are significant at 0.20. The consistency of the results across different camera locations (even though not all are significant at $\alpha = 0.200$) lends further support to the premise that the presence of the fyke systematically reduces the impingement rate on the screen surface.

The pattern in impingement behavior probably arises from two effects of the fyke net. First, the fyke net should reduce screen velocities by about 11 to 12 percent based on physical modeling studies because flow through a bay containing a fyke net is 88 to 89 percent of the flow without the fyke net. While the presence of the fyke net appears to affect the angle of flow through the screen (CURR_ANG, P = 0.1308 and CUR_ANG9, P = 0.0522), the detailed hydraulic effects are unclear. It seems that flow with the fyke net in place tends to be more parallel to the screen in the middle cameras. However, the variance is also high suggesting the presence of some flow instabilities. Note also that the imaging rate (R_PERMIN) increases from about 0.065 to 0.073 (P = 0.20) when the fyke net is removed. The increase in R_PERMIN is consistent with the functional increase in unitload thought to occur when the fyke net is removed. That is, when the fyke net is removed, the increased velocity forces smolts closer to the screen where they are more likely to be imaged.

A significant trend between beginning time and the R_IMPNGN (P = 0.0780) was observed. However, this relationship may be spurious or exaggerated because it was not mirrored by the other passage index or the impingement variables (Table 14).

Screen angle

Tables 16 through 19 summarize the effects of screen angle on impingement/passage characteristics and hydraulic variables. This analysis also was affected by relatively low numbers of observations, particularly for camera locations 31 and 38 which will influence those variables that are most data intensive (e.g., impingement index, R_IMPNGD). Table 16 (top block) provides summaries by camera location for screen angles, unitloads, and beginning times combined. Note a general increase in impingement rate (R_IMPNGD P = 0.1174 towards the bottom of the screen but a peak in impingement rate (R_IMPNGI P = 0.1894, Table 19) towards the middle cameras. The imaging rate decreases towards the bottom cameras (R_PERMIN P = 0.0177, Table 19). Note that the proportion of smolts entrained (R_IMPNEN) has a quadratic relationship to camera location, i.e., that R_IMPNEN is highest at the top and bottom of the screen and lowest in the middle of the screen, a distribution similar to the impingement index variable (R_IMPNGI). Significant relationships between camera location and water angle (CURR_ANG, P = 0.0001, Table 19) and variance in water angle (CURR_CV, P = 0.1842, Table 19) were observed. In general, CURR_ANG becomes more parallel to the screen towards the top of the screen and variance in CURR_ANG (CURR_CV) seems to peak at camera location 21. The peak in CURR_CV suggests the presence of a flow instability at camera location 21 that may account for the drop in the passage index. No other effects of camera location were noted. The proportions for different impingement behaviors for camera location 38 (Table 16) are provided for completeness; however, the number of smolts observed is too low for cause-and-effect evaluation.

Table 16
Proportions of Springtime Smolts Exhibiting Different Impingement Behaviors by Camera Location and Unitload for Screen Angle and Beginning Times Combined

Summary Proportions by Camloc

CAMLOC	FREQ	R_IMPNGH	R_IMPNGI	R_IMPNGD	R_IMPNGN	R_IMPNEN	R_IMPNES	FREQ	R_PERMIN	MN_CRANG	MN_CRAN9	MN_CR9CV	MN_CRCV
13	6	0	0.43393	0.15912	0.020833	0.29125	0.45686	7	0.093319	141.667	51.6667	42.5000	9.1667
21	7	0	0.48920	0.11446	0.009524	0.12018	0.54598	8	0.093447	117.273	27.2727	-40.9091	68.1818
26	4	0	0.51786	0.10495	0.000000	0.06923	0.58498	5	0.057778	111.250	21.2500	8.7500	12.5000
31	4	0	0.61905	0.37798	0.000000	0.13988	0.28571	7	0.030646	100.909	10.9091	1.8182	9.0909
38	2	0	0.45833	0.16667	0.000000	0.25000	0.58333	5	0.031717	80.000	10.0000	2.8571	7.1429

All Cameras Combined Except Camera Location 2

UNITLOAD	FREQ	R_IMPNGH	R_IMPNGI	R_IMPNGD	R_IMPNGN	R_IMPNEN	R_IMPNES	FREQ	R_PERMIN	MN_CRANG	MN_CRAN9	MN_CR9CV	MN_CRCV
12	4	0	0.41987	0.13173	0.000000	0.26421	0.48226	9	0.053704	111.875	25.6250	0.0000	25.6250
14	7	0	0.50540	0.15475	0.009524	0.14395	0.55596	10	0.082273	115.294	26.4706	-7.6471	34.1176
16	12	0	0.52292	0.20089	0.010417	0.15506	0.44931	13	0.061119	112.500	26.2500	18.7500	7.5000

Camera Location 2 Only

14	2	0	0.27803	0.00000	0.16667	0.45833	0.45833	2	0.025000	156.667	66.6667	56.6667	10.0000
16	5	0	0.21631	0.00000	0.15655	0.66937	0.16071	2	0.133333	163.333	63.3333	50.0000	13.3333

(Continued)

Note: The ESBS was in unit/bay 6A. For both screen angles (55 and 62 deg) the screen was deployed with no closure gate, no fyke net, in the standard position, and had a screen porosity of 30 percent. A total of 120 measurements were made of the hydraulic variables. Beginning times were rounded to the nearest 2 hr.

Table 16 (Concluded)

UNITLOAD	FREQ	R_IMPNGH	R_IMPNGI	R_IMPNGD	R_IMPNGN	R_IMPNEN	R_IMPNES	FREQ	R_PERMIN	MN_CRANG	MN_CRAN9	MN_CR9CV	MN_CRCV
Camera Location 13 Only													
12	1	0	0.34615	0.07692	0.000000	0.38462	0.38462	1	0.144000	142.5	52.5	45.0	7.5
14	2	0	0.41414	0.05556	0.000000	0.22727	0.66162	3	0.092677	142.5	52.5	35.0	17.5
16	3	0	0.47639	0.25556	0.041667	0.30278	0.34444	3	0.076919	140.0	50.0	47.5	2.5
Camera Location 21 Only													
12	1	0	0.33333	0.00000	0.000000	0.22222	0.44444	2	0.066667	120.0	30	-63.3333	93.333
14	2	0	0.45000	0.06667	0.033333	0.16667	0.53333	2	0.137500	117.5	27.5	-85.0000	112.500
16	4	0	0.54777	0.16696	0.000000	0.07143	0.57768	4	0.084811	115.0	25.0	20.0000	5.0000
Camera Location 26 Only													
12	1	0	0.50000	0.20000		0.20000	0.60000	1	0.055556	115	25	15.0000	10.0000
14	1	0	0.50000	0.07692		0.07692	0.69231	2	0.072349	110	20	13.3333	6.6667
16	2	0	0.53571	0.07143		0.00000	0.52381	2	0.044318	110	20	0.0000	20.0000
Camera Location 31 Only													
12	1	0	0.50000	0.25000		0.25000	0.50000	2	0.038889	97.5	7.5	-5.0000	12.5000
14	1	0	0.64286	0.42857		0.14286	0.14286	2	0.037500	105.0	15.0	7.5000	7.5000
16	2	0	0.66667	0.41667		0.08333	0.25000	3	0.33182	100.0	10.0	3.3333	6.6667
Camera Location 38 Only													
12	0							3	0.024074	80	10	0	10
14	1	0	0.66667	0.33333	0	0.0	0.66667	1	0.050000	85	5	0	5
16	1	0	0.25000	0.00000	0	0.5	0.50000	1	0.036364	75	15	10	5

Table 17
Proportions of Smolts Exhibiting Different Impingement Behaviors by Screen Angle for All Discharges and Beginning Times Combined

SCRNANGL	FREQ	R_IMPNGH	R_IMPNGI	R_IMPNGD	R_IMPNGN	R_IMPNEN	R_IMPNES	FREQ	R_PERMIN	MN_CRANG	MN_CRAN9	MN_CR9CV	MN_CRCV
All Cameras Combined Except Camera Location 2													
55	18	0	0.46091	0.13496	0.010648	0.20696	0.49560	25	0.031717	108.722	23.6111	-3.0556	26.6667
62	5	0	0.63917	0.31833	0.000000	0.04000	0.45833	7	0.038961	123.077	33.0769	21.5385	11.5385
Summary Proportions by Unitload - Camera Location 2 Only													
55	5	0	0.32424	0.053030	0.08333	0.40455	0.48333	5	0.124000	1551.667	61.6667	48.3333	13.3333
62	3	0	0.26190	0.047619	0.18095	0.52381	0.38095	3	0.038889	155.000	65.0000	57.5000	7.5000
Summary Proportions by Unitload - Camera Location 13 Only													
55	5	0	0.38072	0.07094	0.025	0.30950	0.50824	5	0.115040	142.5	52.5	42.5	10.0
62	2	0	0.72500	0.55000	0.000	0.10000	0.35000	2	0.039015	140.0	50.0	42.5	7.5
Summary Proportions by Unitload - Camera Location 21 Only													
55	5	0	0.45238	0.09524	0.013333	0.16825	0.47937	6	0.106540	116.25	26.25	-65.0000	91.25
62	2	0	0.58125	0.16250	0.000000	0.00000	0.71250	2	0.054167	120.00	30.0	23.3333	6.6667
Summary Proportions by Unitload - Camera Location 26 Only													
55	3	0	0.52381	0.13993		0.092308	0.66886	3	0.075842	108.000	18.0000	10.0000	8
62	1	0	0.50000	0.0000		0.000000	0.33333	2	0.030682	116.667	26.6667	6.6667	20
Summary Proportions by Unitload - Camera Location 31 Only													
55	3	0	0.54762	0.28175		0.18651	0.26984	6	0.0378872	97.5	7.5	0.00000	7.5000
62	1	0	0.83333	0.66667		0.00000	0.33333	1	0.0250000	110.0	20.0	6.66667	13.3333
Summary Proportions by Unitload - Camera Location 38 Only													
55	2	0	0.45833	0.16667		0.25000	0.58333	5	0.0317172	80	10	2.85714	7.1429
62	0	•	•	•	•	•	•	•	0	•	•	•	•

Note: The ESBS was in unit/bay 6A, had no fyke net, the screen was deployed with no closure gate, was in the standard position, and had a screen porosity of 30 percent.

Table 18
Proportions of Springtime Smolts Exhibiting Different Impingement Behaviors by Beginning Time for Screen Angles and All Discharges Combined

HOURBEG	FREQ	R_IMPNGH	R_IMPNGI	R_IMPNGD	R_IMPNGN	R_IMPNEN	R_IMPNES	FREQ	R_PERMIN
All Cameras Combined Except Camera Location 2									
20	9	0	0.56794	0.23302	0.000000	0.09715	0.48211	11	0.048485
22	10	0	0.47014	0.13968	0.019167	0.19940	0.49444	12	0.088434
24	4	0	0.41987	0.13173	0.000000	0.26421	0.48226	7	0.062771
Camera Location 2 Only									
20	3	0	0.15079	0.04762	0.20873	0.74603	0.10317	3	0.0666667
22	2	0	0.28977	0.13258	0.04167	0.55303	0.25000	2	0.1600000
24	1	0	0.37500	0.00000	0.25000	0.25000	0.75000	2	0.0916667
Camera Location 13 Only									
20	2	0	0.48636	0.30000	0.000000	0.32727	0.37273	2	0.0666667
22	3	0	0.42824	0.09259	0.041667	0.23611	0.53704	3	0.1130303
24	1	0	0.34615	0.07692	0.000000	0.38462	0.38462	2	0.0904040
Camera Location 21 Only									
20	3	0	0.55417	0.10833	0.000000	0.00000	0.69722	4	0.0416667
22	3	0	0.47619	0.15873	0.022222	0.20635	0.42857	3	0.1603030
24	1	0	0.33333	0.00000	0.000000	0.22222	0.44444	1	0.1000000
Camera Location 26 Only									
20	2	0	0.50000	0.03846		0.03846	0.51282	2	0.0666667
22	1	0	0.57143	0.14286		0.00000	0.71429	1	0.0636364
24	1	0	0.50000	0.20000		0.20000	0.60000	2	0.0459596
Camera Location 31 Only									
20	2	0	0.73810	0.54762		0.07143	0.23810	2	0.0416667
22	1	0	0.50000	0.16667		0.16667	0.16667	3	0.0304040
24	1	0	0.50000	0.25000		0.25000	0.50000	1	0.0444444
26	0	•		•	•	•	•	1	0.0333333
Camera Location 38 Only									
20	0	•		•	•	•	•	1	0.0166667
22	2	0	0.45833	0.16667		0.25000	0.58333	2	0.0431818
24	0	•		•	•	•	•	1	0.0222222
26	0	•		•	•	•	•	1	0.0333333

Note: The hydraulic variables are not included in this analysis because beginning time should have no effect on their values.

Table 19
Summary of Probabilities from Analysis of Variance ($P \leq 0.20$ are in bold) for Effects of Screen Angle, Unitload, Beginning Time, and Camera Location on Entrainment and Hydraulic Variables

SOURCE	R_PERMIN	R_IMPNNEN	R_IMPNES	R_IMPNGI	R_IMPNGH	R_IMPNGN	R_IMPNGD	CURR_ANG	CUR_ANG9	CUR_ANCV	CURR_CV
All Cameras Combined Except Camera Location 2											
COMBINED	**0.0386**	**0.1255**	0.4687	**0.0882**	0.0000	0.8606	**0.1561**	**0.0001**	**0.0001**	**0.1502**	0.3487
SCRNANGL	0.5666	**0.0527**	0.7007	**0.0197**	0.0000	0.8323	**0.0689**	**0.0092**	**0.0174**	0.4034	0.5679
UNITLOAD	0.4647	**0.1097**	0.3168	**0.1210**	0.0000	0.7697	0.3897	**0.1252**	0.6168	0.5716	0.5454
HOURBEG	0.4729	0.2450	0.7452	0.2061	0.0000	0.3396	0.4156	•	•	•	•
CAMLOC	**0.0177**	**0.1453**	0.2387	**0.1894**	0.0000	0.7893	**0.1174**	**0.0001**	**0.0001**	**0.0767**	**0.1842**
N	32	23	23	23	23	23	23	49	49	49	49
ENTRAINMENT SAMPLES - DURATION = 2,370 MIN : TOT_SEEN = 177 SMOLTS : RATE_SEEN = 0.0747 SMOLTS/MIN HYDRAULIC SAMPLES - DURATION = 3,898 MIN : MEASUREMENTS = 265											
Camera Location 2 Only											
SCRANGL	**0.0729**	0.3325	0.3309	0.4063	0.0000	0.2073	0.9508	0.3122	0.3122	0.2306	0.3304
N	8	6	6	6	6	6	6	10	10	10	10
ENTRAINMENT SAMPLES - DURATION = 594 MIN : TOT_SEEN = 62 SMOLTS : RATE_SEEN = 0.10438 HYDRAULIC SAMPLES - DURATION = 829 MIN : MEASUREMENTS = 74											
Camera Location 13 Only											
SCRNANGL	**0.0277**	0.6052	**0.1796**	**0.0586**	0.7040	0.7040	**0.0026**	0.3166	0.3166	1.0000	0.6718
N	7	6	6	6	6	6	6	12	12	12	12
ENTRAINMENT SAMPLES - DURATION = 600 MIN : TOT_SEEN = 58 | RATE_SEEN = 0.096667 HYDRAULIC SAMPLES - DURATION = 985 MIN : MEASUREMENTS = 76											

(Continued)

Note: For each variable there were three classes of unitload (12, 14, and 16 kcfs), 2 screen angles (55 and 62 deg), 4 beginning times (2000, 2200, 2400, and 2,600 hr), and 5 camera locations (13, 21, 26, 31, and 38 ft from the top of the screen). Probabilities are based on Type III sum of squares to reduce confounding effects of other variables. The analysis tests the hypothesis that the means of the different entrainment/impingement and hydraulic variables are not different by the treatment variables. Probabilities less than 0.20 are highlighted to enhance comparability to other tables and to identify trends.

Table 19 (Concluded)

SOURCE	R_PERMIN	R_IMPNNEN	R_IMPNES	R_IMPNGI	R_IMPNGH	R_IMPNGN	R_IMPNGD	CURR_ANG	CUR_ANG9	CUR_ANCV	CURR_CV
Camera Location 21 Only											
SCRNANGL	0.4288	0.2154	**0.1190**	**0.1546**	0.0000	0.5761	0.3848	0.5102	0.5102	0.3597	0.4024
N	8	7	7	7	7	7	7	11	11	11	11
ENTRAINMENT SAMPLES - DURATION = 720 MIN | TOT_SEEN = 64 | RATE_SEEN = 0.088889 HYDRAULIC SAMPLES - DURATION = 889 MIN : MEASUREMENTS = 79											
Camera Location 26 Only											
SCRNANBL	**0.1278**	0.5512	**0.0409**	0.6667	0.0000	0.0000	0.0000	**0.0533**	**0.0533**	0.8221	0.3358
N	5	4	4	4	4	4	4	8	8	8	8
ENTRAINMENT SAMPLES - DURATION = 440 MIN | TOT_SEEN = 28 | RATE_SEEN = 0.063636 HYDRAULIC SAMPLES - DURATION = 715 MIN : MEASUREMENTS = 46											
Camera Location 31 Only											
SCRNANGL	0.5254	**0.1029**	0.8089	**0.0955**	0.000	0.000	**0.1304**	**0.0159**	**0.0159**	0.4602	0.3893
N	7	4	4	4	4	4	4	11	11	11	11
ENTRAINMENT SAMPLES - DURATION = 440 MIN | TOT_SEEN = 20 | RATE_SEEN = 0.045455 HYDRAULIC SAMPLING - DURATION = 835 : MEASUREMENTS = 42											
Camera Location 38 Only											
SCRNANGL	•	•	•	•	•	•	•	•	•	•	•
N	5	2	2	2	2	2	2	7	7	7	7
ENTRAINMENT SAMPLES - DURATION = 170 : TOT_SEEN = 7 : RATE_SEEN = 0.041176 HYDRAULIC SAMPLES - DURATION = 474 MIN : MEASUREMENTS = 22											

The second block of Table 16 presents summaries by unitload for all camera locations combined except camera location two. Note the increase in impingement variables (R_IMPNGI, P = 0.1210 and R_IMPNGD, P = 0.3897, Table 19) as unitload increases and a concomitant decrease in the entrainment index (R_IMPNEN, P = 0.1097, Table 19). Current angle appears to be affected by unitload (CURR_ANG, P = 0.1252, Table 19); however, the difference in means (about 3 deg) is less than the ability to measure angles (about 5 deg). The rest of Table 16 presents summaries by unitload for the different camera locations on the ESBS.

Table 17 summarizes the effects of screen angle. For the combined analysis, note the significant increase in the impingement variables (R_IMPNGD, P = 0.0689 and R_IMPNGI, P = 0.0197, Table 19) and decrease in one of the passage variables (R_IMPNEN, P=0.0527, Table 19) at the flatter screen angles (e.g., the average water angle for the 55 deg angle is about 13 deg more towards perpendicular than the 62 deg angle). An average impingement proportion of 0.31833 for the 62 deg deployment angle is extremely high. It means that about 3 out of every 10 smolts observed were impinged on the screen. This result was unexpected and initially counterintuitive because increasing the angle of approach of the flow increased impingement. Opposite effects probably occur because of a major difference in current angle that occurs nearer the bottom of the screen where fewer smolts are observed (e.g., water angle at screen locations 26 and 31 are 117 and 110 for the 62 deg screen angle and 108 and 98 for the 55 deg screen angle). There is relatively little difference in water angle at camera locations 2, 13, and 21. Consequently, the hydraulic conditions at the upper half of the screen are unchanged and may even exhibit an increase in water velocity because changing the screen angle from 55 to 62 percent opens the throat area of the screen slot making it more efficent for passing flow. The increase in flow at the top of the screen is as evidenced by current angle differences of about 10 deg at the bottom of the screen. These relationships suggest that the upper portion of the screen (near the gate slot) can pass a maximum flow through the gate slots at which the water plug phenomenon familiar to ichthyoplankton samplers occurs. Changing the screen angle will not significantly alter the hydraulic conditions in the upper half of the screen unless the passage of water up the slot or through the upper portions of the screen is increased. This explanation is supported by increasing values of the impingement variables at camera location 13 (R_IMPNGD, P = 0.0026 and R_IMPNGI, P = 0.0586) and camera location 21 ((R_IMPNGD, P = 0.3848 and R_IMPNGI, P = 0.1546) and decreasing values at location 31 (R_IMPNGD, P = 0.01304 and R_IMPNGI, P = 0.0955). Consequently, altering screen angle is a trade-off between improving passage conditions lower on the screen and worsening passage conditions higher on the screen. Since fish lower on the screen must eventually pass through the upper part of the screen, the net effect of increasing screen angle is probably detrimental.

Table 18 presents data summarized by the beginning time. No significant effects of beginning time were observed.

Screen position

Tables 20 through 23 summarize the effects of screen position on impingement/passage characteristics and hydraulic variables. This analysis also was affected by relatively low numbers of observations for all camera locations. Small sample size will particularly influence those variables that are more data intensive (e.g., impingement index, R_IMPNGD). Table 20 (top block) provides summaries by camera location for screen positions, unitloads, and beginning times, combined. Note the general increase in the impingement variables (R_IMPNGD P = 0.0572 and R_IMPNGI P = 0.0421, Table 23) towards the bottom cameras and a decrease in imaging rate towards the bottom cameras (R_PERMIN P = 0.0813, Table 23). The passage variable, R_IMPNEN (P = 0.0485, Table 23) exhibited the same quadratic pattern seen in the screen angle analysis, and to a lesser extent, the fyke net analysis. Passage was highest at the top and bottom of the screen and lowest in the middle of the screen. The reasons for the quadratic response of R_IMPNEN are unknown but may be related to the flow at the bottom camera going past perpendicular to the screen under some conditions. Thus, smolts at the bottom of the screen are entrained, do not touch the screen, but are carried under the toe of the screen and into the turbine. Significant relationships between camera location and water angle (CURR_ANG, P = 0.0001, Table 23) were observed. As is the case in all analyses of camera location, there is a general trend for water angle to become increasingly parallel towards the top of the screen. At the bottom of the screen, water angles go past perpendicular and flow towards the bottom of the screen.

The second block of Table 20 presents summaries by unitload for all camera locations combined except camera location two. Unitload affects R_IMPNGI (P = 0.1076, Table 23) and imaging rate (P = 0.1230, Table 23), but the pattern is not consistent. These patterns are discounted because supporting patterns in correlated impingement variables are not observed.

The rest of Table 20 presents summaries by unitload for the different camera locations on the ESBS. No consistent effects of location-specific unitloads are noted.

Table 21 summarizes the effects of screen position. The effect of screen position on imaging rate was significant at P = 0.20 at most camera locations. However, screen position and unitload were weakly correlated (R = 0.13711, P = 0.0599, Table 4) suggesting that part of this effect was due to unitload. Lowered screen position significantly increased variance in current angle (P = 0.0269, Table 23) at camera location 38, suggesting that flow instabilities are possible at this location. An increase in variance in current angle was also observed at camera location 31 (P = 0.2244, Table 23).

The large and statistically significant difference in imaging rate between the screen positions and a lack of effect of beginning time (Table 23) suggest that

Table 20
Proportions of Springtime Smolts Exhibiting Different Impingement Behaviors by Camera Location and Unitload for Screen Position and Beginning Times Combined

Summary Proportions by Camloc

CAMLOC	FREQ	R_IMPNGH	R_IMPNGI	R_IMPNGD	R_IMPNGN	R_IMPNEN	R_IMPNES	FREQ	R_PERMIN	MN_CRANG	MN_CRAN9	MN_CR9CV	MN_CRCV
13	7	0	0.35528	0.05067	0.017857	0.34012	0.51184	9	0.077800	141.538	51.5385	43.0769	8.462
21	6	0	0.46032	0.07937	0.011111	0.14021	0.56614	10	0.073369	117.692	27.6923	-30.7692	58.462
26	5	0	0.54762	0.15062	0.000000	0.05538	0.63465	6	0.057365	109.000	19.0000	9.0000	10.000
31	5	0	0.52857	0.25905	0.000000	0.20190	0.34190	10	0.036899	98.462	8.4615	-91.5385	100.000
38	2	0	0.45833	0.16667	0.000000	0.25000	0.58333	6	0.027820	79.091	10.9091	-0.9091	11.818

Summary Proportions by Unitload
(All Cameras Combined Except Camera Location 2)

UNITLOAD	FREQ	R_IMPNGH	R_IMPNGI	R_IMPNGD	R_IMPNGN	R_IMPNEN	R_IMPNES	FREQ	R_PERMIN	MN_CRANG	MN_CRAN9	MN_CR9CV	MN_CRCV
12	4	0	0.41987	0.13173	0.000000	0.26421	0.48226	13	0.043590	108.889	24.4444	1.6667	22.7778
14	9	0	0.52272	0.17962	0.007407	0.13418	0.55093	12	0.077778	111.667	23.8889	-10.0000	33.8889
16	12	0	0.43021	0.08909	0.010417	0.22867	0.51181	16	0.050874	110.000	24.1667	-33.3333	57.5000

Camera Location 2 Only

12	3	•	•	•	•	•	•	2	0.25000	153.333	63.3333	53.3333	10.0000
14	2	0	0.27083	0.00000	0.16667	0.45833	0.45833	3	0.10000	150.000	60.0000	43.3333	16.6667
16	3	0	0.23022	0.08838	0.02778	0.62795	0.20370	3	0.131667	153.333	63.3333	46.6667	16.6667

(Continued)

Note: The ESBS was in unit/bay 6A. For both screen positions (standard and lowered 24 in.), the 55 deg screen angle was deployed with no closure gate, had no fyke net, was in the standard position, and had a screen porosity of 30 percent. A total of 41 measurements were made of the hydraulic variables.

Table 20 (Concluded)

UNITLOAD	FREQ	R_IMPNGH	R_IMPNGI	R_IMPNGD	R_IMPNGN	R_IMPNEN	R_IMPNES	FREQ	R_PERMIN	MN_CRANG	MN_CRAN9	MN_CR9CV	MN_CRCV
Camera Location 13 Only													
12	1	0	0.34615	0.07692	0.000000	0.38462	0.38462	2	0.080556	142.5	52.5	45.0000	7.5
14	2	0	0.41414	0.05556	0.000000	0.22727	0.66162	3	0.086111	142.5	52.5	35.0000	17.5
16	4	0	0.32812	0.04167	0.03125	0.38542	0.46875	4	0.070189	140.0	50.0	47.0000	2.0
Camera Location 21 Only													
12	1	0	0.33333	0.00000	0.000000	0.22222	0.44444	3	0.050000	120.0	30.0	-42.5	72.5
14	2	0	0.45000	0.06667	0.033333	0.16667	0.53333	3	0.102778	117.5	27.5	-85.0	112.5
16	3	0	0.50952	0.11429	0.000000	0.09524	0.62857	4	0.068838	116.0	26.0	22.0	4.0
Camera Location 26 Only													
12	1	0	0.50000	0.20000	0	0.20000	0.60000	2	0.044444	110.000	20.0000	10.0	10.0000
14	2	0	0.58333	0.20513	0	0.03846	0.67949	2	0.079167	106.667	16.6667	0	16.6667
16	2	0	0.53571	0.07143	0	0.00000	0.60714	2	0.048485	110.000	20.0000	14.0	6.0000
Camera Location 31 Only													
12	1	0	0.50000	0.25000	0	0.25000	0.50000	3	0.031482	95	5	-2.5	7.5
14	2	0	0.57143	0.31429	0	0.17143	0.27143	3	0.052779	100	10	5.0	5.0
16	2	0	0.50000	0.20833	0	0.20833	0.33333	4	0.29053	100	10	-240.0	250.0
Camera Location 38 Only													
12	•	•	•	•	•	•	•	3	0.024074	77.5000	12.5000	2.5	10.0000
14	1	0	0.66667	0.33333	0	0.0	0.66667	1	0.050000	83.3333	6.6667	0.0	6.6667
16	1	0	0.25000	0.00000	0	0.5	0.50000	2	0.022349	77.5000	12.5000	-5.0	17.5000

Table 21
Proportions of Smolts Exhibiting Different Impingement Behaviors by Screen Angle for All Discharges and Beginning Times Combined

SCRNANGL	FREQ	R_IMPNGH	R_IMPNGI	R_IMPNGD	R_IMPNGN	R_IMPNEN	R_IMPNES	FREQ	R_PERMIN	MN_CRANG	MN_CRAN9	MN_CR9CV	MN_CRCV
All Cameras Combined Except Camera Location 2													
L24	7	0	0.46429	0.11190	0.000000	0.18333	0.58690	16	0.030382	110.833	25.0000	-35.0000	60.0000
STD	18	0	0.46091	0.13496	0.010648	0.20696	0.49560	25	0.073115	109.722	23.6111	-3.0556	26.6667
Summary Proportions by Unitload - Camera Location 2 Only													
L24	3	0	0.37037	0.000000	0.000000	0.25926	0.37037	3	0.041667	153.333	63.3333	46.6667	16.6667
STD	5	0	0.32424	0.053030	0.083333	0.40455	0.48333	5	0.124000	151.667	61.6667	48.3333	13.3333
Summary Proportions by Unitload - Camera Location 13 Only													
L24	4	0	0.27083	0.000000	0.000	0.45833	0.26042	4	0.031250	140.0	50.0	44.0	6.0000
STD	5	0	0.38072	0.070940	0.025	0.30950	0.50824	5	0.115040	142.5	52.5	42.5	10.0000
Summary Proportions by Unitload - Camera Location 21 Only													
L24	1	0	0.50000	0.000000	0.000000	0.00000	1.00000	4	0.0236111	120.00	30.00	24	6.00
STD	5	0	0.45238	0.095238	0.013333	0.16825	0.47937	6	0.1065404	116.25	26.25	-65	91.25
Summary Proportions by Unitload - Camera Location 26 Only													
L24	2	0	0.58333	0.16667	0	0.000000	0.583333	3	0.0388889	110	20	8	12
STD	3	0	0.52381	0.13993	0	0.092305	0.66886	3	0.0758418	108	18	10	8
Summary Proportions by Unitload - Camera Location 31 Only													
L24	2	0	0.50000	0.22500	0	0.22500	0.45000	4	0.0654167	100.0	10.0	-238	248.0
STD	3	0	0.54762	0.28175	0	0.18651	0.26984	6	0.0378872	97.5	7.5	0	7.5
Summary Proportions by Unitload - Camera Location 38 Only													
L24	•	•	•	•	•	•	•	1	0.0083333	77.5	12.5	-7.50000	20.0000
STD	2	0	0.45833	0.16667	0	0.25	0.58333	5	0.0317172	80.0	10.0	2.85714	7.1429

Note: The ESBS was in unit/bay 6A and had no fyke net. The screen was deployed with no closure gate, was in the standard position, and had a screen porosity of 30 percent.

Table 22
Proportions of Springtime Smolts Exhibiting Different Impingement Behaviors by Beginning Time for Screen Positions and All Discharges Combined

HOURBEG	FREQ	R_IMPNGH	R_IMPNGI	R_IMPNGD	R_IMPNGN	R_IMPNEN	R_IMPNES	FREQ	R_PERMIN
All Cameras Combined Except Camera Location 2									
20	9	0	0.44432	0.08394	0.000000	0.19530	0.56544	13	0.041667
22	10	0	0.47014	0.13968	0.019167	0.19940	0.49444	13	0.082486
24	6	0	0.47436	0.17671	0.000000	0.20947	0.49929	13	0.048718
Camera Location 2 Only									
20	2	0	0.13889	0.00000	0.04167	0.72222	0.13889	2	0.087500
22	2	0	0.28977	0.13258	0.04167	0.55303	0.25000	2	0.160000
24	1	0	0.37500	0.00000	0.25000	0.25000	0.75000	3	0.072200
Camera Location 13 Only									
20	3	0	0.28535	0.00000	0.000000	0.42929	0.52904	3	0.061111
22	3	0	0.42824	0.09259	0.041667	0.23611	0.53704	3	0.113030
24	1	0	0.34615	0.07692	0.000000	0.38462	0.38462	3	0.059259
Camera Location 21 Only									
20	2	0	0.50000	0.00000	0.000000	0.00000	0.83333	3	0.030556
22	3	0	0.47619	0.15873	0.022222	0.20635	0.42857	4	0.123005
24	1	0	0.33333	0.00000	0.000000	0.22222	0.44444	3	0.050000
Camera Location 26 Only									
20	2	0	0.50000	0.03846	0	0.03846	0.59615	2	0.0708333
22	1	0	0.57143	0.14286	0	0.00000	0.71429	1	0.0636364
24	2	0	0.58333	0.26667	0	0.10000	0.63333	3	0.4262963
Camera Location 31 Only									
20	2	0	0.57143	0.33929	0	0.19643	0.32143	3	0.0333333
22	1	0	0.50000	0.16667	0	0.16667	0.16667	3	0.0304040
24	2	0	0.50000	0.22500	0	0.22500	0.45000	3	0.0481481
Camera Location 38 Only									
22	2	0	0.45833	0.16667	0	0.25	0.58333	2	0.0431818

Note: The hydraulic variables are not included in this analysis because beginning time should have no effect on their values.

Table 23
Summary of Probabilities from Analysis of Variance (P ≤ 0.20 are in bold) for Effects of Screen Position, Unitload, Beginning Time, and Camera Location on Entrainment and Hydraulic Variables

SOURCE	R_PERMIN	R_IMPNNEN	R_IMPNES	R_IMPNGI	R_IMPNGH	R_IMPNGN	R_IMPNGD	CURR_ANG	CUR_ANG9	CUR_ANCV	CURR_CV
All Cameras Combined Except Camera Location 2											
COMBINED	**0.0192**	**0.1673**	0.3907	**0.0900**	0.0000	0.8872	**0.0946**	**0.0001**	**0.0001**	0.6025	0.8149
SCRN-POS	**0.0032**	0.2595	0.2144	0.3099	0.0000	0.8652	0.6444	0.5305	0.3637	0.5641	0.5488
UNITLOAD	**0.1230**	0.2378	0.5781	**0.1076**	0.0000	0.9341	0.2270	0.4347	0.8919	0.8634	0.8746
HOURBEG	0.4978	0.4791	0.6902	0.2978	0.00000	0.5256	0.2686	•	•	•	•
CAMLOC	**0.0813**	**0.0485**	**0.1859**	**0.0421**	0.00000	0.7822	**0.572**	**0.0001**	**0.0001**	0.3298	0.5833
N	41	25	25	25	25	25	25	60	60	60	60
ENTRAINMENT SAMPLES - DURATION = 2,490 MIN : TOT_SEEN = 184 SMOLTS : RATE_SEEN = 0.073896 SMOLTS/MIN HYDRAULIC SAMPLES - DURATION = 5,028 MIN : MEASUREMENTS = 299											
Camera Location 2 Only											
COMBINED	**0.0867**	0.8205	0.5636	0.4128	0.0000	0.4397	0.5421	0.6263	0.6263	0.7980	0.6263
SCRN_POS	**0.0867**	0.8205	0.5636	0.4128	0.0000	0.4397	0.5421	0.6263	0.6263	0.7980	0.6263
N	8	5	5	5	5	5	5	9	9	9	9
ENTRAINMENT SAMPLES - DURATION = 474 MIN : TOT_SEEN = 59 SMOLTS : RATE_SEEN = 0.12447 HYDRAULIC SAMPLES - DURATION = 714 MIN : MEASUREMENTS = 71											
Camera Location 13 Only											
COMBINED	**0.0031**	0.4803	0.9367	0.3480	0.0000	0.5761	0.2465	0.2600	0.2600	0.7424	0.4591
SCRN_POS	**0.0031**	0.4803	0.9367	0.3480	0.0000	0.5761	0.2465	0.2600	0.2600	0.7424	0.4591
N	9	77	7	7	7	7	7	13	13	13	13
ENTRAINMENT SAMPLES - DURATION = 720 MIN : TOT_SEEN = 64 | RATE_SEEN = 0.088889 HYDRAULIC SAMPLES - DURATION = 1,110 MIN : MEASUREMENTS = 82											

(Continued)

Note: For each variable there were 3 classes of unitload (12, 14, and 16 kcfs), 2 screen positions (standard and lowered 24 in.), 4 beginning times (2000, 2200, 2400, and 2600 hr), and 5 camera locations (13, 21, 26, 31, and 38 ft from the top of the screen).

Table 23 (Concluded)

SOURCE	R_PERMIN	R_IMPNNEN	R_IMPNES	R_IMPNGI	R_IMPNGH	R_IMPNGN	R_IMPNGD	CURR_ANG	CUR_ANG9	CUR_ANCV	CURR_CV
Camera Location 21 Only											
COMBINED	**0.0857**	0.3876	**0.0366**	0.6917	0.0000	0.7040	0.3916	0.4533	0.4533	0.2286	0.2696
SCRN_POS	**0.0857**	0.3876	**0.0366**	0.6917	0.0000	0.7040	0.3916	0.4533	0.4533	0.2286	0.2696
N	10	6	6	6	6	6	6	13	13	13	13
ENTRAINMENT SAMPLES - DURATION = 600 MIN | TOT_SEEN = 55 | RATE_SEEN = 0.091667 HYDRAULIC SAMPLES - DURATION = 1,044 MIN : MEASUREMENTS = 79											
Camera Location 26 Only											
COMBINED	**0.0999**	0.3071	0.3467	0.4535	0.0000	0.0000	0.8529	0.3466	0.3466	0.7494	0.4714
SCRN_POS	**0.0999**	0.3071	0.3467	0.4535	0.0000	0.0000	0.8529	0.3466	0.3466	0.7494	0.4714
N	6	5	5	5	5	5	5	10	10	10	10
ENTRAINMENT SAMPLES - DURATION = 500 MIN | TOT_SEEN = 32 | RATE_SEEN = 0.064 HYDRAULIC SAMPLES - DURATION = 960 MIN : MEASUREMENTS = 50											
Camera Location 31 Only											
COMBINED	0.8811	0.4631	0.3250	0.4950	0.0000	0.0000	0.6150	0.6462	0.6462	0.2201	0.2244
SCRN_POS	0.8811	0.4631	0.3250	0.4950	0.0000	0.0000	0.6150	0.6462	0.6462	0.2201	0.2244
N	10	5	5	5	5	5	5	13	13	13	13
ENTRAINMENT SAMPLES - DURATION = 500 MIN | TOT_SEEN = 26 | RATE_SEEN = 0.052 HYDRAULIC SAMPLING - DURATION = 1,080 : MEASUREMENTS = 54											
Camera Location 38 Only											
COMBINED	**0.1757**	•	•	•	•	•	•	0.4889	0.4889	**0.1171**	**0.0269**
SCRN_POS	**0.1757**	•	•	•	•	•	•	0.4889	0.4889	**0.1171**	**0.0269**
N	6	2	2	2	2	2	2	11	11	11	11
ENTRAINMENT SAMPLES - DURATION = 170 : TOT_SEEN = 7 : RATE_SEEN = 0.041176 HYDRAULIC SAMPLES - DURATION = 834 MIN : MEASUREMENTS = 34											

smolts are pressed closer to the screen under the normal screen position where they are more likely to be imaged. Thus, it is suspected that substantial proportions of smolts are moving up the gate slot but out of range of the imaging field of the cameras on the top of the screen. Note that the imaging rate towards the bottom of the screen is approximately the same for the two screen positions (R_PERMIN is approximately 0.04 smolts per min - Table 21) but that the imaging rate at the screen top for the lowered screen position is substantially less (R_PERMIN is approximately 3 to 4 times lower at camera location 21 and higher on the screen). If beginning time was affecting the results because screen elevation and beginning time were confounded, then beginning time should occur as a statistically significant variable.

Table 22 summarizes the effects of starting time on dependent variables. No statistically significant effects were noted for the combined analysis. However, imaging rate appeared to peak at 2200 hr for the cameras near the top to middle of the screen, but peaked later or earlier for the bottom cameras. However, imaging rate was low, and observations were limited; therefore, it is unknown if this effect is valid.

Spring closure gate position and unitload

Tables 24 through 27 summarize the effects of gate position and unitload on impingement/passage characteristics and hydraulic variables. This analysis was also affected by relatively low numbers of observations, particularly for camera locations 31 and 38 which will influence those variables that are most data intensive (e.g., impingement index, R_IMPNGD).

Table 24 (top block) provides summaries by camera location for closure gate position, unitload, and beginning times combined. Relatively few statistically significant relationships were observed between camera location and the impingement/passage variables. As is usually observed, more smolts are observed with cameras high on the screens than those low on the screen ($P = 0.0223$, Table 27). The quadratic relationship between entrainment rate (R_IMPNEN, $P = 0.1951$, Table 27) and camera location observed for several other treatments was observed. Camera location had no other consistent or significant effect on the passage/impingement variables. As expected, the values for hydraulic variables were heavily influenced by camera location (e.g., CURR_ANG $P = 0.0001$, Table 27). Notably, the variance in water angle was substantially higher at camera location 21 than at the other camera locations. The cause for this increase is unknown although it suggests the presence of a flow instability near this point.

Table 24
Proportions of Springtime Smolts Exhibiting Different Impingement Behaviors by Camera Location and Unitload for Closure Gate Position and Beginning Times Combined

Summary Proportions by Camloc

CAMLOC	FREQ	R_IMPNGH	R_IMPNGI	R_IMPNGD	R_IMPNGN	R_IMPNEN	R_IMPNES	FREQ	R_PERMIN	MN_CRANG	MN_CRAN9	MN_CR9CV	MN_CRCV
13	11	0	0.40126	0.00964	0.081494	0.2971	0.46234	17	0.070204	141.429	51.4286	42.8571	8.5714
21	12	0	0.45813	0.09933	0.028170	0.1738	0.52734	20	0.071647	119.091	29.0909	-13.6364	42.7273
26	10	0	0.48804	0.09555	0.14286	0.11948	0.58447	15	0.047428	108.500	18.5000	11.0000	7.5000
31	7	0	0.49592	0.14116	0.000000	0.14932	0.37143	16	0.046798	98.636	8.6364	-2.7273	11.3636
38	4	0	0.48958	0.1667	0.000000	0.18750	0.50000	13	0.024748	75.556	14.4444	7.2222	7.2222

All Cameras Combined Except Camera Location 2

UNITLOAD	FREQ	R_IMPNGH	R_IMPNGI	R_IMPNGD	R_IMPNGN	R_IMPNEN	R_IMPNES	FREQ	R_PERMIN	MN_CRANG	MN_CRAN9	MN_CR9CV	MN_CRCV
12	9	0	0.47550	0.14585	0.015873	0.18251	0.55349	25	0.041167	109.118	24.4118	7.0588	17.3529
14	17	0	0.47063	0.10014	0.060738	0.15888	0.50495	26	0.070808	112.941	25.2941	1.7647	23.5294
16	18	0	0.44119	0.10463	0.011218	0.22225	0.46071	30	0.051271	106.857	24.2857	6.8571	7.4286

Camera Location 2 Only

12	2	0	0.14286	0.07143	0.23810	0.78571	0.14286	4	0.040217	156.697	66.6667	60.0000	6.6667
14	4	0	0.16667	0.00000	0.1667	0.66667	0.29167	5	0.071884	151.667	61.6667	50.0000	11.6667
16	4	0	0.15878	0.06629	0.17639	0.74874	0.15278	5	0.089000	157.143	67.1429	52.8571	14.2857

(Continued)

Note: The ESBS was in unit/bay 6A. A sufficient number of observations was available to treat unitload and closure simultaneously. For all unitloads and closure gate positions, the screen angle was 55 deg, had no fyke net, was in the standard position, and had a screen porosity of 30 percent. A total of 95 measurements of the hydraulic variables were made.

Table 24 (Concluded)

UNITLOAD	FREQ	R_IMPNGH	R_IMPNGI	R_IMPNGD	R_IMPNGN	R_IMPNEN	R_IMPNES	FREQ	R_PERMIN	MN_CRANG	MN_CRAN9	MN_CR9CV	MN_CRCV
Camera Location 13 Only													
12	2	0	0.38736	0.03846	0.00000	0.26374	0.54945	4	0.065676	141.667	51.6667	46.6667	5.0000
14	4	0	0.38564	0.06349	0.19286	0.29221	0.53081	6	0.077778	141.250	51.2500	36.2500	15.0000
16	5	0	0.41932	0.15303	0.02500	0.31439	0.37273	7	0.066299	141.429	51.4286	47.1429	4.2857
Camera Location 21 Only													
12	3	0	0.47778	0.16667	0.000000	0.17407	0.48227	7	0.049760	125.000	35.0000	-15.0000	50.0000
14	4	0	0.47153	0.05417	0.065278	0.11111	0.59306	6	0.084058	117.143	27.1429	-41.4286	68.5714
16	5	0	0.43563	0.09507	0.015385	0.22381	0.51481	7	0.082895	114.286	24.2857	15.7143	8.5714
Camera Location 26 Only													
12	3	0	0.52381	0.16190	0.047619	0.11429	0.61270	5	0.039588	106.667	16.6667	8.3333	8.3333
14	4	0	0.46562	0.08173	0.000000	0.15048	0.47933	5	0.063333	108.571	18.5714	11.4286	7.1429
16	3	0	0.48214	0.04762	0.000000	0.08333	0.69643	5	0.039394	110.000	20.0000	12.8571	7.1429
Camera Location 31 Only													
12	1	0	0.50000	0.25000	0	0.25000	0.50000	4	0.028140	97.143	7.1429	-1.42857	8.5714
14	4	0	0.51071	0.14286	0	0.12143	0.37619	6	0.076944	101.250	11.2500	-1.25000	12.5000
16	2	0	0.46429	0.08333	0	0.15476	0.29762	6	0.029091	97.143	7.1429	-5.71429	12.8571
Camera Location 38 Only													
12	.	.	.	.	.	.	.	.	.	77.1429	12.8571	5.7143	7.1429
14	1	0	0.66667	0.33333	0	0.00	0.66667	3	0.030556	80.0000	10.0000	-2.5000	12.5000
16	3	0	0.43056	0.11111	0	0.25	0.44444	5	0.024452	71.4286	18.5714	14.2857	4.2857

Table 25
Proportions of Springtime Smolts Exhibiting Different Impingement Behaviors by Closure Gate for All Discharges, Camera Locations, and Beginning Times Combined

GATESET	FREQ	R_IMPNGH	R_IMPNGI	R_IMPNGD	R_IMPNGN	R_IMPNEN	R_IMPNES	FREQ	R_PERMIN	MN_CRANG	MN_CRAN9	MN_CR9CV	MN_CRCV
Summary Proportions by Closure Gate - All Cameras Combined Except Camera Location 2													
NG	18	0	0.46091	0.13496	0.010648	0.20696	0.49560	25	0.073115	109.722	23.6111	-3.0556	26.6667
NO	2	0	0.37500	0.00000	0.000000	0.25000	0.50000	5	0.021667	108.000	26.0000	14.0000	12.0000
PR	24	0	0.46563	0.10288	0.019402	0.17162	0.49740	51	0.048473	109.677	25.1613	15.0000	10.1613
Camera Location 2 Only													
NG	5	0	0.32424	0.05303	0.08333	0.40455	0.48333	5	0.124000	151.667	61.6667	48.3333	13.3333
NO	1	0	0.50000	0.00000	0.00000	0.00000	1.00000	1	0.008333	160.000	70.0000	40.0000	30.0000
PR	8	0	0.12078	0.01786	0.24147	0.77629	0.20585	8	0.042120	156.667	66.6667	58.3333	8.3333
Camera Location 13 Only													
NG	5	0	0.38072	0.07094	0.025000	0.30950	0.50824	5	0.115040	142.5	52.5	42.5	10.0000
NO	1	0	0.37500	0.00000	0.000000	0.25000	0.50000	1	0.033333	150.0	60.0	50.0	10.0000
PR	11	0	0.33048	0.06740	0.070130	0.40643	0.41314	11	0.053175	140.0	50.0	42.5	7.5000

(Continued)

Note: The ESBS was in unit/bay 6A and had no fyke net. The screen was deployed with no closure gate, was in the standard position, and had a screen porosity of 30 percent. NG = No gate; NO = Normal strange position; PR = Partial gate position.

Table 25 (Concluded)

UNITLOAD	FREQ	R_IMPNGH	R_IMPNGI	R_IMPNGD	R_IMPNGN	R_IMPNEN	R_IMPNES	FREQ	R_PERMIN	MN_CRANG	MN_CRAN9	MN_CR9CV	MN_CRCV
Camera Location 21 Only													
NG	5	0	0.45238	0.09524	0.013333	0.16825	0.47937	6	0.106540	116.250	26.2500	-65.0000	91.2500
NO	.	.	.	.	.	.	.	1	0.016667	110.000	20.0000	10.0000	10.0000
PR	7	0	0.46224	0.10226	0.038767	0.17778	0.56160	13	0.059771	121.538	31.5385	16.1538	15.3846
Camera Location 26 Only													
NG	3	0	0.52381	0.13993	0.000000	0.09231	0.66886	3	0.075842	108.000	18.0000	10.0000	8.0000
NO	.		.	.	.	.	.	1	0.016667	110.000	20.0000	10.0000	10.0000
PR	7	0	0.47270	0.07653	0.020408	0.13112	0.54830	11	0.042476	108.571	18.5714	11.4286	7.1426
Camera Location 31 Only													
NG	3	0	0.54762	0.28175	0	0.18651	0.26984	6	0.037887	97.500	7.5000	0.0000	7.5000
NO	.	.	.	.	.	.	.	1	0.008333	100.000	10.0000	-20.0000	30.0000
PR	4	0	0.45714	0.03571	0	0.12143	0.44762	9	0.057013	99.231	9.2308	-3.0769	12.3077
Camera Location 38 Only													
NG	2	0	0.45833	0.16667	0	0.25	0.58333	5	0.031717	80.000	10.0000	2.8571	7.14286
NO	1	0	0.37500	0.00000	0	0.25	0.50000	1	0.033333	70.000	20.0000	20.0000	0.00000
PR	1	0	0.66667	0.33333	0	0.00	0.33333	7	0.018543	73.000	17.0000	9.0000	8.00000

Table 26
Proportions of Springtime Smolts Exhibiting Different Impingement Behaviors by Beginning Time for All Gate Positions, Camera Locations, and Discharges Combined

HOURBEG	FREQ	R_IMPNGH	R_IMPNGI	R_IMPNGD	R_IMPNGN	R_IMPNEN	R_IMPNES	FREQ	R_PERMIN
Summary Proportions by Beginning Time for Each Replicate - All Cameras Combined Except Camera Location 2									
20	16	0	0.44961	0.10337	0.042659	0.20415	0.47205	27	0.042646
22	20	0	0.48075	0.11921	0.030572	0.15771	0.53466	29	0.066714
24	8	0	0.42660	0.10753	0.010417	0.24044	0.45155	23	0.054588
Camera Location 2 Only									
20	3	0	0.09722	0.00000	0.16111	0.80556	0.13889	5	0.040000
22	5	0	0.18416	0.08160	0.15635	0.71328	0.17937	5	0.101174
24	2	0	0.18750	0.00000	0.29167	0.62500	0.37500	3	0.075362
Camera Location 13 Only									
20	4	0	0.36134	0.13988	0.14286	0.41721	0.30303	6	0.055676
22	6	0	0.43706	0.07660	0.05417	0.20247	0.58151	7	0.083090
24	1	0	0.34615	0.07692	0.00000	0.38462	0.38462	4	0.069444
Camera Location 21 Only									
20	4	0	0.47222	0.06389	0.027778	0.11944	0.58056	7	0.051191
22	5	0	0.51341	0.17062	0.028718	0.14381	0.49560	7	0.103743
24	3	0	0.34722	0.02778	0.027778	0.29630	0.50926	6	0.058067
Camera Location 26 Only									
20	4	0	0.41875	0.01923	0.000000	0.18173	0.67724	5	0.045000
22	4	0	0.52009	0.10714	0.035714	0.06696	0.63393	5	0.055568
24	2	0	0.56250	0.2250	0.000000	0.10000	0.30000	5	0.041717
Camera Location 31 Only									
20	2	0	0.57143	0.21429	0	0.07143	0.23810	5	0.045000
22	3	0	0.47619	0.10317	0	0.15079	0.34127	6	0.055568
24	2	0	0.45000	0.12500	0	0.22500	0.55000	4	0.041717
Camera Location 38 Only									
22	2	0	0.52083	0.16667	0	0.125	0.41667	4	0.020833
24	2	0	0.45833	0.16667	0	0.250	0.58333	4	0.028022

Note: The hydraulic variables are not included in this analysis because beginning time should have no effect on their values.

Table 27
Summary of Probabilities from Analysis of Variance (P ≤ 0.20 are in bold) for Effects of Spring Closure Gate Position, Unitload, Beginning Time, and Camera Location on Entrainment and Hydraulic Variables

All Cameras Combined Except Camera 2											
SOURCE	R_PERMIN	R_IMPNNEN	R_IMPNES	R_IMPNGI	R_IMPNGH	R_IMPNGN	R_IMPNGD	CURR_ANG	CUR_ANG9	CUR_ANCV	CURR_CV
COMBINED	**0.0043**	0.4303	0.4615	0.6590	0.0	0.4468	0.8392	**0.0001**	**0.0001**	**0.0057**	**0.1230**
GATESET	**0.0387**	0.7964	0.7052	0.9046	0.0	0.3889	0.2849	0.9098	**0.1673**	**0.1856**	0.2995
UNITLOAD	**0.0511**	0.3974	0.2618	0.5304	0.0	0.3180	0.5150	**0.1188**	0.7963	0.4116	0.4265
HOURBEG	0.4660	**0.1756**	0.2031	0.2895	0.0	0.7870	0.8628	.	.	.	.
CAMLOC	**0.0023**	**0.1951**	0.2597	0.3797	0.0	0.2706	0.6510	**0.0001**	**0.0001**	**0.0020**	**0.0813**
N	81	44	44	44	44	44	44	103	103	103	130
ENTRAINMENT SAMPLES - DURATION = 4,602 MIN : TOT_SEEN = 340 SMOLTS : RATE_SEEN = 0.073 SMOLTS/MIN HYDRAULIC SAMPLES - DURATION = 8,577 MIN : MEASUREMENTS = 527											
Camera Location 2 Only											
COMBINED	**0.0245**	0.2351	0.4618	0.2570	0.0	0.6334	0.2710	**0.0491**	**0.0491**	**0.0057**	**0.0392**
GATESET	**0.0109**	**0.0619**	**0.1901**	**0.0628**	0.0	0.2635	**0.1875**	**0.0786**	**0.0786**	**0.0053**	**0.0304**
UNITLOAD	0.2550	0.7701	0.7305	0.7498	0.0	0.9960	0.2210	**0.0949**	**0.0949**	**0.0475**	0.3399
N	14	10	10	10	10	10	10	19	19	19	19
ENTRAINMENT SAMPLES - DURATION = 1,004 MIN : TOT_SEEN = 81 SMOLTS : RATE_SEEN = 0.08068 HYDRAULIC SAMPLES - DURATION = 1,651 MIN : MEASUREMENTS = 108											

(Sheet 1 of 3)

Note: For each variable there were 3 classes of unitload (12, 14, and 16 kcfs), 3 closure gate positions (no gate, partial gate, and normal gate), 4 beginning times (2000, 2200, 2400, and 2600 hr), and 5 camera locations (13, 21, 26, 31, and 38 ft from the top of the screen).

Table 27 (Continued)

Camera Location 13 Only

SOURCE	R_PERMIN	R_IMPNNEN	R_IMPNES	R_IMPNGI	R_IMPNGH	R_IMPNGN	R_IMPNGD	CURR_ANG	CUR_ANG9	CUR_ANCV	CURR_CV
COMBINED	**0.0566**	0.9970	0.8316	0.9634	0.0000	0.4877	0.4169	**0.0436**	**0.0436**	**0.0684**	**0.0993**
GATESET	**0.0156**	0.9593	0.7731	0.8274	0.0000	0.5416	0.3104	**0.0098**	**0.0098**	**0.9072**	**0.5710**
UNITLOAD	0.9372	0.9539	0.6009	0.8914	0.0000	0.3761	0.3031	0.7195	0.7195	**0.0220**	**0.0294**
N	17	11	11	11	11	11	11	21	21	21	21

ENTRAINMENT SAMPLES - DURATION = 1,175 MIN : TOT_SEEN = 99 | RATE_SEEN = 0.08426
HYDRAULIC SAMPLES - DURATION = 1,750 MIN : MEASUREMENTS = 129

Camera Location 21 Only

COMBINED	0.2755	0.8969	0.5239	0.9691	0.0000	**0.0581**	0.5798	**0.1427**	**0.1427**	0.4030	0.4737
GATESET	**0.1636**	0.9945	0.3148	0.9021	0.0000	**0.1208**	0.9507	0.3791	0.3791	0.2418	0.3194
UNITLOAD	0.3999	0.7559	0.4978	0.8948	0.0000	**0.0428**	0.3974	**0.1073**	**0.1073**	0.6606	0.6435
N	20	12	12	12	12	12	12	12	22	22	22

ENTRAINMENT SAMPLES - DURATION = 1,242 MIN | TOT_SEEN = 121 | RATE_SEEN = 0.09742
HYDRAULIC SAMPLES - DURATION = 1,831 MIN : MEASUREMENTS = 157

Camera Location 26 Only

COMBINED	**0.0510**	0.9351	0.5800	0.8291	0	0.4799	0.6180	0.8322	0.8322	0.8511	0.9667
GATESET	**0.0426**	0.7667	0.5250	0.5541	0	0.4973	0.4954	0.9300	0.9300	0.8334	0.8287
UNITLOAD	**0.1724**	0.8714	0.5069	0.8122	0	0.3664	0.5437	0.5321	0.5321	0.5636	0.8660
N	15	10	10	10	10	10	10	20	20	20	20

ENTRAINMENT SAMPLES - DURATION = 1,095 MIN : TOT_SEEN = 64 | RATE_SEEN = 0.05845
HYDRAULIC SAMPLES - DURATION = 1,740 MIN : MEASUREMENTS = 97

(Sheet 2 of 3)

Table 27 (Concluded)

Camera Location 31 Only											
SOURCE	R_PERMIN	R_IMPNNEN	R_IMPNES	R_IMPNGI	R_IMPNGH	R_IMPNGN	R_IMPNGD	CURR_ANG	CUR_ANG9	CUR_ANCV	CURR_CV
COMBINED	0.6181	0.6256	**0.1609**	0.2308	0	0	**0.1193**	0.5117	0.5117	0.3946	**0.1386**
GATESET	0.8492	0.7465	**0.0613**	**0.8000**	0	0	**0.0408**	0.6926	0.6926	0.2234	**0.0567**
UNITLOAD	0.4099	0.6544	**0.1802**	0.3184	0	0	0.3921	0.2632	0.2632	0.9207	0.6690
N	16	7	7	7	7	7	7	22	22	22	22
ENTRAINMENT SAMPLES - DURATION = 680 MIN : TOT_SEEN = 42 | RATE_SEEN = 0.06177 HYDRAULIC SAMPLES - DURATION = 1,780 : MEASUREMENTS = 98											
Camera Location 38 Only											
COMBINED	**0.1657**	.	.	.	.	.	.	**0.0163**	**0.0163**	**0.0865**	0.5062
GATESET	**0.0780**	.	.	.	.	.	.	**0.0482**	**0.0482**	0.4932	0.7665
UNITLOAD	0.2815	.	.	.	.	.	.	**0.0643**	**0.0643**	0.0733	0.3199
N	13	4	4	4	4	4		18	18	18	18
ENTRAINMENT SAMPLES - DURATION = 410 : TOT_SEEN = 14 : RATE_SEEN = 0.03415 HYDRAULIC SAMPLES - DURATION = 1,476 MIN : MEASUREMENTS = 56											

(Sheet 3 of 3)

a. *Unitload.* The second block of Table 24 presents summaries by unitload for all camera locations combined except camera location 2. The rest of Table 24 presents summaries by unitload for the different camera locations on the ESBS. Unitload had a statistically significant effect on imaging rate (P = 0.0511, Table 27), but the normal pattern of increased imaging rate with increasing discharge was not observed. In this case, the 14 kcfs unitload had the highest imaging rate. The reason for this relationship between unitload and imaging rate is unknown. Unitload also affected average current angle through the screen (P = 0.1188, Table 27), but the change was near the detection limit of 5 deg.

Relatively few significant relationships at the other camera locations were observed. There appeared to be several nearly significant relationships between unitload and hydraulic variables at camera location 2. However, differences in means were approximately equal to the accuracy of the measurements (5 deg). However, at camera location 38 the differences in current angles appeared to be statistically significant and larger than our sampling accuracy. Increased discharge caused the current angle at this location to deviate more towards the toe of the screen (current angle was about 80 deg at 12 and 14 kcfs and about 70 deg at 16 kcfs suggesting the presence of a water plug effect (maximum conveyance has been reached) higher on the screen that manifests itself by causing progressively more of the flow to bend under the screen).

b. *Closure gate.* Table 25 summarizes the effects of closure gate position. Closure gate position has little effect on dependent variables averaged across the different camera locations. However, there were several trends observed at specific camera locations, particularly camera location 2. At camera location 2, gate setting had a significant (P = 0.05) or nearly significant effect (P = 0.20) on most passage/impingement variables and hydraulic variables. Specifically, the impingement variables are three times higher under no closure gate operation than they are under the partial gate condition (R_IMPNGD, P = 0.1875, and R_IMPNGI, P = 0.0628, Table 27). The passage variables were much higher under the partial gate positions than under the no closure gate position (R_IMPNEN, P = 0.0619, R_IMPNGN, P = 0.2635, Table 27). The normal closure gate storage position had too few observations for interpretation. At camera location 2, the angle of flow was more parallel to the screen surface by about 5 deg (CURR_ANG, P = 0.0786, Table 27) under the partial closure gate position. Closure gate appeared to effect imaging rate at a number of camera locations; however, the reasons for this pattern are unclear. Probably, part of the variation in imaging rate attributed to gate setting is caused by beginning time because gate setting and beginning time are significantly correlated (R = -0.20798, P = 0.0041, Table 4). In the case of the hydraulic variables no other significant patterns were observed across more than one variable or that exceeded the accuracy of measurements made from the video images.

No consistent pattern between beginning time and any of the passage/impingement variables was observed.

Summer Bypass Screen Analysis

The organization of results of the bypass screen evaluation for summer is identical to that for the spring. It is separated into four sections. The first section presents summary statistics to describe general patterns among and between variables. The first section also includes correlation analysis of the dependent and independent variables. The second section describes the results of studies to determine the response of smolts to localized hydraulic conditions (unitload was used as a velocity surrogate and current angle was estimated from imaging) on the screen surface 13, 21, 26, 31, and 38 ft from the top of the screen. Section two includes summary tables and ANOVA to determine the effect of hydraulic variables on impingement behavior. In the third section, regression analysis is used to determine if local hydraulic variables can be used to predict impingement behavior. The fourth section presents tabular summaries and results from ANOVA to determine the effect of unitload and gate setting.

Summary statistics

a. *Summary tabulations*. Table 28 presents summary data and simple statistics for the dependent and independent variables used in the analyses. The imaging rate was much higher in the summer than in the spring. Hydraulic data from physical model studies of the ESBS were unavailable for summer. Hydraulic variables obtained from physical model studies for the summer analysis could not be incorporated because data were only available for camera locations 2 and 13. Only hydraulic variables obtained from measurements made during imaging (water current angle and derivatives such as variance of current angle) were used.

The summer tests were all performed without the fyke nets in place. The number of observations in the summer is considerably higher in the summer than in the spring primarily because the density of fishes increases in the summer. Results from summer testing are more definitive than those from spring.

b. *Correlation analysis*. Correlation analysis results (Table 29) of the impingement/passage variables and hydraulic variables for the summer analysis generally followed the same patterns observed in the spring analysis except that water velocity information was unavailable. A few notable differences were observed and are noted below.

Table 28
Simple Statistics for Analysis of Localized Hydraulic Conditions

Variable	N	Mean	Std Dev	Sum	Minimum	Maximum
R-PERMIN	170	0.607178	0.831643	103.220259	0.024390	5.600000
R_IMPNEN	170	0.490560	0.206179	83.395277	0	1.000000
R_IMPNES	170	0.259320	0.164124	44.084329	0	0.750000
R_IMPNGI	164	0.250042	0.095054	41.006881	0	0.500000
R_IMPNGD	170	0.051671	0.071158	8.784040	0	0.333333
R_IMPNGN	170	0.175367	0.180050	29.812387	0	1.000000
R_SDEAD	170	0.001382	0.011379	0.234890	0	0.125000
HOURBEG	170	22.235294	1.520254	3780.000000	20.000000	24.000000
CAMLOC	170	27.270588	7.036487	4636.000000	13.000000	38.000000
CURR_ANG	170	108.294118	21.401390	18410	70.000000	140.000000
CUR_ANG9	170	25.705882	11.400533	4370.000000	10.000000	50.000000
CURR_CV	170	6.352941	6.589764	1080.000000	0	30.000000
CUR ANCV	170	19.352941	13.723565	3290.000000	-10.000000	50.000000

Note: Results combined for all cameras except camera 2. Variables defined on pages 29 and 30 of text.

(1) Passage variables (no impingement or screen contact - R_IMPNEN and R_IMPNGN) were negatively correlated to the impingement variables (impingement or screen contact - R_IMPNGI and R_IMPNGD). The headfirst impingement without escape index (R_IMPNGH) was dropped from the analysis because too few non-zero observations occurred.

(2) Increasing water angle increases the impingement indices and decreases the headfirst passage index. The opposite response was observed in the spring. This difference may result from differences in the depth distribution of smolts between the summer and spring as evidenced by imaging rate (compare Tables 5 and 31, top block), or it could be related to the presence of the fyke net for all summer video imaging.

(3) The effects of beginning time (HOURBEG) appear to have some effect on the passage variables. However, changes in unitload and hence corresponding changes in water velocity were not random but appeared to increase with time confounding the HOURBEG and UNITLOAD variables. The effects on impingement/passage variables attributed to HOURBEG are probably associated with decreases in UNITLOAD.

Table 29
Pearson Correlation Coefficients for the Summer Analysis of Localized Hydraulic Effects

	R_PERMIN	R_IMPNEN	R_IMPNES	R_IMPNGI	R_IMPNGD	R_IMPNGN	R_SDEAD	HOURBEG	CAMLOC	CURR_ANG	CUR_ANG9	CURR_CV	CUR_ANCV
R_PERMIN	1.00000 0.0	0.12073 **0.1168**	-0.04607 0.5508	0.17860 **0.0221**	0.25652 **0.0007**	-0.18583 **0.0153**	-0.04560 0.5549	-0.06953 0.3676	-0.33634 **0.0001**	0.30581 **0.0001**	0.22845 **0.0027**	-0.15521 **0.0433**	0.26431 **0.0005**
R_IMPEN	0.12073 **0.1168**	1.00000 0.0	-0.22820 **0.0028**	-0.57839 **0.0001**	-0.02646 0.7320	0.20180 **0.0083**	0.00392 0.9596	-0.15246 **0.0472**	-0.06539 0.3969	0.03563 0.6446	0.04548 0.5559	-0.24914 **0.0011**	0.15742 **0.0404**
R_IMPNES	-0.04607 0.5508	-0.22820 **0.0028**	1.00000 0.0	0.48418 **0.0001**	-0.17066 **0.0261**	0.40392 **0.0001**	-0.05907 0.4442	0.11043 **0.1517**	0.27495 **0.0003**	-0.25779 **0.0007**	-0.30346 **0.0001**	-0.12013 **0.1187**	-0.19441 **0.0111**
R_IMPNGI	0.17860 **0.0221**	-0.57839 **0.0001**	0.48418 **0.0001**	1.00000 0.0	0.55555 **0.0001**	-0.12920 **0.0992**	0.10719 **0.1719**	0.09071 0.2481	-0.19111 **0.0142**	0.17384 **0.0260**	0.11728 **0.1348**	-0.14085 **0.0720**	0.16157 **0.0387**
R_IMPNGD	0.25652 **0.0007**	-0.02646 0.7320	-0.17066 **0.0261**	0.55555 **0.0001**	1.00000 0.0	-0.31033 **0.0001**	0.18777 **0.0142**	0.00504 0.9480	-0.43574 **0.0001**	0.38937 **0.0001**	0.36201 **0.0001**	-0.10825 **0.1600**	0.35271 **0.0001**
R_IMPNGN	-0.18583 **0.0153**	0.20180 **0.0083**	0.40392 **0.0001**	-0.12920 **0.0992**	-0.31033 **0.0001**	1.00000 0.0	-0.09761 0.2054	-0.14790 **0.0543**	0.54271 **0.0001**	-0.55549 **0.0001**	-0.41671 **0.0001**	0.07248 0.3476	-0.38098 **0.0001**
R_SDEAD	-0.04560 0.5549	0.00392 0.9596	-0.05907 0.4442	0.10719 **0.1719**	0.18777 **0.0142**	-0.09761 0.2054	1.00000 0.0	-0.01890 0.8067	-0.08540 0.2682	0.08550 0.2676	0.08109 0.2931	-0.01912 0.8046	0.07655 0.3211
HOURSBEG	-0.06953 0.3676	-0.15246 **0.0472**	0.11043 **0.1517**	0.09071 0.2481	0.00504 0.9480	-0.14790 **0.0543**	-0.01890 0.8067	1.00000 0.0	0.00508 0.9476	-0.00941 0.9030	-0.02330 0.7630	0.01529 0.8432	-0.02669 0.7297
CAMLOC	-0.33634 **0.0001**	-0.06539 0.3969	0.27495 **0.0003**	-0.19111 **0.0142**	-0.43574 **0.0001**	0.54271 **0.0001**	-0.08540 0.2682	0.00508 0.9476	1.00000 0.0	-0.95685 **0.0001**	-0.79902 **0.0001**	0.14136 **0.0659**	-0.73165 **0.0001**
CURR_ANG	0.30581 **0.0001**	0.03563 0.6446	-0.25779 **0.0007**	0.17384 **0.0260**	0.38937 **0.0001**	-0.55549 **0.0001**	0.08550 0.2676	-0.00941 0.9030	-0.95685 **0.0001**	1.00000 0.0	0.75071 **0.0001**	-0.14507 **0.0591**	0.69330 **0.0001**
CUR_ANG9	0.22845 **0.0027**	0.04548 0.5559	-0.30346 **0.0001**	0.11728 **0.1348**	0.36201 **0.0001**	-0.41671 **0.0001**	0.08109 0.2931	-0.02330 0.7630	-0.79902 **0.0001**	0.75071 **0.0001**	1.00000 0.0	-0.09943 **0.1971**	0.87847 **0.0001**
CURR_CV	-0.15521 **0.0433**	-0.24914 **0.0011**	-0.12013 **0.1187**	-0.14085 **0.0720**	-0.10825 **0.1600**	0.07248 0.3476	-0.01912 **0.8046**	0.01529 0.8432	0.14136 **0.0659**	-0.14507 **0.0591**	-0.09943 **0.1971**	1.00000 0.0	-0.56277 **0.0001**
CUR_ANVC	0.26431 **0.0005**	0.15742 **0.0404**	-0.19441 **0.0111**	0.16157 **0.0387**	0.35271 **0.0001**	-0.38098 **0.0001**	0.07655 0.3211	-0.02669 0.7297	-0.73165 **0.0001**	0.69330 **0.0001**	0.87847 **0.0001**	-0.56277 **0.0001**	1.00000 0.0

Note: Variables are defined on pages 29 and 30. Each comparison is based on 170 observations except the R_IMPNGD index which is based on 164 observations.

(4) R_IMPNGI and R_IMPNGD are highly correlated (r = 0.5555, P = 0.0001) suggesting that when observations are sparse R_IMPNGI (which has reduced data requirements) is a good surrogate for R_IMPNGD.

(5) The rate at which fish are imaged (R_PERMIN) appears to be related to current angle; however, this relationship may be spurious since water angle increases significantly towards the top of the screen. Consequently, more fish should be seen at the topmost camera (at location 13 because camera 2 is not used in the correlation analysis) because most of the fishes intercepted by the screen would have to pass this camera.

The only significant correlation among independent variables for the summer data occurred between unitload and beginning time (R = 0.7790, P = 0.0001, Table 30). This is a high correlation coefficient indicating that unitload and its associated variables, such as current velocity and R_PERMIN (imaging rate) are confounded with beginning time. The R_PERMIN variable is affected because all other factors being equal, the passage of fishes will increase linearly as the discharge increases. Increased unitload also results in increased water velocities on the screen which are more likely to press smolts closer to the screen where they are more likely to be imaged. No way to statistically eliminate these confounding effects is known.

Table 30
Correlation Matrix for Independent Variables for Summer

Pearson Correlation Coefficients / Prob > |R| under Ho: Rho = 0 / N = 170

	UNITLOAD	HOURBEG	CAMLOC	GATSET
UNITLOAD	1.00000 0.0	0.77900 **0.0001**	0.1676 0.8283	0.05141 0.5055
HOURBEG	0.77900 **0.0001**	1.00000 0.0	0.00508 0.9476	0.05709 0.4596
CAMLOC	0.01676 0.8283	0.00508 0.9476	1.00000 0.0	0.05314 0.4913
GATSET	0.05141 0.5055	0.05709 0.4596	0.05314 0.4913	1.00000 0.0

Note: The non-numeric variables GATSET (closure gate setting) were converted to numeric variables by replacing alphameric configuration descriptions with 0, 1, or 2. For example, gate setting has a value of 0 if the gate is not stored, 1 if it is in the partial storage position, and 2 if it is in the normal storage position.

Effects of local hydraulic conditions

a. *Data tabulation and analysis of variance.* Summaries of impingement/entrainment variables by camera location, current angle, beginning time, and unitload are presented in Table 31, and associated statistics from ANOVA are presented in Table 32. The top block of Table 31 summarizes results by camera location for all treatments combined. Note that in contrast to the spring analysis, the values for impingement variables (R_IMPNGD, P = 0.0616 and R_IMPNGI, P = 0.2616, Table 32) tended to decrease with distance away from the top of the screen. The reason for this pattern is unclear; however, reference to Table 13 (details effects of the presence of the fyke net) indicates that the pattern of increased impingement towards the bottom of the screen is not observed when the fyke net is in place. Instead, impingement appears to be reduced and sporadic with no trends becoming apparent. Probably, at least part of the reversal in impingement patterns from the spring to the summer imaging is associated with the presence of the fyke net for all summer sampling.

The second and third blocks of Table 31 summarize impingement behavior as a function of local hydraulic conditions. No significant relationships were observed for current angle (second block). However, R_IMPNGD increased systematically with increasing current angle and R_IMPNGN exhibited the opposite trend. In the third block, (water angle plus variance of water angle) the only consistent pattern appears to be a propensity for summer smolts to have a pattern of increasing values for the R_IMPNEN (entrainment without strike) and R_IMPNES indices (contact with escape) that decreases with increasing values of CUR_ANCV. Imaging rate appears to be bimodal with peaks at camera locations 21 and 31 ft from the top of the screen.

Note the differences in the values of the indices between the spring (Table 5) and summer (Table 31) samples. Values for impingement indices and impingement proportions are substantially higher for the spring samples than for the summer samples. Fyke nets were usually not used in the spring but were used in the summer.

b. *Regression analysis.* In the summer, no equations were found with an R^2 for the impingement indices that would be of value (Table 33). However, an R^2 of 0.3320 was found for the entrainment index (R_IMPNGN). While the summer analysis did not provide as useful results as the spring, keep in mind that no velocity information was available for use as independent variables, and the presence of the fyke probably had a major effect on the hydraulic patterns on the screen surface.

Table 31
Proportions of Smolts Responding to Different Localized Hydraulic Conditions for Summertime Using Imaging Determined Angles and Other Variables Suitable for Analysis of Localized Conditions

Summary Proportions by Camloc

CAMLOC	FREQ	R_IMPNGH	R_IMPNGI	R_IMPNGD	R_IMPNGN	R_IMPNEN	R_IMPNES	FREQ	R_PERMIN
13	7	0.00476	0.29170	0.12658	0.10264	0.54318	0.12997	7	0.59810
21	58	0.00331	0.26992	0.08080	0.08117	0.50575	0.23105	58	1.06261
26	36	0.00000	0.22910	0.05200	0.12985	0.49542	0.21345	36	0.37716
31	33	0.00224	0.26215	0.02959	0.21462	0.44616	0.33144	33	0.59867
38	36	0.00000	0.21710	0.01009	0.35080	0.49169	0.30977	36	0.15577

Summary Proportions by Angle

CURR_ANG	FREQ	R_IMPNGH	R_IMPNGI	R_IMPNGD	R_IMPNGN	R_IMPNEN	R_IMPNES	FREQ	R_PERMIN
70	27	0.00000	0.22050	0.01345	0.34365	0.47330	0.29773	27	0.16675
80	9	0.00000	0.20804	0.00000	0.37225	0.54687	0.34589	9	0.17307
100	30	0.00247	0.25792	0.02884	0.22498	0.47966	0.34977	30	0.58351
110	13	0.00000	0.27013	0.04892	0.11155	0.43793	0.23274	13	0.60545
120	51	0.00224	0.24038	0.07029	0.11305	0.49357	0.20406	51	0.63562
130	35	0.00221	0.27565	0.07853	0.07905	0.50820	0.23611	35	1.02732
140	5	0.00667	0.29338	0.11722	0.09037	0.53046	0.14863	5	0.68233

Summary Proportions by Variance in Approach Angle (Surrogate for Turbulence)

CURR_ANCV	FREQ	R_IMPNGH	R_IMPNGI	R_IMPNGD	R_IMPNGN	R_IMPNEN	R_IMPNES	FREQ	R_PERMIN
-10	2	0.00000	•	0.00000	0.00000	0.00000	0.00000	2	0.04375
0	27	0.00274	0.21770	0.02050	0.26708	0.49011	0.27479	27	0.33824
10	40	0.00000	0.24893	0.01781	0.26976	0.46574	0.35104	40	0.41564
20	42	0.00272	0.25841	0.07671	0.16415	0.49339	0.24707	42	0.61271
30	31	0.00000	0.23514	0.05839	0.08549	0.55452	0.19821	31	0.80694
40	26	0.00426	0.28563	0.08454	0.07976	0.51328	0.22397	26	0.97843
50	2	0.00000	0.29327	0.14423	0.09615	0.55769	0.13942	2	0.59333

(Continued)

Table 31 (Concluded)

Summary Proportions by Beginning Hour

HOURBEG	FREQ	R_IMPNGH	R_IMPNGI	R_IMPNGD	R_IMPNGN	R_IMPNEN	R_IMPNES	FREQ	R_PERMIN
20	40	0.00415	0.24123	0.05830	0.22693	0.52497	0.23467	40	0.40349
22	70	0.00060	0.24408	0.04343	0.16531	0.50892	0.25423	70	0.94607
24	60	0.00154	0.26248	0.05686	0.15273	0.44620	0.28169	60	0.34760

Summary Proportions by Unitload

UNITLOAD	FREQ	R_IMPNGH	R_IMPNGI	R_IMPNGD	R_IMPNGN	R_IMPNEN	R_IMPNES	FREQ	R_PERMIN
13	82	0.00159	0.24403	0.04962	0.18629	0.49731	0.24242	82	0.53400
15	32	0.00242	0.24397	0.04750	0.17705	0.55957	0.25747	32	1.28502
16	56	0.00165	0.26199	0.05705	0.15841	0.44124	0.28512	56	0.41857

Table 32
Summary of Probabilities from Analysis of Variance ($P \leq 0.20$ are in bold) for Summertime for Effects of Localized Hydraulic Variables on Smolt Entrainment and Impingement Behavior

Combined Analysis

SOURCE	R_PERMIN	R_IMPNEN	R_IMPNES	R_IMPNGI	R_IMPNGH	R_IMPNGN	R_IMPNGD
COMBINED	**0.0001**	**0.0353**	**0.0006**	0.1822	0.5512	**0.0001**	**0.0001**
CURR_ANG	0.5893	0.2341	0.2627	0.8189	0.7372	0.8313	0.9007
CUR_ANCV	0.9465	**0.0844**	**0.0315**	0.3342	0.6428	0.4337	0.2061
CAMLOC	**0.0020**	0.7052	0.5633	0.2616	0.3003	0.3129	**0.0616**
HOURBEG	**0.0001**	**0.0711**	0.3278	0.4014	**0.1074**	**0.0204**	0.4840
N	170	170	170	170	170	170	170

ENTRAINMENT SAMPLES - DURATION = 8767 MIN : TOT_SEEN = 2480 SMOLTS : RATE_SEEN = 0.28288 SMOLTS/MIN

Summer closure gate position and unitload

Tables 34 through 37 summarize effects of gate position and unitload on impingement/passage characteristics and hydraulic variables for the summer season. Summaries of data are presented for all variables by camera location (Table 34) and for unitload (Table 34), closure gate setting (Table 35), and beginning time (Table 36). Significance levels for the data summaries are presented in Table 37. This analysis was not affected by low numbers of

Table 33
Summary of Multiple Regression Analysis Using Backward Elimination of Summer Entrainment Against Select Hydraulic Variables

Dependent Variable	R-square	DF reg/err/tot	Equation Prob > F	Independent Variables	Parameter Estimates	Individual Probabilities
R_PERMIN	0.1131	1/168/169	0.0001	INTERCEP CAMLOC	1.691230 -0.039752	0.0001 0.0001
R_IMPNEN	0.0844	3/166/169	0.0021	INTERCEP CUR_ANG9 CUR_ANCV HOURBEG	0.978305 -0.007350 0.007669 -0.020113	0.0001 0.0098 0.0012 0.0475
R_IMPNES	0.1149	2/167/169	0.0001	INTERCEP CUR_ANG9 CUR_ANCV	0.40125 -0.008367 0.003781	0.0001 0.0002 0.0395
R_IMPNGI	0.365	1/162/163	0.0142	INTERCEP CAMLOC	0.320220 -0.002596	0.0001 0.0142
R_IMPNGN	0.3320	2/167/169	0.0001	INTERCEP CURR_ANG HOURBEG	1.086075 -0.004686 -0.018138	0.0001 0.0001 0.0165
R_IMPNGD	0.1899	1/168/169	0.0001	INTERCEP CAMLOC	0.171841 -0.004407	0.0001 0.0001

observations, and consequently the results are the most robust of all analyses of bypass screen design or deployment alternatives.

Table 34 (top block) provides summaries by camera location for closure gate position, unitload, camera location, and beginning times combined. Note that imaging rate (R_PERMIN) is significantly affected by all independent variables (GATESET, P = 0.0002; UNITLOAD, P = 0.0026; HOURBEG, P = 0.0038; CAMLOC, P = 0.0001 - Table 37). However, the effect of HOURBEG should be evaluated with caution because it is highly correlated with UNITLOAD. All three impingement variables are significantly affected by camera locations (R_IMPNGD, P = 0.0001; R_IMPNGI, P = 0.0483; R_IMPNES, P = 0.0001, Table 38). Impingement rate (R_IMPNGD) and impingement index (R_IMPNGI) decrease towards the bottom of the ESBS (opposite of the spring pattern), and contact with escape (R_IMPNES) increases towards the bottom of the ESBS (Table 34). In general, imaging rate is higher towards the top of the screen. However, there is a secondary peak in R_PERMIN at camera location 31 (Table 34) and a corresponding secondary peak in R_IMPNGI and R_IMPNES at the same locations. The reasons for this bimodal distribution are unclear, but it is doubtful that the bimodal distribution is a statistical artifact because several variables are affected. A possible explanation is that two distinct groups of smolts are passing (e.g., hatchery and nonhatchery) through the system each with substantially different passage characteristics. As has been found for most

Table 34
Proportions of Summertime Smolts Exhibiting Different Impingement Behaviors by Camera Location and Unitload for Closure Gate Position and Beginning Times Combined

CAMLOC	FREQ	R_IMPNGH	R_IMPNGI	R_IMPNGD	R_IMPNGN	R_IMPNEN	R_IMPNES	FREQ	R_PERMIN	MN_CRANG	MN_CRAN9	MN_CR9CV	MN_CRCV
Summary Proportions by CAMLOC													
13	7	0.00476	0.29170	0.12658	0.10264	0.54318	0.12997	7	0.59810	137.143	47.1429	40.0000	7.14286
21	54	0.00355	0.26901	0.08679	0.08240	0.54877	0.21869	58	1.05977	125.690	35.6897	30.8621	4.82759
26	30	0.00000	0.23951	0.05129	0.13359	0.57228	0.23392	36	0.38364	117.222	27.2222	20.2778	6.94444
31	29	0.00255	0.27448	0.03367	0.23273	0.48471	0.36566	33	0.56448	100.909	10.9091	4.5455	6.36364
38	30	0.00000	0.22215	0.01210	0.42096	0.56781	0.34950	38	0.17522	72.500	17.5000	9.4444	8.05556
Summary Proportions by Unitload - All Cameras Combined Except Camera Location 2													
13	72	0.00180	0.24993	0.05651	0.20395	0.55666	0.26325	82	0.56198	108.293	26.0976	19.0244	7.07317
15	32	0.00242	0.24397	0.04750	0.17705	0.55957	0.25747	32	1.28502	110.625	25.0000	20.8375	4.06250
16	46	0.00200	0.27339	0.06221	0.17836	0.51543	0.29637	56	0.32671	106.964	25.5357	18.9286	6.60714
Camera Location 2 Only													
13	11	0	0.09538	0.05619	0.20316	0.85917	0.00627	14	0.16934	167.857	77.8571	74.2857	3.5714
15	3	0	0.14487	0.10483	0.13226	0.81510	0.00000	3	0.42582	163.333	73.3333	63.3333	10.0000
16	11	0	0.09624	0.06417	0.13471	0.87169	0.00848	13	0.29048	166.923	76.9231	74.6154	2.3077
Camera Location 13 Only													
13	5	0.00000	0.27338	0.09388	0.13703	0.54712	0.15696	5	0.67333	136	46	38	8
16	2	0.01667	0.33750	0.20833	0.01667	0.53333	0.06250	2	0.41000	140	50	45	2

(Continued)

Note: The ESBS was in unit/bay 6A. There were sufficient observations to treat unitload and closure simultaneously. For all unitloads and closure gate positions, the screen angle was 55 deg, had no fyke net, was in the standard position, and had a screen porosity of 30 percent. A total of 120 measurements of the hydraulic variables were made.

Table 34 (Concluded)

CAMLOC	FREQ	R_IMPNGH	R_IMPNGI	R_IMPNGD	R_IMPNGN	R_IMPNEN	R_IMPNES	FREQ	R_PERMIN	MN_CRANG	MN_CRAN9	MN_CR9CV	MN_CRCV
Camera Location 21 Only													
13	25	0.00222	0.26958	0.09474	0.09813	0.55537	0.21613	26	0.99084	124.615	34.6154	30.0000	4.61538
15	13	0.00595	0.26843	0.06477	0.07197	0.52791	0.23517	13	1.89077	129.231	39.2308	36.1538	3.07692
16	16	0.00368	0.26842	0.09225	0.06630	0.55541	0.20931	19	0.58551	124.737	34.7368	28.4211	6.31579
Camera Location 26 Only													
13	14	0	0.22542	0.04634	0.18861	0.59551	0.22398	17	0.29044	120.0	30.0	21.7647	8.23529
15	7	0	0.24047	0.06069	0.11089	0.57975	0.23759	7	0.86676	110.0	20.0	17.1429	2.85714
16	9	0	0.266067	0.05168	0.06568	0.53033	0.24653	12	0.22611	117.5	27.5	20.0000	7.50000
Camera Location 31 Only													
13	13	0.005698	0.25225	0.02786	0.21567	0.52336	0.34824	16	0.49133	101.250	11.2500	1.87500	9.37500
15	8	0.000000	0.25634	0.03164	0.21432	0.51896	0.30860	8	1.06910	100.000	10.0000	6.25000	3.75000
16	8	0.000000	0.32875	0.04514	0.27888	0.38765	0.45103	9	0.22971	101.111	11.1111	7.77778	3.33333
Camera Location 38 Only													
13	15	0	0.23005	0.01469	0.40676	0.55459	0.34020	18	0.16365	72.222	17.7778	10.5556	7.2222
15	4	0	0.14583	0.00000	0.55982	0.70833	0.26250	4	0.48011	72.500	17.5000	7.5000	10.0000
16	11	0	0.23912	0.01299	0.38983	0.53474	0.39383	14	0.09566	72.857	17.1429	8.5714	8.5714

Table 35
Proportions of Summertime Smolts Exhibiting Different Impingement Behaviors by Closure Gate for All Discharges, Camera Locations, and Beginning Times Combined

Summary Proportions By Closure Gate - All Cameras Combined Except Camera Location 2												
GATESET	FREQ	R_IMPNGH	R_IMPNGI	R_IMPNGD	R_IMPNGN	R_IMPNEN	R_IMPNES	FREQ	R_PERMIN	MN_CRANG	MN_CRAN9	MN_CR9CV	MN_CRCV
NG	67	0.00276	0.26147	0.05086	0.18634	0.52793	0.28090	71	0.60072	108.592	27.8873	22.3944	5.49296
NO	56	0.00105	0.25701	0.05632	0.20108	0.54229	0.28761	59	0.97818	104.915	22.7119	17.1186	5.5932
PR	27	0.00206	0.23951	0.06997	0.17810	0.59095	0.21850	40	0.13333	112.750	26.2500	17.2500	9.00000
Camera Location 2 Only													
NG	11	0	0.10431	0.07809	0.17991	0.86947	0.00848	11	0.27051	167.273	77.2727	74.5455	2.72727
NO	5	0	0.11616	0.05267	0.13069	0.80656	0.01379	5	0.46395	160.000	70.0000	64.0000	6.00000
PR	9	0	0.09046	0.05735	0.16455	0.87642	0.00000	14	0.14143	169.286	79.2857	75.7143	3.57143
Camera Location 13 Only													
NG	7	0.00476	0.29170	0.12658	0.10264	0.54318	0.12997	7	0.59810	137.143	47.1429	40	7.14286
Camera Location 21 Only													
NG	24	0.003224	0.27466	0.07330	0.08130	0.52399	0.22816	25	1.17025	129.200	39.2000	35.6	3.60000
NO	18	0.003268	0.27229	0.10474	0.07091	0.56015	0.22090	18	1.16346	124.444	34.4444	30.0	4.44444
PR	12	0.004630	0.25278	0.08684	0.10184	0.58128	0.19644	15	0.18578	121.333	31.3333	24.0	7.33333

(Continued)

Note: The ESBS was in unit/bay 6A, had no fyke net, the screen was deployed with no closure gate, was in the standard position, and had a screen porosity of 30 percent.

Table 35 (Concluded)

GATESET	FREQ	R_IMPNGH	R_IMPNGI	R_IMPNGD	R_IMPNGN	R_IMPNEN	R_IMPNES	FREQ	R_PERMIN	MN_CRANG	MN_CRAN9	MN_CR9CV	MN_CRCV
Camera Location 26 Only													
NG	7	0	0.23990	0.03827	0.15601	0.55847	0.25158	7	0.16157	120.000	30.0000	25.7143	4.28571
NO	15	0	0.25955	0.04491	0.12220	0.52581	0.28108	15	0.73215	113.333	23.3333	17.3333	6.00000
PR	8	0	0.20158	0.07465	0.13535	0.67149	0.13005	14	0.10110	120.000	30.0000	20.7143	9.28571
Camera Location 31 Only													
NG	11	0.006734	0.26146	0.03199	0.17225	0.50906	0.33514	12	0.49496	100.833	10.8333	6.66667	4.1667
NO	14	0.000000	0.26857	0.02675	0.27107	0.48961	0.36826	14	0.79765	100.000	10.0000	5.71429	4.2857
PR	4	0.000000	0.33095	0.06250	0.26488	0.40060	0.44048	7	0.07846	102.857	102.857	-1.42857	14.2857
Camera Location 38 Only													
NG	18	0	0.24051	0.00794	0.37935	0.52692	0.38816	20	0.10687	73.500	16.5000	8.0000	8.5000
NO	9	0	0.20425	0.02448	0.48401	0.61598	0.30647	12	0.35661	70.833	19.1667	10.8333	8.3333
PR	3	0	0.16567	0.00000	0.48148	0.66865	0.24669	4	0.10994	72.500	17.5000	12.5000	5.0000

Table 36
Proportions of Summertime Smolts Exhibiting Different Impingement Behaviors by Beginning Time for All Gate Positions, Camera Locations, and Discharges Combined

HOURBEG	FREQ	R_IMPNGH	R_IMPNGI	R_IMPNGD	R_IMPNGN	R_IMPNEN	R_IMPNES	FREQ	R_PERMIN
Summary Proportions by Beginning Time for Each Replicate - All Cameras Combined Except Camera Location 2									
20	36	0.00459	0.24074	0.06478	0.24289	0.58330	0.24222	40	0.42276
22	64	0.00065	0.25090	0.04750	0.17677	0.54570	0.27403	70	0.98186
24	50	0.00184	0.27307	0.06157	0.16994	0.51544	0.29136	60	0.34767
Camera Location 2 Only									
20	8	0	0.09557	0.06014	0.23907	0.86901	0.00431	9	0.15819
22	6	0	0.11987	0.07524	0.11984	0.82401	0.00575	8	0.27807
24	11	0	0.09624	0.06417	0.13471	0.87169	0.00848	13	0.29048
Camera Location 13 Only									
20	2	0.000000	0.28750	0.15000	0.13333	0.57500	0.08333	2	0.38750
22	3	0.000000	0.26397	0.05647	0.13950	0.52854	0.20604	3	0.86389
24	2	0.016667	0.33750	0.20833	0.01667	0.53333	0.06250	2	0.41000
Camera Location 21 Only									
20	12	0.007606	0.26424	0.09997	0.10601	0.57149	0.20561	13	0.67981
22	24	0.001736	0.27510	0.08170	0.08264	0.53150	0.22679	24	1.66768
24	18	0.003268	0.26406	0.08478	0.06634	0.55666	0.21661	21	0.60021
Camera Location 26 Only									
20	7	0	0.20569	0.05585	0.23321	0.64447	0.16647	8	0.20996
22	13	0	0.23424	0.03969	0.13405	0.57121	0.26348	15	0.59635
24	10	0	0.27002	0.06318	0.06328	0.52313	0.24271	13	0.26146
Camera Location 31 Only									
20	7	0.01058	0.23337	0.03711	0.29297	0.57037	0.33666	8	0.50569
22	13	0.00000	0.26397	0.02735	0.18075	0.49940	0.34329	15	0.82242
24	9	0.00000	0.32163	0.04012	0.26097	0.39686	0.42053	10	0.24452
Camera Location 38 Only									
20	8	0	0.23093	0.02273	0.44023	0.56088	0.32051	9	0.15409
22	11	0	0.19879	0.00350	0.43808	0.60592	0.32626	13	0.27551
24	11	0	0.23912	0.01299	0.38983	0.53474	0.39383	14	0.09566

Note: The hydraulic variables are not included in this analysis because beginning time should have no effect on their values.

Table 37
Summary of Probabilities From Analysis of Variance (P ≤ 0.20 are in Bold) for Effects of Summer Closure Gate Position, Unitload, Beginning Time, and Camera Location on Entrainment and Hydraulic Variables

Combined Analysis											
SOURCE	R_PERMIN	R_IMPNNEN	R_IMPNES	R_IMPNGI	R_IMPNGH	R_IMPNGN	R_IMPNGD	CURR_ANG	CUR_ANG9	CUR_ANCV	CURR_CV
COMBINED	**0.0001**	**0.1025**	**0.0001**	**0.1403**	0.5520	**0.0001**	**0.0001**	**0.0001**	**0.0001**	**0.0001**	**0.0195**
GATESET	**0.0002**	**0.1105**	**0.0952**	0.3674	0.8985	**0.1339**	0.2816	**0.0001**	**0.0036**	**0.0020**	**0.0163**
UNITLOAD	**0.0026**	0.5777	0.3589	0.5879	0.6393	0.8301	0.8470	0.9709	0.7841	0.7668	0.4649
HOURBEG	**0.0038**	0.3780	0.3936	0.7975	**0.1373**	**0.0633**	0.2606	.	.	.	.
CAMLOC	**0.0001**	**0.1289**	**0.0001**	**0.0483**	0.3871	**0.0001**	**0.0001**	**0.0001**	**0.0001**	**0.0001**	**0.1289**
N	164	150	150	150	150	150	150	150	170	170	170
ENTRAINMENT SAMPLES - DURATION = 7,459 MIN : TOT_SEEN = 2,417 SMOLTS : RATE_SEEN = 0.320 SMOLTS/MIN HYDRAULIC SAMPLES - DURATION = 8,767 MIN : MEASUREMENTS = 2,480											
Camera Location 2 Only											
COMBINED	**0.0003**	0.8133	0.5149	0.9486	0.0	0.4539	0.9211	**0.0001**	**0.0001**	**0.0002**	**0.0448**
GATESET	**0.0004**	0.4996	**0.1915**	0.8664	0.0	0.8676	0.8815	**0.0001**	**0.0001**	**0.0003**	**0.0819**
UNITLOAD	**0.0285**	0.5572	0.2995	0.4706	0.0	0.6122	0.4856	**0.0554**	**0.0554**	**0.0016**	**0.0154**
HOURSBEG	**0.1146**	0.6906	0.5820	0.8107	0.0	**0.1388**	0.8206	.	.	.	.
N	29	25	25	25	25	25	25	30	30	30	30
ENTRAINMENT SAMPLES - DURATION = 1,925 MIN : TOT_SEEN = 451 SMOLTS : RATE_SEEN = 0.23429 HYDRAULIC SAMPLES - DURATION = 2,155 MIN : MEASUREMENTS = 466											

(Sheet 1 of 3)

Note: For each variable there were 3 classes of unitload (12, 14, and 16 kcfs), 3 closure gate positions (no gate, partial gate, and normal gate), 4 beginning times (2000, 2200, 2400, and 2600 hr), and 5 camera locations (13, 21, 26, 31, and 38 ft from the top of the screen). Probabilities based on Type III sum of squares to reduce confounding effects of other variables. The analysis tests the hypothesis that the means of the different entrainment/impingement and hydraulic variables are not different by the treatment variables. Probabilities less than 0.20 are highlighted to enhance comparability to other tables and to identify trends.

Table 37 (Continued)

SOURCE	R_PERMIN	R_IMPNNEN	R_IMPNES	R_IMPNGI	R_IMPNGH	R_IMPNGN	R_IMPNGD	CURR_ANG	CUR_ANG9	CUR_ANCV	CURR_CV
Camera Location 13 Only											
COMBINED	**0.1575**	0.7761	0.4200	0.3027	0.3403	**0.1815**	**0.0612**	0.3739	0.3739	0.3503	0.5133
GATESET	.	.	.	.	.	.	.	.	.	.	.
UNITLOAD	.	.	.	.	.	.	.	.0.3739	0.3739	.0.3503	0.5133
HOURBEG	**0.1023**	0.5228	0.3222	0.5951	.	0.9186	**0.1046**	.	.	.	.
N	7	7	7	7	7	7	7	7	7	7	7
ENTRAINMENT SAMPLES - DURATION = 290 MIN : TOT_SEEN = 152 | RATE_SEEN = 0.52414 HYDRAULIC SAMPLES - DURATION = 290 MIN : MEASUREMENTS = 152											
Camera Location 21 Only											
COMBINED	**0.0001**	0.7624	0.8902	0.9607	0.6556	0.5620	0.6513	**0.0001**	**0.0001**	**0.0014**	0.3302
GATESET	**0.0002**	0.4020	0.7393	0.6783	0.5619	0.5008	0.5541	**0.0001**	**0.0001**	**0.0033**	0.3124
UNITLOAD	**0.0023**	0.8503	0.7082	0.7125	0.3018	0.6523	0.6230	0.9581	0.9581	0.8292	0.6307
HOURSBEG	**0.0339**	0.5232	0.6378	0.7127	0.2632	0.7868	0.4533	.	.	.	.
N	58	54	54	54	54	54	54	58	58	58	58
ENTRAINMENT SAMPLES - DURATION = 2,097 MIN | TOT_SEEN = 1,025 | RATE_SEEN = 0.48879 HYDRAULIC SAMPLES - DURATION = 2,412 MIN : MEASUREMENTS = 1,040											
Camera Location 26 Only											
COMBINED	**0.0001**	**0.0771**	0.1261	0.2559	0	**0.1124**	0.5742	**0.0001**	**0.0001**	0.2331	0.3110
GATESET	**0.0002**	**0.0246**	**0.0300**	**0.1928**	0	0.8286	0.4534	**0.0005**	**0.0005**	**0.1405**	0.3352
UNITLOAD	**0.1522**	0.3501	0.4236	0.4148	0	0.7463	0.2410	**0.0001**	**0.0001**	0.7991	0.3095
HOURSBEG	0.2789	0.4723	0.5967	0.2463	0	**0.1926**	0.2651	.	.	.	.
N	35	30	30	30	30	30	30	36	36	36	36
ENTRAINMENT SAMPLES - DURATION = 1,675 MIN | TOT_SEEN = 467 | RATE_SEEN = 0.27881 HYDRAULIC SAMPLES - DURATION = 2,083 MIN : MEASUREMENTS = 485											

(Sheet 2 of 3)

Table 37 (Concluded)

Camera Location 31 Only											
SOURCE	R_PERMIN	R_IMPNNEN	R_IMPNES	R_IMPNGI	R_IMPNGH	R_IMPNGN	R_IMPNGD	CURR_ANG	CUR_ANG9	CUR_ANCV	CURR_CV
COMBINED	**0.0558**	0.6343	0.2928	0.6929	0.7200	**0.4111**	0.9289	0.3548	0.3548	**0.0026**	**0.0022**
GATESET	0.4828	0.7747	0.3595	0.7005	0.7275	**0.0248**	0.6177	**0.1894**	**0.1894**	**0.0046**	**0.0027**
UNITLOAD	**0.1954**	0.9073	0.1247	0.9057	0.9948	**0.1501**	0.6887	0.9875	0.9875	**0.0140**	**0.0333**
HOURBEG	0.3589	0.6718	0.5958	0.8220	0.4336	**0.0507**	0.8144	.	.	.	.
N	31	29	29	29	29	29	29	33	33	33	33
ENTRAINMENT SAMPLES - DURATION = 1,318 MIN : TOT_SEEN = 451 | RATE_SEEN = 0.34219 HYDRAULIC SAMPLES - DURATION = 1,563 MIN : MEASUREMENTS = 463											
Camera Location 38 Only											
COMBINED	**0.0001**	0.5160	0.6324	0.5233	0	0.7500	0.4601	0.4653	0.4653	0.3791	0.6327
GATESET	**0.0233**	0.4830	0.4469	0.4748	0	0.7276	**0.1851**	**0.1894**	**0.1894**	0.2096	0.4811
UNITLOAD	**0.0088**	0.2277	0.6051	**0.1758**	0	0.3731	**0.1634**	0.6304	0.6304	0.3652	0.5770
HOURSBEG	**0.1074**	0.7847	0.8112	0.6481	0	0.7852	0.2977	.	.	.	.
N	33	30	30	30	30	30		36	36	36	36
ENTRAINMENT SAMPLES - DURATION = 2,079 : TOT_SEEN = 322 : RATE_SEEN = 0.15488 HYDRAULIC SAMPLES - DURATION = 2,419 MIN : MEASUREMENTS = 340											

(Sheet 3 of 3)

analyses, camera location has a significant effect (Tables 34 and 37) on current angle ($P = 0.0001$) and standard deviation of current angle ($P = 0.0001$).

a. *Unitload.* The second block of Table 34 presents summaries by unitload for all camera locations combined except camera location 2. The rest of Table 34 presents summaries by unitload for the different camera locations on the ESBS. Unitload had a statistically significant effect on imaging rate ($P = 0.0026$, Table 37) for all cameras combined, but the normal pattern of increased imaging rate with increasing discharge was discontinuous. However, for the summer analysis, beginning time and unitload, particularly for the 16 kcfs unitload (usually run near or after midnight) were highly correlated so that the effects of these two variables are confounded and cannot be separated. The pattern of reduction in passage noted around midnight conflicts with the increase in passage associated with increases in discharge. No other consistent patterns of unitload effects on impingement behavior were observed for the combined analysis.

Relatively few significant relationships between unitload and the dependent variables at the other camera locations were observed other than for imaging rate (Table 34). The statistically significant results obtained for the hydraulic variables (e.g., CURR_ANG, $P = 0.0554$, Table 37) at the different camera locations generally were less than the accuracy of our measurements and probably should not be considered.

b. *Closure gate position.* Table 35 summarizes the effects of closure gate position. Closure gate position has a nearly significant ($P = <0.14$) effect on the passage variables (R_IMPNEN and R_IMPNGN) and the contact-with-escape variable (R_IMPNES). The impingement variables were not significantly affected by closure gate position ($p > 0.20$, Table 37). Closure gate position also had a statistically significant effect on current angle averaged across the entire screen surface; however, the difference was less than the accuracy of our measurements.

Current angle at camera location 2 showed differences caused by closure gate position, but the pattern was different than that observed for the spring tests. That is, for the summer tests, the highest angle (flow most parallel to the bypass screen and moving towards the gate slot) was observed for the no gate and partial gate positions (about 168 versus 160 deg for CURR_ANG, $P = 0.0001$, Table 37). Additionally, the current angles for the upper screen locations appeared to be about 10 deg higher in the summer than in the spring. During the spring, unitload was varied from 12, 14, and 16 KCFS with the majority (30 out of 81 replicates) of the unitloads occurring at 16 KCFS (Table 24). However, in the spring, the unitloads varied from between 13, 15, and 16 KCFS with the majority of the unitloads occurring at 13 KCFS (82 out of 170 replicates). Alternatively, some of the difference in hydraulic patterns on the screen could be determined by unit or bay effects since spring tests were conducted in different units and bays than the summer

tests or some as yet undetermined factor could be influencing the flow pattern. In both seasons, the intermediate unitload was most parallel to the screen surface. Differences in current angles between closure gate positions were noted for camera locations 21 and 26, also. Only the no closure gate position (NG) was imaged at camera location 13 so that no statements concerning effects of gate position can be made. Several significant relationships were observed at camera location 26. However, a consistent pattern of increases/decreases among the different passage/impingement variables is not observed suggesting that a consistent effect of closure gate position is not evident at camera locations 21 and 26.

c. *Beginning time*. Occasional significant results were obtained for beginning time; however, the confounding effects of unitload make these relationships impossible to discern.

General Analyses

The general analysis contains four sections. The first section compares the effects of the month on impingement behavior and hydraulic variables. The second section describes the results of evaluations of the effect of the camera body and illumination system on impingement behavior. The third section describes efforts to use imaging to predict the descaling rate. The fourth section describes the results of efforts to estimate FGE using imaging technology.

Month

a. *General*. Tables 38 through 41 summarize the effects of the month on impingement/passage characteristics and hydraulic variables. The results summaries provided by Table 38 should be interpreted with caution because of differences in smolt size and behavior between months. Also, the results between the spring (Tables 24-27) and summer (Tables 34-37) unitload/closure gate evaluations cannot be directly compared because the range and distribution of unitloads were different and made direct comparisons between months difficult. The hydraulic variables were rounded to the nearest 2 kcfs.

Table 38 (top block) provides summaries by camera location for all months, unitloads, and beginning times combined. Camera location (CAMLOC) has a significant effect on imaging rate (R_PERMIN, P = 0.00241, Table 41), impingement rate (R_IMPNGD, P = 0.0115, Table 41), and escape rate (R_IMPNES, P = 0.0772, Table 41), and head first entrainment (R_IMPNGN, P = 0.0001, Table 41). The results for R_PERMIN mirror the findings for the summer analysis largely because the summer rates are high enough that they dominate the combined data. There was a significant effect of camera location on current angle (CURR_ANG, P = 0.0001, Table 41) and standard deviation of current angle (CURR_CV, P = 0.0484,

Table 38
Proportions of Springtime Smolts Exhibiting Different Impingement Behaviors by Camera Location and Unitload for All Months and Beginning Times Combined

Summary Proportions by Camera Location - All Cameras Combined Except Camera Location 2

CAMLOC	FREQ	R_IMPNGH	R_IMPNGI	R_IMPNGD	R_IMPNGN	R_IMPNEN	R_IMPNES	FREQ	R_PERMIN	MN_CRANG	MN_CRAN9	MN_CR9CV	MN_CRCV
13	14	0.0023810	0.28888	0.071695	0.10139	0.49393	0.30543	16	0.315860	140.556	50.5556	-11.6667	62.2222
21	32	0.0024182	0.30290	0.065390	0.07585	0.45958	0.61956	35	0.856150	123.889	33.8889	30.0000	3.8889
26	10	0.0000000	0.26793	0.026786	0.12920	0.49093	0.29111	14	0.103645	111.111	21.1111	13.8889	7.2222
31	14	0.0052910	0.30067	0.039418	0.15915	0.43807	0.35380	18	0.350528	96.818	6.8182	-1.3636	8.1818
38	19	0.0000000	0.24539	0.007219	0.35938	0.51673	0.38527	24	0.093064	75.385	14.6154	3.0769	11.5385

Summary Proportions by Unitload - All Cameras Combined Except Camera Location 2

UNITLOAD	FREQ	R_IMPNGH	R_IMPNGI	R_IMPNGD	R_IMPNGN	R_IMPNEN	R_IMPNES	FREQ	R_PERMIN	MN_CRANG	MN_CRAN9	MN_CR9CV	MN_CRCV
12	5	0.0000000	0.38167	0.000000	0.17333	0.23667	0.59000	9	0.041482	112.000	23.3333	9.3333	14.0000
14	40	0.0018519	0.25615	0.038910	0.20788	0.52661	0.30524	48	0.320518	105.660	23.2075	6.4151	16.7925
16	44	0.0025162	0.29850	0.056872	0.11394	0.45986	0.33015	50	0.585097	111.538	28.0769	13.2692	14.8079

Summary Proportions by Unitload - All Cameras Combined Except Camera Location 2 Only

12	3	0.0	0.38889	0.000000	0.00000	0.22222	0.61111	4	0.071667	150.000	60.0000	55.0000	5.00000
14	8	0.0	0.14774	0.059052	0.18675	0.76358	0.14181	8	0.156689	161.250	71.2500	65.0000	6.25000
16	9	0.0	0.18506	0.094633	0.07611	0.72451	0.11972	9	0.299035	162.222	72.2222	67.7778	4.44444

Summary Proportions by Unitload - All Cameras Combined Except Camera Location 13 Only

12	1	0.0000000	0.37500	0.000000	0.00000	0.25000	0.75000	2	0.041667	150.000	60.0000	53.3333	6.66670
14	7	0.0000000	0.31432	0.067059	0.14550	0.43842	0.35021	8	0.441667	136.667	46.6667	-18.8889	65.55560
16	6	0.0055556	0.24485	0.089052	0.06683	0.59935	0.17910	6	0.239516	141.667	51.6667	-33.3333	85.00000

(Continued)

Note: The ESBS was in unit/bay 6A in the spring and in unit/bay 5B in the summer. For both months, the 55 deg angled screen was deployed with no closure gate; the fyke net was present, was in the standard position, and had a screen porosity of 30 percent. A total of 128 measurements was made of the hydraulic variables.

Table 38 (Concluded)

CAMLOC	FREQ	R_IMPNGH	R_IMPNGI	R_IMPNGD	R_IMPNGN	R_IMPNEN	R_IMPNES	FREQ	R_PERMIN	MN_CRANG	MN_CRAN9	MN_CR9CV	MN_CRCV
Summary Proportions by Unitload - Camera Location 21 Only													
12	2	.0000000	0.50000	0.000000	0.16667	0.00000	0.83333	3	0.388889	115.000	25.0000	20.0000	5.00000
14	9	.0000000	0.27193	0.080138	0.08691	0.53627	0.22529	10	0.367389	123.000	33.0000	26.0000	7.00000
16	21	.0036848	0.29741	0.065297	0.06246	0.47048	0.31103	22	1.189759	125.909	35.9091	33.6364	2.27273
Summary Proportions by Unitload - Camera Location 26 Only													
12	1	0	0.20000	0.000000	0.20000	0.60000	0.20000	2	0.051667	105.000	15.0000	5.0000	10.0000
14	6	0	0.27358	0.020833	0.17159	0.47367	0.30701	7	0.128922	113.750	23.7500	20.0000	3.7500
16	3	0	0.27927	0.047619	0.02083	0.48909	0.28968	5	0.089048	111.667	21.6667	11.6667	10.0000
Summary Proportions by Unitload - Camera Location 31 Only													
12	1	0.000000	0.33333	0.000000	0.33333	0.33333	0.33333	2	0.035000	90.000	0.0000	-15.0000	15.0000
14	8	0.009259	0.21715	0.030093	0.17017	0.59579	0.28443	10	0.577045	96.923	6.9231	0	6.9231
16	5	0.000000	0.42778	0.062222	0.10667	0.20667	0.46889	6	0.078175	98.571	8.5714	0	8.5714
Camera Location 38 Only													
12	0	.	.	.	.	.	.	.	.	85.000	5.0000	-45.0000	50.0000
14	10	0	0.22196	0.000000	0.41235	0.55608	0.36130	13	0.115751	74.615	15.3846	6.9231	8.4615
16	9	0	0.27143	0.015873	0.30053	0.47302	0.41190	11	0.066252	74.546	15.4545	7.2727	8.1818

Table 39
Proportions of Smolts Exhibiting Different Impingement Behaviors by Month for All Discharges and Beginning Times Combined

Summary Proportions by Month - All Cameras Combined Except Camera Location 2												
MONTH	FREQ	R_IMPNGH	R_IMPNGI	R_IMPNGD	R_IMPNGN	R_IMPNEN	R_IMPNES	FREQ	R_PERMIN	MN_CRANG	MN_CRAN9	MN_CR9CV	MN_CRCV
5	22	0.0000000	0.35320	0.029590	0.07775	0.32320	0.49392	36	0.065617	109.592	21.6327	-8.5714	30.2041
7	67	0.0027580	0.26147	0.050862	0.18634	0.52793	0.28090	71	0.600716	108.592	27.8873	22.3944	5.4930
Camera Location 2 Only													
5	10	0	0.33667	0.046515	0.02000	0.37317	0.39520	10	0.125590	151.000	61.0000	53.0000	8.00000
7	11	0	0.10431	0.078087	0.17991	0.86947	0.00848	11	0.270509	167.273	77.2727	74.5455	2.72727
Camera Location 13 Only													
5	9	0.0000000	0.22249	0.01307	0.07789	0.56808	0.37403	9	0.096344	142.727	52.7273	-44.5455	97.27270
7	7	0.0047619	0.29170	0.12658	0.10264	0.54318	0.12997	7	0.598095	137.143	47.1429	40.0000	7.14290
Camera Location 21 Only													
5	8	0.0000000	0.38765	0.041667	0.059524	0.26637	0.59375	10	0.070897	111.818	21.8182	17.2727	4.54545
7	24	0.0032242	0.27466	0.073297	0.081296	0.52399	0.22816	25	1.170251	129.200	39.2000	35.6000	3.60000
Camera Location 26 Only													
5	3	0	0.33333	0.000000	0.06667	0.33333	0.38333	7	0.045714	105.455	15.4545	6.3636	9.09091
7	7	0	0.23990	0.038265	0.15601	0.55847	0.25158	7	0.161575	120.000	30.0000	25.7143	4.28571
Camera Location 31 Only													
5	3	0.00000	0.44444	0.066667	0.11111	0.17778	0.42222	6	0.061667	92.000	2.0000	-11.0000	13.0000
7	11	0.00673	0.26146	0.031987	0.17225	0.50906	0.33514	12	0.494958	100.833	10.8333	6.6667	4.1667
Camera Location 38 Only													
5	1	0	0.33333	0.000000	0.00000	0.33333	0.33333	4	0.024039	81.667	8.3333	-13.3333	21.6667
7	18	0	0.24051	0.007937	0.37935	0.52692	0.38816	20	0.106869	73.500	16.5000	8.0000	8.5000

Note: The ESBS was in unit/bay 6A in the spring and in unit/bay 5B in the summer. For both months, the screen was deployed with no closure gate, had no fyke net, had a screen angle of 55 deg, was in the standard position, and had a screen porosity of 30 percent.

Table 40
Proportions of Springtime Smolts Exhibiting Different Impingement Behaviors by Beginning Time for Both Months and All Discharges Combined

All Cameras Combined Except Camera Location 2												
HOURBEG	FREQ	R_IMPNGH	R_IMPNGI	R_IMPNGD	R_IMPNGN	R_IMPNEN	R_IMPNES	FREQ	R_PERMIN	MN_CRANG	MN_CRAN9	MN_CR9CV	MN_CRCV
20	26	0.0042226	0.26940	0.078027	0.20822	0.53922	0.28114	27	0.434251	108.333	25.0000	17.6667	7.3333
22	30	0.0013889	0.27092	0.032358	0.15825	0.49052	0.30887	36	0.752781	112.143	26.9048	18.5714	8.3333
24	29	0.0011494	0.30096	0.36528	0.13910	0.43461	0.38641	38	0.151736	106.098	24.3902	5.3659	19.0244
26	4	0.0000000	0.35714	0.00000	0.00000	0.28571	0.47619	6	0.070370	110.000	22.8571	-51.4286	74.2857
Camera Location 2 Only													
20	6	0	0.13323	0.06479	0.22457	0.79833	0.08150	6	0.198234	165.000	75.0000	73.3333	1.6667
22	6	0	0.27306	0.06333	0.05722	0.51722	0.30556	7	0.20217	157.143	67.1429	61.4286	5.7143
24	7	0	0.16806	0.05077	0.06975	0.71466	0.18899	7	0.220662	158.571	68.5714	61.4286	7.1429
26	1	0	0.40000	0.20000	0.00000	0.40000	0.40000	1	0.083333	150.000	60.0000	50.0000	10.0000
Camera Location 13 Only													
20	4	0.0000000	0.21728	0.10441	0.15858	0.66985	0.10049	4	0.279968	137.500	47.5000	37.500	10.000
22	4	0.0000000	0.29172	0.04235	0.10462	0.45891	0.34203	5	0.535000	145.000	55.0000	48.333	6.667
24	4	0.0083333	0.26994	0.10417	0.09167	0.56429	0.23363	5	0.204000	138.333	48.3333	-45.000	93.333
26	2	0.0000000	0.46429	0.00000	0.00000	0.07143	0.78571	2	0.119444	140.000	50.0000	-190.000	240.000

(Continued)

Table 40 (Concluded)

HOURBEG	FREQ	R_IMPNGH	R_IMPNGI	R_IMPNGD	R_IMPNGN	R_IMPNEN	R_IMPNES	FREQ	R_PERMIN	MN_CRANG	MN_CRAN9	MN_CR9CV	MN_CRCV
Camera Location 21 Only													
20	9	0.0039683	0.31725	0.12726	0.11041	0.49276	0.26495	9	0.802170	125.55	35.5556	32.222	3.333
22	13	0.0032051	0.31352	0.05395	0.08207	0.42690	0.32108	14	1.404524	124.66	34.6667	30.000	4.667
24	9	0.0000000	0.30688	0.02731	0.04074	0.41356	0.40747	11	0.274156	122.72	32.7273	30.000	2.727
26	1	0.0000000	0.00000	0.00000	0.00000	1.00000	0.00000	1	0.066667	110.00	20.0000	10.000	10.000
Camera Location 26 Only													
20	2	0	0.26136	0.062500	0.35227	0.53977	0.35227	3	0.058333	108.00	18.0000	8.000	10.0000
22	3	0	0.17292	0.000000	0.17500	0.65417	0.12917	4	0.166029	111.66	21.6667	16.667	5.0000
24	5	0	0.32756	0.028571	0.01250	0.37345	0.36381	6	0.096429	113.33	23.3333	15.000	8.3333
26	0	•	•	•	•	•	•	•	•	110.00	20.0000	20.000	0.0000
Camera Location 31 Only													
20	5	0.014815	0.25481	0.068148	0.18159	0.55852	0.34370	5	0.521301	98.33	8.3333	-3.3333	11.6667
22	5	0.000000	0.25930	0.020000	0.15736	0.50141	0.29805	7	0.454849	97.14	7.1429	0.0000	7.1429
24	3	0.000000	0.37963	0.037037	0.17778	0.27778	0.47037	5	0.090476	95.71	5.7143	0.0000	5.7143
26	1	0.000000	0.50000	0.000000	0.00000	0.00000	0.33333	1	0.066667	95.00	5.0000	-5.0000	10.0000
Camera Location 38 Only													
20	6	0	0.24722	0.000000	0.36222	0.50556	0.35000	6	0.100646	73.33	16.6667	11.6667	5.0000
22	5	0	0.21392	0.000000	0.39004	0.57215	0.36926	6	0.152284	77.50	12.5000	-7.5000	20.0000
24	8	0	0.26369	0.017857	0.33810	0.49048	0.42173	11	0.063571	74.54	15.4545	6.3636	9.0909
26	0	•	•	•	•	•	•	•		80.00	10.0000	0.0000	10.0000

Table 41
Summary of Probabilities from Analysis of Variance (P ≤ 0.20 are in bold) for Effects of Unitload, Month, Beginning Time, and Camera Location on Entrainment and Hydraulic Variables

Combined Analysis

SOURCE	R_PERMIN	R_IMPNNEN	R_IMPNES	R_IMPNGI	R_IMPNGH	R_IMPNGN	R_IMPNGD	CURR_ANG	CUR_ANG9	CUR_ANCV	CURR_CV
COMBINED	**0.0001**	**0.0196**	**0.0006**	**0.1781**	0.8025	**0.0001**	**0.0030**	**0.0001**	**0.0001**	**0.0740**	**0.0335**
MONTH	**0.1304**	**0.0180**	**0.0013**	**0.0840**	0.3314	**0.1173**	0.1715	**0.0001**	**0.0001**	**0.0100**	**0.0542**
UNITLOAD	**0.0023**	0.5150	**0.1999**	0.6124	0.7573	**0.0935**	0.2707	**0.1117**	0.5189	0.5189	0.5423
HOURBEG	**0.0005**	0.3358	**0.1307**	0.8043	0.6299	0.3923	**0.0162**	•	•	•	•
CAMLOC	**0.0241**	0.6079	**0.0772**	0.6867	0.6129	**0.0001**	**0.0115**	**0.0001**	0.3211	0.3211	**0.0484**
N	107	89	89	89	89	89	89	120	120	120	120

ENTRAINMENT SAMPLES - DURATION = 4,934 MIN : TOT_SEEN = 1,118 SMOLTS : RATE_SEEN = 0.22659 SMOLTS/MIN
HYDRAULIC SAMPLES - DURATION = 8,767 MIN : MEASUREMENTS = 2,480

Camera Location 2 Only

COMBINED	**0.0162**	**0.0002**	**0.0001**	**0.0026**	0.0000	**0.0130**	0.3568	**0.0001**	**0.0001**	**0.0011**	0.2937
MONTH	**0.1215**	**0.0001**	**0.0002**	**0.0045**	0.0000	**0.0162**	0.9789	**0.0001**	**0.0001**	**0.0003**	**0.0692**
UNITLOAD	**0.0638**	**0.1381**	**0.0603**	0.2948	0.0000	**0.1203**	0.2643	0.8201	0.8201	0.8117	0.5341
N	21	20	202	0	20	20	20	21	21	21	21

ENTRAINMENT SAMPLES - DURATION = 1,482 MIN : TOT_SEEN = 294 SMOLTS : RATE_SEEN = 0.19838
HYDRAULIC SAMPLES - DURATION = 2,155 MIN : MEASUREMENTS = 466

(Sheet 1 of 3)

Note: For each variable there were 3 classes of unitload (12, 14, and 16 kcfs), 2 months (May and July), 4 beginning times (2000, 2200, 2400, and 2600 hr), and 5 camera locations (13, 21, 26, 31, and 38 ft from the top of the screen). Probabilities are based on Type III sum of squares to reduce confounding effects of other variables. The analysis tests the hypothesis that the means of the different entrainment/impingement and hydraulic variables are not different by the treatment variables.

Table 41 (Continued)

SOURCE	R_PERMIN	R_IMPNNEN	R_IMPNES	R_IMPNGI	R_IMPNGH	R_IMPNGN	R_IMPNGD	CURR_ANG	CUR_ANG9	CUR_ANCV	CURR_CV
Camera Location 13 Only											
COMBINED	**0.0004**	0.4187	**0.0150**	0.7527	0.3369	0.3887	**0.0182**	**0.1252**	**0.1252**	0.5875	0.4850
MONTH	**0.0036**	0.3626	**0.0081**	0.9350	**0.1529**	0.4420	**0.0037**	0.6608	0.6608	0.3217	**0.1683**
UNITLOAD	0.8235	0.3151	**0.0492**	0.5650	0.2971	0.2367	**0.1679**	**0.1335**	**0.1335**	0.5168	0.5428
N	16	14	14	14	14	14	14	18	18	18	18
ENTRAINMENT SAMPLES - DURATION = 700 MIN : TOT_SEEN = 199 | RATE_SEEN = 0.28429 HYDRAULIC SAMPLES - DURATION = 290 MIN : MEASUREMENTS = 152											
Camera Location 21 Only											
COMBINED	**0.0538**	**0.0028**	**0.0001**	**0.0619**	0.6860	**0.1102**	0.6813	**0.0001**	**0.0001**	**0.0001**	**0.0825**
MONTH	**0.0647**	**0.0526**	**0.0001**	**0.1668**	0.4971	**0.1013**	0.6560	**0.0001**	**0.0001**	**0.0001**	0.9933
UNITLOAD	0.3153	**0.0559**	**0.0113**	0.2688	0.6594	**0.0633**	0.6851	**0.0335**	**0.0335**	**0.0518**	**0.0422**
N	35	32	32	32	32	32	32	36	36	36	36
ENTRAINMENT SAMPLES - DURATION = 1,410 MIN | TOT_SEEN = 549 | RATE_SEEN = 0.38936 HYDRAULIC SAMPLES - DURATION = 965 MIN : MEASUREMENTS = 1,040											
Camera Location 26 Only											
COMBINED	**0.1304**	**0.1421**	0.5723	**0.1667**	0.0000	**0.0566**	0.8388	**0.0001**	**0.0001**	**0.0074**	0.3450
MONTH	**0.0386**	**0.0336**	0.2113	**0.0437**	0.0000	**0.0268**	0.5987	**0.0001**	**0.0001**	**0.0020**	0.3402
UNITLOAD	0.6944	**0.1910**	0.5465	**0.1758**	0.0000	**0.0383**	0.9475	0.6517	0.6517	0.2598	0.3744
N	14	10	10	10	10	10	10	18	18	18	18
ENTRAINMENT SAMPLES - DURATION = 722 MIN | TOT_SEEN = 80 | RATE_SEEN = 0.11080 HYDRAULIC SAMPLES - DURATION = 2,083 MIN : MEASUREMENTS = 485											

(Sheet 2 of 3)

Table 41 (Concluded)

Camera Location 31 Only											
SOURCE	R_PERMIN	R_IMPNNEN	R_IMPNES	R_IMPNGI	R_IMPNGH	R_IMPNGN	R_IMPNGD	CURR_ANG	CUR_ANG9	CUR_ANCV	CURR_CV
COMBINED	**0.0796**	**0.0508**	0.3515	**0.0458**	0.8912	0.2122	0.5303	**0.0001**	**0.0001**	**0.0001**	**0.0285**
MONTH	0.4105	0.3884	0.9813	0.2821	1.0000	**0.1481**	0.3062	**0.0001**	**0.0001**	**0.0001**	**0.0095**
UNITLOAD	0.2182	**0.1115**	0.2646	**0.1063**	0.8260	**0.1406**	0.4650	**0.0287**	**0.0287**	**0.1728**	0.8621
N	18	14	14	14	14	14	14	22	22	22	22
ENTRAINMENT SAMPLES - DURATION = 687 MIN | TOT_SEEN = 161 | RATE_SEEN = 0.23435 HYDRAULIC SAMPLING - DURATION = 1,563 : MEASUREMENTS = 463											
Camera Location 38 Only											
SOURCE	**0.0864**	0.4853	0.7820	0.4759	0.0000	0.2886	0.5296	**0.0088**	**0.0088**	**0.0010**	**0.0023**
MONTH	**0.0841**	0.4469	0.6755	0.5252	0.0000	0.2109	0.6212	**0.0212**	**0.0212**	0.5040	0.8882
UNITLOAD	**0.1692**	0.4722	0.5237	0.3970	0.0000	0.5312	0.2764	0.4910	0.4910	**0.0049**	**0.0033**
N	24	19	19	19	19	19	19	26	26	26	26
ENTRAINMENT SAMPLES - DURATION = 1,415 : TOT_SEEN = 129 : RATE_SEEN = 0.091166 HYDRAULIC SAMPLES - DURATION = 2,419 MIN : MEASUREMENTS = 340											

(Sheet 3 of 3)

Table 41). Flow is most parallel to the screen nearest the slot and tends to be perpendicular or past perpendicular at the toe of the screen (Table 38).

b. *Unitload.* Unitload (combined for all camera locations except location 2 - Table 38, second block) has a highly significant effect on R_PERMIN (P = 0.0023, Table 41) and a significant effect on contact and escape (R_IMPNES, P = 0.1999, Table 41) and headfirst entrainment without contact (R_IMPNGN, P = 0.0935, Table 41). R_PERMIN follows the expected pattern of increased imaging rate with increased discharge (Table 38, second block). Impingement rate (R_IMPNGD) and head first impingement (R_IMPNGH) also increase with discharge although the increase is not significant. In general, it seems that increased unitload results in increased screen contact.

The rest of Table 38 presents the effects of unitload at specific camera locations on impingement/entrainment variables and hydraulic variables. Replicate values for variables for the 12 kcfs unitload occur more than once only at camera locations 2 and 21. Consequently, trends based on the full range of unitloads are probably difficult to discern. However, the 14 and 16 kcfs unitloads are reasonably well represented, and several patterns are apparent. Headfirst entrainment without screen contact (R_IMPNGN) decreases with increasing unitload at all camera locations. Entrainment without screen contact (R_IMPNEN) decreases with unitload for all camera locations except 13 and 26.

c. *Month.* Table 39 presents data summaries by month for all discharges and beginning times combined. Month has a significant effect on all variables except headfirst impingement. Imaging rate (R_PERMIN) is an order of magnitude higher in the summer (0.60 vs 0.07 smolts per min, P = 0.1304, Table 18) than in the spring. The passage variables (R_IMPNGN and R_IMPNEN) are significantly higher in the summer than in the spring (0.08 versus 0.19 for R_IMPNGN, P = 0.12; 0.32 versus 0.53 for R_IMPNEN, P = 0.02). The two impingement variables behave differently across the two seasons. R_IMPNGI is higher in the spring (0.35 versus 0.26, P = 0.08) than in the summer. R_IMPNGD is higher in the summer. However, inspection of the camera-by-camera values indicates that there were few smolts observed in the spring at the deeper cameras. The 0.0's observed for the R_IMPNGD index probably reflect low numbers of smolts as opposed to impingement on the screen. Consequently, the results provided by the R_IMPNGI index more realistically reflect the impingement characteristics of smolts in the two months (i.e., screen contact and probably impingement are higher in the spring). Surprisingly, there were statistically significant differences in the hydraulic variables between the two months (P = 0.0001 for water angle and P = 0.05 for variance of water angle, Table 41). Inspection of the hydraulic variables at specific camera locations indicates that in the spring, flows were more nearly perpendicular to the screen (P = 0.0001 for water angle,

Table 18), and this flow characteristic may account for increased impingement and decreased passage of smolts in the spring.

The cause of these differences in hydraulic patterns between months is not completely known because bay and unit effects were not controlled, but probably they reflect differences in unitloads between the months. During the spring, unitload was varied from 12, 14, and 16 kcfs with the majority (30 out of 81 replicates) of the unitloads occurring at 16 kcfs (Table 24). However, in the summer, the unitloads varied from between 13, 15, and 16 kcfs with the majority of the unitloads occurring at 13 kcfs (82 out of 170 replicates).

d. Beginning time. Table 40 (top block) summarizes the effects of starting time on the impingement/passage variables. The R_IMPNGD index (P = 0.0162, Table 41) decreased as starting time increased. However, this analysis suffers from low numbers of observations after 2400 hr. Consequently, the analysis is probably weighted by the 0.0 value for R_IMPNGD after midnight and does not reflect a valid assessment. Starting time also heavily influenced imaging rate (R_PERMIN, P = 0.0005, Table 41) with the majority of smolts observed at 2200 hr. The imaging rate of the summer probably dominated this pattern since it is almost an order of magnitude higher than the imaging rate of the spring. Screen contact with escape also increases with later beginning times (R_IMPNES, P = 0.1307, Table 41). However, the reason for this is unknown.

The rest of Table 40 presents camera location specific summaries of the effects of beginning time on the impingement behavior and hydraulic variables.

Camera body and light system bias

a. Camera mounting system bias. Observation of fishes swimming past the camera mounting system on the central beam of the SSTS indicates that smolts do not concentrate in the wake of the mounting system. The smolts swim around the mount without apparent response other than to avoid contact with the structure of the mount (Figure 16). Based on these qualitative assessments, it is concluded that the mounting system does not alter the response of the smolts to the screen design or deployment configuration being evaluated.

b. Camera illumination system bias. In light bias studies, video images of 208 smolts were collected, and the data was separated into 44 replicates placing no restrictions on the denominator of the proportions, as was done for the R_PERMIN variable reported for the bypass screen studies. However, analysis was restricted to blocks in which 5 or more smolts were observed. The restricted analysis separated 132 smolts separated into 18 replicates. Limiting the data to those proportions based on 5 or more smolts maximized the sensitivity of the

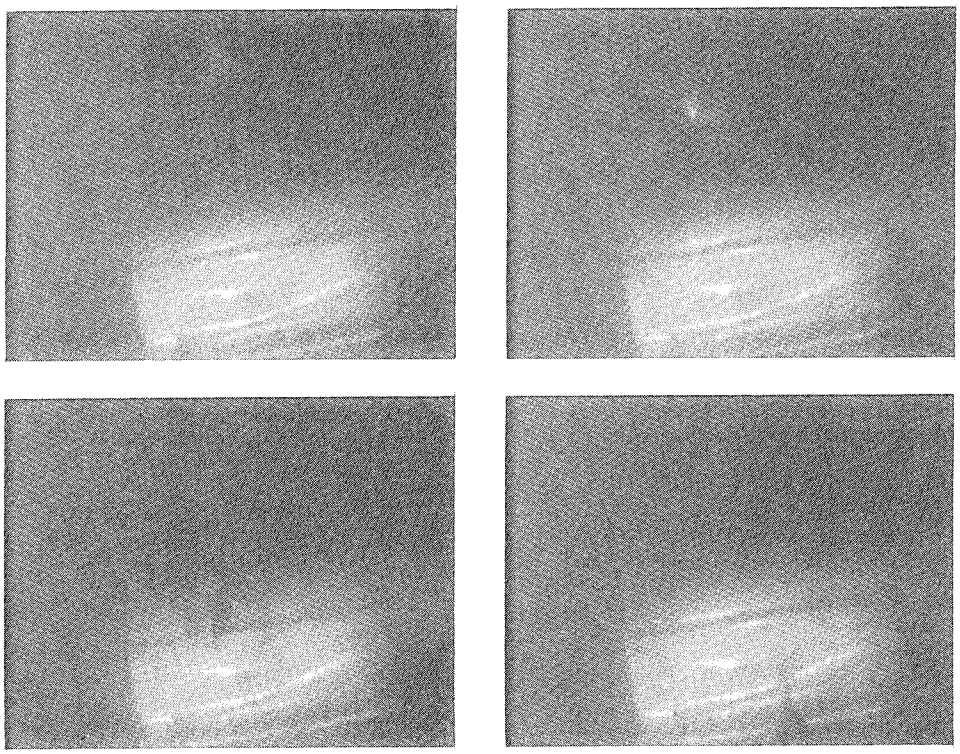

Figure 16. Sequence of photographs showing passage of a smolt around camera and camera mounting hardware going clockwise beginning with the upper left hand corner. a) The smolt is approaching directly over the camera mounting pipe (turned cross wise against the field of view), b) is directly over the mounting pipe, c) is moving over the pipe mount towards the camera, d) proceeds past the mounting pipe without hesitation. The presence of the camera mounting pipe appeared to have no influence on the passage of the smolt over the center beam of the screen, other than a small deviation in path to avoid hitting the pipe mount

index and still provided for sufficient degrees of freedom to perform the analysis.

Data summaries by camera location, beginning time, and illumination setting are presented in Tables 42 through 44. Note that the majority (12 of 18) of the replicates were obtained from camera locations 13 and 31 (Table 42). Camera location 21 provided no observations. No consistent pattern of effect caused by camera location was observed (Table 45). However, when better representation for camera location was obtained by using time blocks when 3 or more smolts were observed (not reported) instead of the blocks where 5 or more smolts were observed, camera location became a significant variable.

Data summaries of results by beginning time are presented in Table 43. Beginning time could not be evaluated by ANOVA concurrently with illumination setting and camera location because too few observations were

Table 42
Summary of Impingement Variables by Camera Location (LOCATION)

		Mean			Standard Deviation			Coefficient of Variation		
Location	Freq	R-IMPNGI	IMPINGED	SEEN	R_IMPNGI	IMPINGED	SEEN	R_IMPNGI	IMPINGED	SEEN
2	2	0.30000	1.50000	5.0	0.00000	0.00000	0.00000	0.0000	0.0000	0.0000
13	6	0.40394	4.25000	10.5	0.11097	2.20794	4.72229	27.4731	51.9515	44.9742
26	2	0.45000	2.25000	5.0	0.07071	0.35355	0.00000	15.7135	15.7135	0.0000
31	6	0.43333	2.41667	5.5	0.08165	0.73598	0.83666	18.8422	30.4543	15.2120
38	2	0.28636	2.25000	8.0	0.01928	1.06066	4.24264	6.7344	47.1405	53.0330

Table 43
Summary of Impingement Variables by Beginning Time (HOURBEG)

		Mean			Standard Deviation			Coefficient of Variation		
Hourbeg	Freq	R-IMPNGI	IMPINGED	SEEN	R_IMPNGI	IMPINGED	SEEN	R_IMPNGI	IMPINGED	SEEN
20	2	0.5000	4.7500	9.500	0.0000	3.1820	6.3640	0.0000	66.9891	66.989
21	2	0.5000	2.7500	5.500	0.0000	0.3536	0.7071	0.0000	12.8565	12.857
22	2	0.3306	4.0000	11.500	0.0432	3.5355	9.1924	13.0726	88.3883	79.934
23	6	0.3975	3.0000	7.667	0.0936	1.1402	2.5033	23.5485	38.0058	32.652
24	6	0.3417	1.8333	5.500	0.0917	0.4083	1.2247	26.8514	22.2681	22.268

Table 44
Summary of Impingement Variables by Illumination Setting (ILLUMSET)

		Mean			Standard Deviation			Coefficient of Variation		
Illumset	Freq	R-IMPNGI	IMPINGED	SEEN	R_IMPNGI	IMPINGED	SEEN	R_IMPNGI	IMPINGED	SEEN
63	3	0.36667	1.83333	5.000	0.013333	0.3333	0.0000	31.4918	31.4918	0.0000
125	8	0.36690	2.31250	6.625	0.009656	0.2812	4.8393	26.7821	22.9332	33.2051
188	2	0.33056	4.00000	11.500	0.001867	12.5000	84.5000	13.0726	88.3883	79.9338
250	5	0.48000	4.00000	8.200	0.002000	4.1250	14.7000	9.3169	50.7752	46.7568

available. However, there appears to be a decrease of the impingement index after 2100 hr. No effect of beginning time on the number of impinged fish (TOT_IMP) or number seen per replicate (TOT_SEEN) could be discerned.

Table 44 presents summaries of the data by illumination setting (ILLUMSET). Illumination setting did not affect the impingement index (R_IMPNGI, P = 0.4336, Table 46); however, it did affect both the number

Table 45
Summary of Regression Analysis to Determine Descaling Rate from Video Imaging Variables

Dependent variable - DESCALE

R-square = 0.57550493 C(p) = 3.93973857

	DF	Sum of Squares	Mean Square	F	Prob > F
Regression	2	0.00928925	0.00464463	4.75	0.0498
Error	7	0.00685179	0.00097883		
Total	9	0.01614104			

Variable	Parameter Estimate	Standard Error	Type II Sum of Squares	F	Prob > F
INTERCEP	-0.04815256	0.07405438	0.00041385	0.42	0.5363
R_IMPNGI	-0.36579344	0.15492377	0.00545685	5.57	0.0503
CURR_ANG	0.00256410	0.00083705	0.00918490	9.38	0.0182

Note: Note the reverse slopes of the coefficients from expected relationships.

Table 46
Summary of Probabilities from ANOVA (P ≤ 0.20 are in bold) for Light Bias Testing

SOURCE	R_PERMIN	R_IMPNGI	TOT_IMP	SEEN
COMBINED	**0.0178**	0.2581	**0.0502**	**0.0164**
CAMLOC	**0.0051**	0.4794	**0.0749**	**0.0150**
ILLUMSET	0.4556	0.3995	**0.0717**	**0.0311**
N	44	18	18	18

DURATION = 1,080 MIN
TOT_SEEN = 132 SMOLTS
RATE_SEEN = 0.12222 SMOLTS/MIN

of fishes meeting the impingement index requirements (TOT_IMP, P = 0.0717, Table 45) and the total of fishes seen (SEEN, P = 0.0311, Table 45). It is inferred that increased setting of the light intensity expanded the field of vision which resulted in an increased ability to image smolts on the screen surface. However, the light setting did not appear to affect impingement behavior. Experience has shown that optimum light setting for video imaging is approximately 60 percent of maximum (about 150 W). Note that the highest values for the number seen and the number impinged occurs at the 75 percent setting (about 188 W) and not at the maximum illumination setting.

Figure 17 shows the illumination fields associated with the four light settings used in the light bias testing.

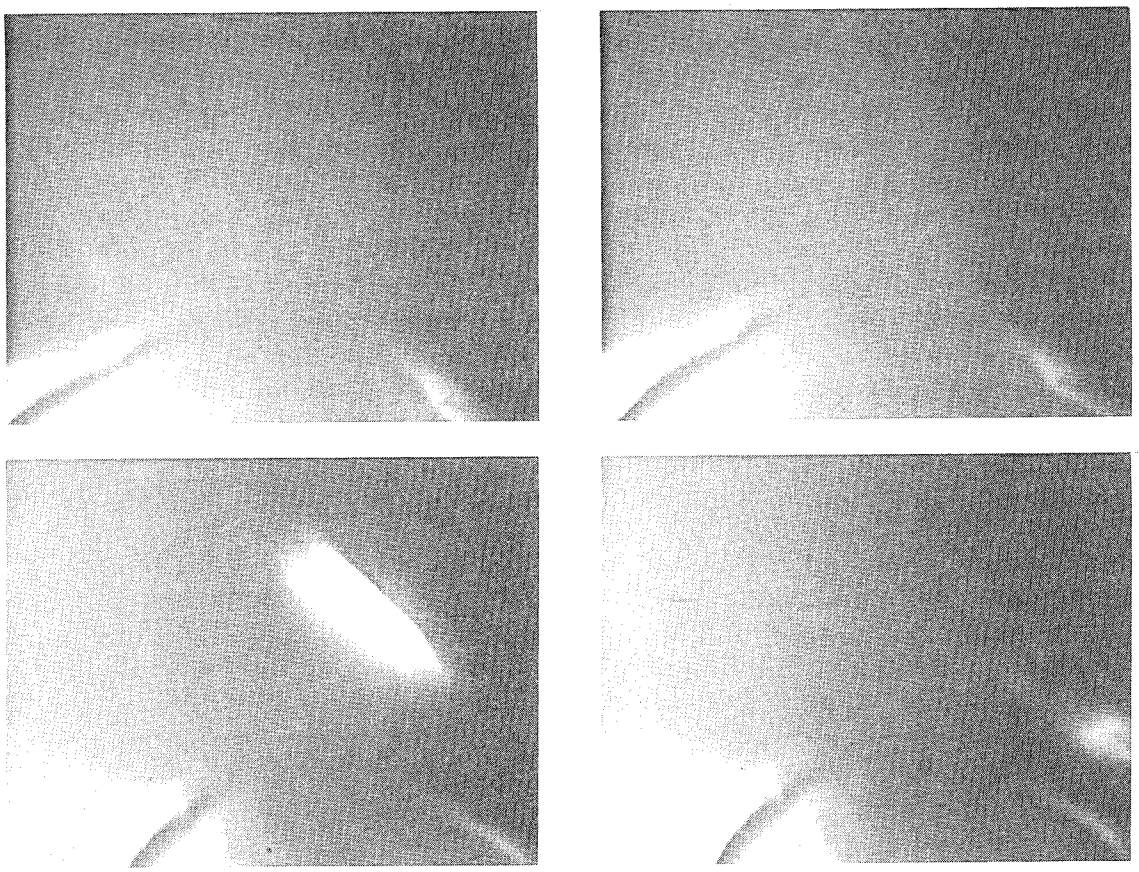

Figure 17. Sequence of photographs taken from video images showing changes in light field associated with 25 percent (upper) and 100 percent (lower) light intensity setting. Note the increase in illumination field associated with the increased light intensity. Screen mesh is at the bottom of each photograph. Two tie-down bars are visible on the mesh. Smolts can be seen passing from left to right on upper (faint) and lower (bright) photographs

Evaluations in this report of the potential bias introduced by the light field were restricted to the SSTS. Our observations of the bar screen video images indicate a considerable reflection off of the bar screen that may affect smolt behavior. Future video imaging work should include an evaluation of the light bias on a bar screen as well as during the summer months for both screen designs.

All fish collection gears have inherent biases. The problems associated with interpreting and reconciling conflicting data obtained from gillnets, electroifishing, and hydroacoustics are well known. Video imaging also has inherent limitations and biases that cannot be completely eliminated. However, video imaging provided direct characterization of the hydraulic environment within the intake and provided the first evidence of smolt

behavior in the vicinity of prototype screens under prototype operations. The information obtained by video imaging is valuable even if a component of the information is biased.

Descaling

Results of regression analysis to predict descaling rates from video imaging information are presented in Table 45. The descaling summary variable DESCALE is defined as the total number of smolts of all species combined exhibiting descaling damage divided by the total number of smolts of all species captured in gatewell dipping. Note that video imaging information explained 57 percent of the variability in the descaling rate. The two video imaging variables, R_IMPNGI (impingement index) and CURR_ANG (current angle of the water to the screen) were highly significant. A three variable model, which included R_IMPNGD (impingement rate) explained over 70 percent of the variability in descaling. The three variable model was not selected because only 9 observations were available for the analysis. However, the trend suggested by the three variable model suggests that video imaging information has the potential for directly determining the descaling rate.

Surprisingly, the slopes of the coefficients for the video imaging variables were opposite from what was expected. As R_IMPNGI increases, descaling rate decreases. Similarly as the flow becomes more parallel to the screen, descaling rate increases. The significant probabilities and relatively high R-square both indicate that these results are probably not spurious and that an effort should be made to reconcile these conflicting patterns. Several explanations are possible for these counterintuitive results. First, the descaling data and video imaging data were collected in different units and bay numbers; hydraulic model studies suggest that there may be significant bay effects. Consequently, the results may represent the effect of yet undetermined bay or unit effects. A more likely explanation is that, for a bar screen, the conditions thought to result in increased descaling manifest themselves by increasing gap loss. Many of the smolts observed passing through the gap were observed to be stunned or injured. Thus, increased descaling may be a product of decreased gap loss and not a product of poor guidance on the screen surface. Conversely, a portion of the descaling rates reported during FGE tests may be due to upriver causes or handling methods during collection. The apparent reverse effect of video imaging variables on descaling rate, particularly in light of the findings from the gap loss portion of this study, is a major source of uncertainty and should be resolved by more detailed studies in the future.

Future studies of descaling using video cameras should include simultaneous imaging of the bypass screen, the gap, and the VBS. As the results suggest, locating cameras on only part of the system may produce an incomplete or misleading conclusion.

Using video imaging to estimate FGE

No specific studies or analyses were performed to determine the potential use of video imaging methods to estimate FGE. However, field experience and evaluation of the video imaging data suggest that, with some modification from those methods used in this study, video imaging technology can be employed to quantify or optimize the efficiency of parts or all of a bypass system (at least from the bypass screen to the orifice).

Use of cameras to quantify guidance (but not FGE) in the same sense that fyke nets are employed is not possible because video imaging cannot determine the proportion of fishes that is not intercepted by the bypass system. However, video imaging could be employed as a component of a system in which non-video based methods (e.g., fixed-aspect hydroacoustics or gated, intensified video systems) were employed to quantify the total number of smolts entering the intake or to determine the number of smolts not intercepted by the bypass system.

Estimating fish passage rates on the bypass screens is hindered by the effects of unquantified effects on smolts such as unit/bay/operational conditions pressing smolts closer to the screen and hence increasing the probability of imaging. That is, imaging rates may increase because the imaging efficiency of the video cameras increases not because more smolts are passing through the bypass system. Variability of the hydraulic field makes selection of standard imaging locations difficult. The relatively short imaging distance of 2 to 4 ft and unpredictable changes in turbidity require multiple cameras and introduce uncertainty in fish passage rates estimated using video imaging.

Fish in the gate slot can be relatively easily imaged because the narrow confines of the slot force most of the smolts within range of the cameras. However, the rate at which fish exit through the orifice is probably reduced from the rate at which they enter the slot from the bypass screen. Hence, any effort to estimate fish passage up the VBS must incorporate the effects of slot-departure rates through the orifice. Estimating slot-departure rates with sufficient confidence for estimating smolt passage is problematic at best. Thus, video imaging of the orifices probably would provide the best deployment for estimating fish passage through the bypass system.

VBS

The VBS evaluation is separated into three sections. The first section (Tables 47 and 48) presents simple statistical descriptions of the dependent and independent variables and a correlation analysis of the independent and dependent variables. Correlation analysis was used to identify potentially confounding influences among the independent variables and to identify overlap among the dependent variables. The second section (Tables 49 through 52) describes the relationship between available simple hydraulic variables, i.e., current angle, standard deviation of current angle (used as a surrogate for

Table 47
Simple Statistics for Dependent and Independent Variables for Analysis of MBFVBS

Variable	N	Mean	Std Dev	Sum	Minimum	Maximum
Dependent Variables						
R_PERMIN	59	16.946348	17.753717	999.834519	0.066667	66.030769
R_TSCRN	59	0.490349	0.103611	28.930608	0	0.731707
R_TCAMR	59	0.004688	0.012067	0.276584	0	0.062500
R_WFLOW	59	0.780403	0.149123	46.043794	0.516539	1.000000
R_NOCTRL	59	0.007966	0.35815	0.469977	0	0.265306
R_CONTCT	59	0.229794	0.139563	13.557858	0.014493	0.666667
R_CONTES	59	0.165384	0.136564	9.757660	0	0.555556
R_CONTNO	59	0.064410	0.077298	3.800199	0	0.375000
Independent Variables						
CAMLOC	59	3.067797	1.472324	181.000000	1.000000	5.000000
UNITLOAD	59	13.813559	1.332286	815.000000	12.000000	16.000000
GATE	59	2.389831	0.743175	141.000000	1.000000	3.000000
HOURBEG	59	21.508475	1.369280	1269.000000	20.000000	24.000000
CURR_ANG	59	149.491525	26.091598	8820.000000	60.000000	180.000000
VAR CURR	59	11.186441	13.009909	660.000000	0	60.000000

Note: A total 33,334 smolts were imaged and analyzed over a total imaging duration of 1977.5 min (all cameras combined).

turbulence), and unitload (used as a very crude surrogate for velocity). This section includes the presentation of data summaries combined for all camera locations except camera location 1B and separately for each camera location to aid in identifying trends and patterns of the variables across the MBFVBS surface. An ANOVA, using the data blocked by camera location (excluding camera location 1B which is located on the bypass screen and was used to determine gap loss), was used to describe the strength of the effects of the hydraulic variables. The value of the hydraulic variables for predictive purposes is explored with multiple regression. The third section evaluates the influence of operating conditions (unitload) and deployment configuration (gate setting) on both impingement variables and hydraulic variables. Sufficient numbers of observations were available to analyze data for both unitload and gate setting.

Table 48
Pearson Correlation Coefficients for Dependent and Independent Variables for the Summer MBFVBS Analysis

Dependent Variables

	R_PERMIN	R_TSCRN	R_TCAMR	R_WFLOW	R_NOCTRL	R_CONTCT	R_CONTES	R_CONTNO
R_PERMIN	1.00000 0.0	-0.03548 0.7896	-0.14375 0.2774	-0.57500 0.0001	-0.11351 0.3920	0.06780 0.6099	0.23436 0.0740	-0.29461 0.0250
R_TSCRN	-0.03548 0.7896	1.00000 0.0	-0.07764 0.5589	-0.02093 0.8750	-0.36658 0.0043	-0.38230 0.0028	-0.42395 0.0008	0.05876 0.6585
R_TCAMR	-0.14375 0.2774	-0.07764 0.5589	1.00000 0.0	0.12371 0.3506	0.43839 0.0005	0.16879 0.2013	-0.07588 0.5679	0.43881 0.0005
R_WFLOW	-0.57500 0.0001	-0.02093 0.8750	0.12371 0.3506	1.00000 0.0	0.20300 0.1231	-0.12239 0.3558	-0.36396 0.0046	0.42203 0.0009
R_NOCTRL	-0.11351 0.3920	-0.36658 0.0043	0.43839 0.0005	0.20300 0.1231	1.00000 0.0	-0.01892 0.8869	-0.10320 0.4367	0.14816 0.2628
R_CONTCT	0.06780 0.6099	-0.38230 0.0028	0.16879 0.2013	-0.12239 0.3558	-0.01892 0.8869	1.00000 0.0	0.84349 0.0001	0.31531 0.0150
R_CONTES	0.23436 0.0740	-0.42395 0.0008	-0.07588 0.5679	-0.36396 0.0046	-0.10320 0.4367	0.84349 0.0001	1.00000 0.0	-0.24378 0.0628
R_CONTNO	-0.29164 0.0250	0.05876 0.6585	0.43881 0.0005	0.42203 0.0009	0.14816 0.2628	0.31531 0.150	-0.24378 0.0628	1.00000 0.0

Independent Variables

	CAMLOC	UNITLOAD	GATE	HOURBEG	CURR_ANG	VAR_CURR	
CAMLOC	1.00000 0.0	-0.05497 0.6792	0.10149 0.4444	0.05958 0.6540	-0.60050 0.0001	0.58980 0.0001	
UNITLOAD	-0.05497 0.6792	1.00000 0.0	-0.01240 0.9258	-0.49530 0.0001	0.06170 0.6425	-0.05665 0.6700	
GATE	0.10149 0.4444	-0.01240 0.9258	1.00000 0.0	0.34403 0.0076	-0.24746 0.0588	0.11183 0.3991	
HOURBEG	0.05958 0.6540	-0.49530 0.0001	0.34403 0.0076	1.00000 0.0	-0.07950 0.5495	0.19783 0.1331	
CURR_ANG	-0.60050 0.0001	0.06170 0.6425	-0.24746 0.0588	-0.07950 0.5495	1.00000 0.0	-0.39945 0.0017	
VAR_CURR	0.58980 0.0001	-0.05665 0.6700	0.11183 0.3991	0.19783 0.1331	-0.39945 0.0017	1.00000 0.0	

Note: For each block of numbers, the top number is the correlation coefficient and the second number is the probability of obtaining the test statistic (F-value) for the listed correlation coefficient if the null hypothesis (slope = 0.0) is true. Each correlation is based on 59 observations.

Table 49
Proportions of Smolts Exhibiting Different Impingement Behaviors by Water Current Angle for All Beginning Times, Unitloads, and Gate Settings Combined

CURR_ANG	FREQ	R_PERMIN	R_CONTCT	R_CONTES	R_CONTNO	R_TSCRN	R_TCAMR	R_WFLOW	R_NOCTRL	VAR_CURR
Summary Proportions by Water Current Angle - All Cameras Combined Except Camera 1B										
60	1	27.8182	0.16732	0.09935	0.067974	0.51242	0.028758	0.73725	0.024837	20.0000
80	1	0.2750	0.18182	0.18182	0.000000	0.36364	0.000000	0.63636	0.000000	0.0000
100	2	16.1841	0.34226	0.28709	0.055169	0.46042	0.000571	0.75595	0.000000	20.0000
120	6	29.6722	0.31956	0.28491	0.034653	0.49248	0.002162	0.63625	0.004274	16.6667
140	18	25.7153	0.30004	0.22766	0.072389	0.48955	0.008633	0.66826	0.000969	20.0000
160	17	11.4975	0.17368	0.11232	0.061356	0.51657	0.004393	0.85502	0.019488	5.8824
180	14	7.3577	0.16097	0.08469	0.076280	0.47038	0.000260	0.91264	0.005055	2.8571
Camera Location 1B										
140	13	1.1729	0.10698	0.02505	0.08193	0.56848	0.000000	0.79803	0.026648	0.0000
Camera Location IV										
140	1	1.0667	0.37500	0.00000	0.37500	0.50000	0.062500	0.96875	0.000000	20.0000
160	5	3.7958	0.06002	0.01266	0.04736	0.65221	0.000000	0.84817	0.000000	0.0000
180	6	3.0269	0.24107	0.10434	0.13672	0.47504	0.000000	0.94010	0.000000	0.0000
Camera Location 2										
80	1	0.2750	0.18182	0.18182	0.00000	0.36364	0.000000	0.63636	0.000000	0.0000
160	4	5.4325	0.12013	0.04513	0.07501	0.43485	0.012836	0.93698	0.068958	10.0000
180	6	11.9840	0.07778	0.05740	0.02038	0.49963	0.000000	0.90951	0.000280	3.3333

(Continued)

Table 49 (Concluded)

CURR_ANG	FREQ	R_PERMIN	R_CONTCT	R_CONTES	R_CONTNO	R_TSCRN	R_TCAMR	R_WFLOW	R_NOCTRL	VAR_CURR
Camera Location 3										
100	1	0.5500	0.40909	0.31818	0.09091	0.45455	0.000000	0.81818	0.000000	0.0000
140	1	29.0133	0.19577	0.16636	0.02941	0.49908	0.000000	0.74081	0.000000	40.0000
160	7	20.9450	0.23392	0.17003	0.06389	0.48351	0.003335	0.82608	0.007923	5.7143
180	2	6.4708	0.17025	0.10759	0.06266	0.36867	0.001818	0.83963	0.034545	10.0000
Camera Location 4										
60	1	27.8182	0.16732	0.09935	0.06797	0.51242	0.028758	0.73725	0.024837	20.0000
120	1	0.3250	0.53846	0.38462	0.15385	0.46154	0.000000	0.84615	0.000000	0.0000
140	8	26.9058	0.27475	0.22123	0.07352	0.48220	0.009418	0.65768	0.001753	15.00000
160	1	8.1333	0.53443	0.47541	0.05902	0.39672	0.000000	0.76393	0.000000	20.0000
Camera Location 5										
100	1	31.8182	0.27543	0.25600	0.01943	0.46629	0.001143	0.69371	0.000000	40.0000
120	5	35.5417	0.27578	0.26497	0.01081	0.49866	0.002594	0.59427	0.005128	20.0000
140	8	27.1936	0.30901	0.27020	0.3881	0.49440	0.002193	0.63220	0.000427	22.5000

Table 50
Proportions of Smolts Exhibiting Different Impingement Behaviors by Standard Deviation of Water Current Angle (surrogate for turbulence) for All Beginning Times, Unitloads, and Gate Settings Combined

VAR_CURR	FREQ	R_PERMIN	R_CONTCT	R_CONTES	R_CONTNO	R_TSCRN	R_TCAMR	R_WFLOW	R_NOCTRL	CURR_ANG
Summary Proportions by Standard Deviation of Water Current Angle - All Cameras Combined Except Camera 1B										
0	30	11.1107	0.20131	0.13540	0.065913	0.50441	0.000899	0.85741	0.001936	160
20	26	22.9487	0.25779	0.19140	0.066392	0.47455	0.009162	0.69820	0.015711	140
40	2	30.4158	0.23560	0.21118	0.024420	0.48268	0.000571	0.71726	0.000000	120
60	1	9.0154	0.34471	0.29693	0.047782	0.49488	0.010239	0.73379	0.003413	140
Camera Location 1V										
0	13	1.1729	0.10698	0.02505	0.08193	0.56848	0.000000	0.79803	0.026648	140.000
Camera Location IB										
0	11	3.3764	0.15877	0.06267	0.09610	0.55557	0.000000	0.89831	0.000000	170.909
20	1	1.0667	0.37500	0.00000	0.37500	0.50000	0.062500	0.96875	0.000000	140.000
Camera Location 2										
0	8	9.6470	0.08573	0.06710	0.01863	0.48098	0.000000	0.89889	0.000210	162.500
20	3	5.5778	0.14773	0.05664	0.09109	0.41765	0.017114	0.88341	0.091944	166.667
Camera Location 3										
0	7	17.8112	0.25626	0.19412	0.06214	0.47819	0.003335	0.81030	0.007923	154.286
20	3	11.8094	0.19774	0.12157	0.07617	0.40971	0.001212	0.86930	0.023030	166.667
40	1	29.0133	0.19577	0.16636	0.02941	0.49908	0.000000	0.74081	0.000000	140.000
Camera Location 4										
0	3	31.3671	0.38222	0.30716	0.07506	0.46044	0.001214	0.73330	0.000311	133.333
20	8	19.6777	0.30644	0.22596	0.08048	0.48087	0.012558	0.67611	0.004741	132.500
Camera Location 5										
0	1	0.2250	0.66667	0.55556	0.11111	0.44444	0.000000	0.77778	0.000000	140.000
20	11	35.0925	0.25814	0.23945	0.01869	0.50083	0.001843	0.59249	0.002331	130.909
40	1	31.8182	0.27543	0.25600	0.01943	0.46629	0.001143	0.69371	0.000000	100.000
60	1	9.0154	0.34471	0.29693	0.04778	0.49488	0.010239	0.73379	0.003413	140.000

Table 51
Summary of Probabilities from ANOVA (P ≤ 0.20 are in bold) of Effects of Hydraulic Variables on Smolt Entrainment/Impingement Behavior on MBFVBS

All Cameras Combined Except Camera 1B								
SOURCE	R_PERMIN	R-CONTCT	R_TSCRN	R_TCAMR	R_WFLOW	R_NOCTRL	R_CONTES	R_CONTNO
COMBINED	**0.0991**	**0.1189**	0.9277	**0.0621**	**0.0001**	0.3784	**0.0544**	0.7670
UNITLOAD	0.5928	0.7575	0.9953	**0.0436**	0.2428	**0.2013**	0.7717	**0.1691**
CURR_ANG	**0.1329**	**0.0471**	0.6270	0.6077	**0.0001**	0.4528	**0.0285**	0.9561
VAR_CURR	0.8432	0.6909	0.5008	0.5347	0.2540	0.2708	0.8888	0.9038

Note: Unitload is a surrogate for velocity, and the standard deviation of current angle is a surrogate for turbulence. Results from all cameras except 1B are combined. The results are based on a sample size of N = 59.

Table 52
Summary of Multiple Regression Analysis Using Backward Elimination of Summer MBFVBS Imaging Data Against Select Hydraulic Variables

Dependent Variable	R-square	DF reg/err/tot	Equation Prob > F	Independent Variables	Parameter Estimates	Individual Probabilities
R_PERMIN	0.33	1/57/59	0.0001	INTERCEPT CAMLOC	-4.222336 1.309804	0.3467 0.0001
R_CONTCT	0.22	1/57/58	0.0002	INTERCEPT CAMLOC	0.094129 0.011105	0.0155 0.0002
R_CONTES	0.47	3/55/58	0.0001	INTERCEPT CAMLOC UNITLOAD VAR_CURR	0.22592 0.07011 -0.01815 -0.00223	0.1231 0.0001 0.0777 0.0866
R_TSCRN	N/S					
R_TCAMR	0.17	3/55/58	0.0144	INTERCEPT CAMLOC CURR_ANG VAR_CURR	0.03280 -0.00363 -0.00014 0.00037	0.0173 0.0139 0.0524 0.120
R_WFLOW	0.59	2/56/58	0.0001	INTERCEPT CAMLOC CURR-AVG	0.80919 -0.06441 0.00113	0.0001 0.0001 0.0687
R_NOCTRL	0.09	1/57/58	0.0194	INTERCEPT UNITLOAD	-0.10481 0.00816	0.300 0.0194
R_CONTNO	0.08	1/57/58	0.0265	INTERCEPT CAMLOC	0.11095 -0.01517	0.0001 0.0265

Summary variable descriptions

Over 30,000 smolts were imaged and their behaviors analyzed over a period of nearly 2,000 min of observation. Proportions of smolts exhibiting different behaviors were summarized in 59 replicates. Smolts were imaged (R_PERMIN) at an average rate of nearly 17 fishes per min (Table 47), a rate more than 20 times higher than the imaging rate for smolts on the bypass screen surface (Table 2). The increase in imaging rate is partially related to the relative small cross-sectional area available for smolt passage up through the gate slot. Proportionately more smolts will be within the field of view of the camera in the gate slot than on the bypass screen. Other reasons will be discussed later in the results section. The increased imaging rate suggests that conclusions reached for the MBFVBS will generally not be limited by small sample size as was the case for the analysis of spring passage on the bypass screens.

An evaluation of the impingement variables indicates extremely low average values for the R_TCAMR (proportions towards camera) and R_NOCTRL (proportion not in control of their movement) variables and relatively low values for the R_CONTNO (significant MBFVBS contact without escape) variable. During evaluations of any of these three variables, care must be taken to check that an analysis is not based on 1 or 2 smolts. The low mean proportion of smolts moving specifically towards the camera (mean for R_TCAMR is 0.004688, Table 47) suggests that the camera and illumination system in the slot are not attracting smolts to any significant extent. The remaining variables, R_TSCRN (proportion moving towards the screen), R_WFLOW (proportion moving with the flow), R_CONTCT (proportion making contact with the screen), and R_CONTES (proportion contacting the screen and escaping), have sufficiently high means that their patterns should not be influenced by low numbers of smolts in any particular replicate.

Correlation analysis of the dependent variables indicated a number of significant relationships (Table 48). R_CONTCT (proportion of smolts contacting the screen) and R_CONTES (proportion contacting the screen with immediate escape) are highly correlated ($R = 0.843$, $P = 0.0001$) because R_CONTES is a subset of R_CONTCT. Similarly, R_CONTNO is also a subset of R_CONTCT, and it is also correlated ($R = 0.31531$, $P = 0.0150$) to R_CONTCT. Generally, the sum of R_CONTNO and R_CONTES should yield R_CONTCT. Consequently, R_CONTCT can be used as a surrogate to evaluate the significance of R_CONTNO and R_CONTES during periods of low fish abundance. Another group of intercorrelated dependent variables are R_NOCTRL to R_TSCRN ($R = -0.367$, $P = 0.0043$), to R_TCAMR ($R = 0.438$, $P = 0.0005$), and to a lesser extent, R_WFLOW ($R = 0.203$, $P = 0.1231$ - Table 48). This last group of variables all identify fish that appear to have little or no control over their movements and are most easily discerned when they are moving toward the screen. The highly significant correlations of R_WFLOW to R_CONTES ($R = -0.364$, $P = 0.0046$) and R_CONTNO ($R = 0.422$, $P = 0.0009$ suggest that impingement is highest when the flow is moving towards the screen.

The most significant result from correlation analysis of the independent variables (Table 48) was the high correlation of both CURR_ANG (R = -0.600, P = 0.0001) and VAR_CURR (0.590, P = 0.0001) to camera location suggesting that differences in hydraulic characteristics of the MBFVBS were determined primarily by the geometry of the system and less determined by operating conditions (unitload) or deployment configuration (gate setting). The high correlations of HOURBEG to GATE (R = 0.344, P = 0.0076) and UNITLOAD (R = -0.495, P = 0.0001) are an unfortunate bias resulting from non-random occurrence of the independent variables. The powerhouse operator generally began each sampling period with the highest unitload and changed to lower unitloads as the night progressed. Similarly, gate position was also related to beginning time. The negative correlation between CURR_ANG and VAR_CURR (R = -0.399, P = 0.0017) is a manifestation of the hydraulic patterns on the screen surface. Flow angles relative to the screen greater than 160 deg tend to be more laminar, whereas flow angles nearer 90 deg are characterized by more turbulent or unstable conditions.

Effects of simple hydraulic variables

Table 49 presents summaries of impingement variables by current angle (CURR_ANG) for all cameras combined (top block) and for each camera location separately. Current angles of 100 deg or less are limited by low numbers of observations and should be interpreted with caution. Table 50 presents summaries of impingement variables by standard deviation of current angle (VAR_CURR), and Table 51 presents results of analysis of variance to determine the significance of the independent variables in explaining the behavior of the dependent variables. Unitload (Table 52) is discussed in this section as a crude surrogate for velocity although it could have just as easily been discussed in the next section in its context as an operational variable. Physical model data were available for the MBFVBS but not used because of the uncertainty of transferring average water velocity/angle data from the model to instantaneous data available from the cameras. It would be relatively easy for small changes in discharge to result in major differences between model and prototype behavior because the imaging indicating that hydraulic conditions in the slot tended to change at thresholds (Figure 15) .

The following relationships were observed for the combined analysis. Note the significant increase in imaging rate (R_PERMIN - P = 0.1329) and contact proportion (R_CONTCT - P = 0.0471) as current angle (CURR_ANG) decreases, (i.e., R_PERMIN and R_CONTCT both increase as flow becomes more perpendicular to the screen, Tables 49 and 52). The variation in current angle (VAR_CURR) increases as CURR_ANG decreases (significance level not analyzed using ANOVA). Contact with escape (R_CONTES) increases with decreasing current angle between angles of 180 to 120 deg (Table 51, P = 0.0285). The proportion of smolts moving with the flow (R_WFLOW) is highest at higher water current angles (Table 51, P = 0.0001). Camera-specific relationships were obscured by low numbers

of observations. In a number of instances, only one observation was available for analysis and consequently, few conclusions can be reached.

No statistically significant results were obtained for the analysis of variation in current angle with the impingement variables (Table 51).

It appears that the impingement variables separate into two groups (Table 51): those whose patterns are explained by unitload (R_TCAMR and R_NOCTRL) and those whose patterns are explained by CURR_ANG (R_PERMIN, R_CONTCT, R_WFLOW, and R_CONTES). However, the underlying reasons for the separation of the variables into the two groups are unknown because impingement behaviors observed in the gatewell reflect both conditions in the gatewell and on the bypass screen. Therefore, it is difficult to confidently assign causality because the bypass screen was not imaged concurrently with the VBS.

Regression analysis was used to evaluate the relative importance of the different independent variables and to also determine if design criteria could be developed for the MBFVBS (Table 52). The results indicated that imaging could probably be employed for this purpose. Several of the R-square values were near or over 0.50 - relatively high values for biological data. With refinements in the way hydraulic data are collected (direct measurement of velocity and telltales to better reflect flow angles), it may be possible to obtain higher R-square values. Camera location was the independent variable explaining most of the variation (based on p values) in the dependent variables except for R_NOCTRL which was explained by unitload. However, as previously discussed, the effect of unitload on R_NOCTRL may be a manifestation of smolt interaction with the bypass screen and not with the MBFVBS. Secondarily, CURR_ANG and VAR_CURR also explained some of the variability in the dependent variables; however, their contribution was overshadowed by camera location. Consequently, improvement of conditions on the MBFVBS may require redesign of the MBFVBS to generate better flow patterns throughout its length. Relatively simple adjustments obtained through unitload changes or alterations in gate position may be inadequate since their effect is reduced compared to camera location.

Effects of operating conditions and deployment configuration

Table 53 summarizes the impingement variables and hydraulic variables as a function of camera location (top block), unitload for all cameras combined (second block), and unitload for each camera separately (third and subsequent blocks). Similar summaries are presented by gate setting (Table 54) and beginning time (Table 55) for the impingement and hydraulic variables.

Table 53
Summary Proportions of Smolts Exhibiting Different Impingement Behaviors by Camloc and Unitload

Summary Proportions by Camloc

CAM_NUMB	FREQ	R_PERMIN	R_CONTCT	R_CONTES	R_CONTNO	R_TSCRN	R_TCAMR	R_WFLOW	R_NOCTRL	CURR_ANG	VAR_CURR
1B	13	1.1729	0.10698	0.02505	0.08193	0.56848	.000000	0.79803	0.026648	140.000	0.0000
1V	12	3.1839	0.17679	0.05745	0.11934	0.55094	.0052083	0.90418	0.000000	168.333	1.6667
2	11	8.5372	0.10264	0.06425	0.03839	0.46371	.0046675	0.89467	0.025228	163.636	5.4545
3	11	17.1927	0.23480	0.17181	0.06299	0.46141	.0024528	0.82008	0.011323	156.364	9.0909
4	11	22.8657	0.32711	0.24811	0.07900	0.47529	.0094641	0.69171	0.003533	132.727	14.5455
5	14	30.5054	0.29474	0.26732	0.02742	0.49391	.0022611	0.62305	0.002075	130.000	22.8571

Summary Proportions by Unitload (Discharge) - All Cameras Combined Except Camera Location 1B

UNITLOAD	FREQ	R_PERMIN	R_CONTCT	R_CONTES	R_CONTNO	R_TSCRN	R_TCAMR	R_WFLOW	R_NOCTRL	CURR_ANG	VAR_CURR
12	2	10.9077	0.34663	0.29630	0.05033	0.47220	0.005119	0.73949	0.001706	140.000	40.0000
13	37	16.7800	0.22570	0.17609	0.04961	0.49324	0.001941	0.77134	0.000957	149.189	9.1892
14	5	14.5933	0.29789	0.15976	0.13813	0.48931	0.021195	0.79861	0.006716	148.000	16.0000
16	15	18.9462	0.20161	0.12339	0.07822	0.48598	0.005904	0.80214	0.026505	152.000	10.6667

Summary Proportion by Unitload - Camera Location 1B Only

12	1	0.5846	0.00000	0.00000	0.00000	0.42105	0.000000	0.84211	0.00000	140.000	0.0000
13	8	1.1392	0.10687	0.03968	0.06719	0.56055	0.000000	0.79141	0.00893	140.000	0.0000
14	1	1.3333	0.00000	0.00000	0.00000	0.67500	0.000000	0.70000	0.27500	140.000	0.0000
16	3	1.4056	0.17858	0.00271	0.17587	0.60327	0.000000	0.83368	0.00000	140.000	0.0000

(Continued)

Note: The top block (SUMMARY PROPORTIONS BY CAMLOC) provides proportions of smolts exhibiting different impingement behaviors by camera location for all gate settings, unitloads, and beginning times combined. The other blocks (SUMMARY PROPORTIONS BY UNITLOAD) provide proportions of smolts exhibiting different impingement behaviors by unitload separated out by camera location for each beginning time and gate setting combined.

Table 53 (Concluded)

Summary Proportions by Unitload - Camera Location 1V Only											
UNITLOAD	FREQ	R_PERMIN	R_CONTCT	R_CONTES	R_CONTNO	R_TSCRN	R_TCAMR	R_WFLOW	R_NOCTRL	CURR_ANG	VAR_CURR
13	8	3.7405	0.16166	0.07544	0.08622	0.52257	0.000000	0.87865	0.00000	170.000	0.0000
14	1	1.0667	0.37500	0.00000	0.37500	0.50000	0.062500	0.96875	0.00000	140.000	20.0000
16	3	2.4056	0.15107	0.02862	0.12246	0.64356	0.000000	0.95075	0.00000	173.333	0.0000
Summary Proportion by Unitload - Camera Location 2 Only											
13	7	5.9620	0.07637	0.05860	0.01777	0.48554	0.000000	0.87095	0.00000	160.000	2.8571
14	1	3.1667	0.16842	0.06316	0.10526	0.47368	0.010526	0.90526	0.01053	160.000	20.0000
16	3	16.3361	0.14199	0.07778	0.06421	0.40945	0.013605	0.94647	0.08899	173.000	6.6667
Summary Proportion by Unitload - Camera Location 3 Only											
13	7	13.7874	0.25827	0.19383	0.06444	0.49229	0.002463	0.81685	0.00493	148.571	11.4286
14	1	16.7333	0.16534	0.13745	0.02789	0.45020	0.003984	0.71514	0.00996	160.000	0.0000
16	3	25.2917	0.20319	0.13189	0.07129	0.39310	0.001918	0.86258	0.02670	173.333	6.6667
Summary Proportion by Unitload - Camera Location 4 Only											
12	1	12.8000	0.34856	0.29567	0.05288	0.44952	0.000000	0.74519	0.00000	140.000	20.0000
13	6	22.2321	0.37203	0.30739	0.06464	0.47704	0.008643	0.71891	0.00016	140.000	10.0000
14	1	32.5867	0.35761	0.29460	0.06301	0.48282	0.022095	0.60720	0.01309	140.000	20.0000
16	3	24.2477	0.21995	0.09820	0.12174	0.47788	0.010051	0.64763	0.00828	113.333	20.0000
Summary Proportion by Unitload - Camera Location 5 Only											
12	1	9.0154		0.29693	0.04778	0.49488	0.010239	0.73379	0.00341	140.000	60.0000
13	9	35.4774		0.25562	0.02028	0.48471	0.000302	0.59804	0.00000	128.889	20.0000
14	1	19.4133		0.30357	0.11951	0.53984	0.006868	0.79670	0.00000	140.000	20.0000
16	3	26.4500		0.28046	0.01138	0.50590	0.003945	0.60328	0.00855	126.667	20.0000

Table 54
Summary Proportions of Smolts Exhibiting Different Impingement Behaviors by Gate Setting for All Unitloads and Beginning Times Combined

GATESET	FREQ	R_PERMIN	R_CONTCT	R_CONTES	R_CONTNO	R_TSCRN	R_TCAMR	R_WFLOW	R_NOCTRL	CURR_ANG	VAR_CURR
Summary Proportions by Gate Setting - All Cameras Combined Except Camera 1B											
NG	32	19.0154	0.28846	0.19906	0.089394	0.45749	0.0066274	0.79604	0.013609	143.750	12.5000
NO	9	12.3799	0.13155	0.11070	0.020857	0.52886	0.0001550	0.72760	0.000000	160.000	8.8889
PR	18	15.5512	0.17462	0.13285	0.041771	0.52951	0.0035063	0.77900	0.001916	154.444	10.0000
Camera Location 1B											
NG	7	1.1631	0.09616	0.03291	0.06326	0.49935	0.000000	0.78429	0.039286	140.000	0.0000
NO	2	0.7042	0.10526	0.00000	0.10526	0.68045	0.000000	0.83083	0.000000	140.000	0.0000
PR	4	1.4246	0.12675	0.02381	0.10294	0.63348	0.000000	0.80567	0.017857	140.000	0.0000
Camera Location 1V											
NG	6	1.8547	0.28710	0.09611	0.19099	0.46835	0.010417	0.95701	0.000000	173.333	3.3333
NO	2	4.6125	0.02556	0.01552	0.01004	0.63248	0.000000	0.76468	0.000000	160.000	0.0000
PR	4	4.4635	0.08693	0.02041	0.06652	0.63405	0.000000	0.89469	0.000000	165.000	0.0000
Camera Location 2											
NG	5	11.3817	0.14870	0.08632	0.06238	0.41687	0.010269	0.89583	0.055502	152.000	8.0000
NO	2	2.7221	0.08915	0.7248	0.01667	0.49855	0.000000	0.89657	0.000000	180.000	0.0000
PR	4	7.8892	0.05180	0.03254	0.01926	0.50483	0.000000	0.89225	0.000000	170.000	5.0000

(Continued)

Table 54 (Concluded)

GATESET	FREQ	R_PERMIN	R_CONTCT	R_CONTES	R_CONTNO	R_TSCRN	R_TCAMR	R_WFLOW	R_NOCTRL	CURR_ANG	VAR_CURR
Camera Location 3											
NG	5	21.5167	0.23772	0.17040	0.06732	0.40524	0.001948	0.84048	0.018014	152.000	8.0000
NO	2	5.9183	0.22338	0.16838	0.5955	0.51984	0.000000	0.79784	0.000000	170.000	10.0000
PR	4	17.4250	0.23686	0.17757	0.05929	0.50241	0.004310	0.80570	0.008621	155.000	10.0000
Camera Location 4											
NG	8	27.8424	0.31852	0.22865	0.08988	0.47249	0.007105	0.69301	0.004858	127.500	12.5000
NO	1	17.9250	0.20363	0.19526	0.00837	0.46444	0.001395	0.59601	0.000000	140.000	20.0000
PR	2	5.4292	0.42318	0.35238	0.07079	0.49194	0.022936	0.74435	0.000000	150.000	20.0000
Camera Location 5											
NG	8	26.2667	0.37846	0.33508	0.04339	0.49238	0.003957	0.68822	0.003632	127.500	25.0000
NO	2	33.4942	0.15209	0.14867	0.00341	0.19681	0.000000	0.52712	0.000000	140.000	20.0000
PR	4	37.4883	0.19863	0.17112	0.00751	0.49554	0.000000	0.54068	0.000000	130.000	20.0000

Table 55
Proportions of Smolts Exhibiting Different Impingement Behaviors by Beginning Time for All Unitloads and Gate Settings Combined

HOURSBEG	FREQ	R_PERMIN	R_CONTCT	R_CONTES	R_CONTNO	R_TSCRN	R_TCAMR	R_WFLOW	R_NOCTRL	CURR_ANG	VAR_CURR
Summary Proportions by Gate Setting - All Cameras Combined Except Camera 1B											
20	23	20.5378	0.18593	0.13407	0.05186	0.49697	.0067146	0.78446	0.018825	153.043	9.5652
22	26	13.8186	0.26333	0.18775	0.07558	0.48645	.0040759	0.77732	0.001292	146.923	10.0000
23	3	20.5333	0.30336	0.17953	0.12383	0.46337	.0008178	0.80660	0.000000	140.000	13.3333
24	7	15.2260	0.21786	0.17915	0.03871	0.49464	.0019600	0.76732	0.000488	151.429	20.0000
Camera Location 1B											
20	4	1.9188	0.15950	0.00203	0.15746	0.65736	0.000000	0.83331	0.000000	140.000	0.0000
22	6	0.8011	0.10450	0.05291	0.05159	0.54901	0.000000	0.80079	0.057738	140.000	0.0000
23	1	1.2727	0.08571	0.00000	0.08571	0.48571	0.000000	0.71429	0.000000	140.000	0.0000
24	2	0.7469	0.02000	0.00000	0.02000	0.49053	0.000000	0.76105	0.000000	140.000	0.0000
Camera Location 1V											
20	4	3.4563	0.11214	0.02717	0.08498	0.64000	0.000000	0.92917	0.000000	170.000	0.0000
22	6	3.4465	0.20858	0.09381	0.11477	0.49486	0.010417	0.88225	0.000000	163.333	3.3333
23	1	2.0364	0.32143	0.01786	0.30357	0.48214	0.000000	1.00000	0.000000	180.000	0.0000
24	1	1.6667	0.10000	0.00000	0.10000	0.60000	0.000000	0.84000	0.000000	180.000	0.0000
Camera Location 2											
20	5	12.4383	0.10325	0.05170	0.05155	0.44446	0.008163	0.91295	0.53397	172.000	8.0000
22	5	4.9168	0.11788	0.08778	0.03010	0.47476	0.002105	0.86372	0.002105	152.000	4.0000
24	1	7.1333	0.02336	0.00935	0.01402	0.50437	0.000000	0.95794	0.000000	180.000	0.0000

(Continued)

Table 55 (Concluded)

HOURSBEG	FREQ	R_PERMIN	R_CONTCT	R_CONTES	R_CONTNO	R_TSCRN	R_TCAMR	R_WFLOW	R_NOCTRL	CURR_ANG	VAR_CURR
Camera Location 3											
20	5	22.0750	0.21793	0.14568	0.07225	0.42417	0.004599	0.84411	0.022918	168.000	4.0000
22	5	12.1090	0.25797	0.19641	0.06156	0.50448	0.000797	0.79412	0.001992	144.000	12.0000
24	1	18.2000	0.20330	0.17949	0.02381	0.43223	0.000000	0.82967	0.000000	160.000	20.0000
Camera Location 4											
20	4	28.6247	0.24446	0.19902	0.04544	0.51053	0.019589	0.66643	0.006442	120.000	15.0000
22	4	17.0113	0.42985	0.28866	0.14119	0.44947	0.005524	0.71173	0.003273	140.000	15.0000
23	1	27.7455	0.31324	0.26474	0.04849	0.44168	0.001311	0.72608	0.000000	140.000	0.0000
24	2	20.6167	0.29386	0.25686	0.03699	0.47329	0.001172	0.68502	0.000000	140.000	20.0000
Camera Location 5											
20	5	34.2957	0.24879	0.23838	0.01041	0.49700	0.002454	0.57496	0.005128	132.000	20.0000
22	6	30.9050	0.33273	0.29052	0.4222	0.49742	0.001145	0.63010	0.000000	133.333	16.6667
23	1	31.8182	0.27543	0.25600	0.01943	0.46629	0.001143	0.69371	0.000000	100.000	40.0000
24	2	19.1744	0.30531	0.27574	0.02957	0.48949	0.005688	0.68678	0.001706	130.000	40.0000

a. *General.* As previously indicated by the correlation analysis, camera location is of prime importance in explaining the impingement variables and current pattern variables. Only R_TSCRN and R_NOCTRL are not statistically affected by camera location (Table 53 - top block) with most of the rest of the variables being highly affected ($P < 0.01$, Table 56). Note the general increase in current angle variation with higher camera number ($P = 0.0001$, Table 56). The least turbulent flow conditions and flows most parallel to the screen occur at camera locations 1V, 2, and 3. Camera locations 4 and 5, particularly location 5 are characterized by highly turbulent flows ($P = 0.0001$, Table 56).

Note that the imaging rate increases for the cameras located higher on the slot (Table 53). The imaging rate for camera location 1B (on the top of the bypass screen) is similar in magnitude to the imaging rate of smolts observed elsewhere on the bypass screen. However, imaging rate increases almost 30 times at the top of the MBFVBS. This observation suggests that smolts are "piling up" at the top of the MBFVBS or that the rate at which smolts are able to exit the slot by passing through the orifice into the transport channel is considerably less than the rate at which they enter the slot. The effects associated with increased residence time at the top of the slot cannot be determined from video imaging, but it seems reasonable that increasing the smolts time within the potentially highly turbulent environment at the top of the MBFVBS would be detrimental. Future studies using imaging should explore the possibility of using the slope of the camera location/imaging rate relationship as an overall indicator of passage efficiency through the MBFVBS. That is, similar imaging rates across cameras in the slot would indicate that smolts are exiting the slot at the same rate they are entering the slot.

Other impingement variables also seem to be determined by camera location. Note that R_CONTCT ($P = 0.0001$, Table 56) and R_CONTES ($P = 0.0001$, Table 56) both increase towards the top of the slot, whereas, R_CONTNO decreases ($P = 0.0156$, Table 56) towards the top of the MBFVBS. However, the decrease in R_CONTNO towards the top of the screen must be interpreted with caution because the denominator of the proportion (an estimate of the total numbers of smolts observed) increases by a factor of 30 from the bottom of the slot to the top of the slot. Thus, the absolute number of smolts contacting the screen without escape is higher towards the top of the slot. The R_WFLOW variable decreases at successive locations up the slot from about 90 percent at camera location 1V to about 62 percent at camera location 5. The range of values for R_TSCRN, R_CONTNO, and R_NOCNTL and the general tendency of increases in their values at the bottom of the screen suggest that there may be a relationship between bypass screen conditions and the MBFVBS. That is, patterns of impingement variables on the MBFVBS may be partially determined by conditions on the bypass screen. However, insufficient evidence is available to determine this relationship particularly for the R_NOCTRL variable because its relationship to camera location is not statistically significant. Future video imaging work on the MBFVBS must consider conditions on the bypass screen.

Table 56
Summary of Probabilities from Analysis of Variance (P ≤ 0.20 are in bold) for Effects of Unitload, Screen Type, Beginning Time, and Camera Location on Entrainment/Impingement Variables and Hydraulic Variables

All Cameras Combined Except Camera Number 1B										
SOURCE	R_PERMIN	R_CONTCT	R_CONTES	R_CONTNO	R_TSCRN	R_TCAMR	R_WFLOW	R_NOCTRL	CURR_ANG	VAR_CURR
COMBINED	**0.0100**	**0.0001**	**0.1119**	**0.1038**	**0.0001**	0.4073	**0.0001**	**0.0050**	**0.0015**	**0.0002**
UNITLOAD	0.6191	**0.0908**	0.3530	**0.0203**	0.4907	0.6733	**0.0126**	0.3635	0.7019	**0.0155**
GATESET	0.4771	**0.0001**	**0.0057**	0.5772	**0.0310**	0.2498	**0.0023**	**0.0493**	**0.1202**	0.2593
HOURBEG	0.5997	**0.0026**	0.3211	0.4496	0.6904	0.7830	**0.0173**	0.2988	0.3726	0.4022
CAMLOC	**0.0004**	**0.0001**	**0.1534**	0.6100	0.0001	0.4375	**0.0001**	**0.0156**	**0.0001**	**0.0001**
Camera Location 1B										
COMBINED	0.9329	0.7115	**0.0493**	0.0000	0.9420	**0.0003**	0.8984	0.4979	0.0000	0.0000
UNITLOAD	0.8684	0.4771	**0.1161**	0.0000	0.8264	**0.0001**	0.7549	0.3094	0.0000	0.0000
GATESET	0.6804	0.8401	**0.0203**	0.0000	0.9064	0.5830	0.7021	0.6400	0.0000	0.0000
N	13	13	13	13	13	13	13	13	13	13
Camera Location 1V										
COMBINED	0.7487	**0.1019**	0.3706	0.0000	0.2442	0.0000	0.7744	**0.0813**	**0.0027**	0.0000
UNITLOAD	0.9234	0.5849	0.3386	0.0000	0.4568	0.0000	0.6123	**0.1465**	**0.0078**	0.0000
GATESET	0.5748	**0.0590**	0.2076	0.0000	**0.1315**	0.0000	0.5199	**0.1988**	**0.0110**	0.0000
N	12	12	12	12	12	12	12	12	12	12
Camera Location 2										
COMBINED	0.7103	0.3138	0.3859	0.5315	0.9005	0.5467	0.6491	0.2861	0.6670	0.4945
UNITLOAD	0.4840	0.7730	0.5348	0.4704	0.6320	0.4028	0.8431	0.2620	0.5980	0.3197
GATESET	0.6523	0.3574	0.3177	0.6699	0.8812	0.6645	0.3741	0.6406	0.4084	0.6699
N	11	11	11	11	11	11	11	11	11	11

Note: For each variable there were 4 classes of unitload (12, 13, 14, 16 kcfs), 3 gate settings (no gate, normal gate, and partial gate), 4 beginning times (2000, 2200, 2300, and 2400 hr) and 5 camera locations on the MBFVBS. All combined statistics based on 59 observations.

Table 56 (Concluded)

Camera Location 3										
SOURCE	R_PERMIN	R_CONTCT	R_CONTES	R_CONTNO	R_TSCRN	R_TCAMR	R_WFLOW	R_NOCTRL	CURR_ANG	VAR_CURR
COMBINED	0.7704	0.5986	**0.1863**	0.8996	0.4121	0.5669	0.7295	0.8268	0.3474	0.9628
UNITLOAD	0.6312	0.3064	0.3200	0.8708	0.2204	0.3892	0.4203	0.5474	**0.1973**	0.7837
GATESET	0.5895	0.6387	**0.1857**	0.6531	0.4961	0.5607	0.7982	0.8031	0.3824	0.9677
N	11	11	11	11	11	11	11	11	11	11
Camera Location 4										
COMBINED	0.7643	0.6663	0.9926	0.6664	0.6144	0.4562	**0.1966**	0.6249	0.5996	0.2475
UNITLOAD	0.8838	0.7387	0.9708	0.6560	0.7194	0.3069	**0.1283**	0.4804	0.4936	**0.1739**
GATESET	0.4219	0.7918	0.8982	0.3668	0.5781	0.4876	0.4292	0.3446	0.4557	**0.1768**
N	11	11	11	11	11	11	11	11	11	11
Camera Location 5										
COMBINED	0.7647	**0.1821**	**0.0507**	**0.0935**	**0.0082**	0.5209	**0.1359**	**0.1271**	0.6191	**0.0829**
UNITLOAD	0.6830	0.6682	**0.0187**	**0.1003**	**0.0198**	0.3694	0.9336	**0.1380**	0.5379	**0.0362**
GATESET	0.9219	**0.0565**	**0.1941**	0.5198	**0.0094**	0.6172	**0.0300**	0.4076	0.3546	1.0000
N	14	14	14	14	14	14	14	14	14	14

b. *Unitload.* The relationship between unitload and impingement variables for all cameras combined except camera 1B is presented in the top block of Table 53. Note that unitload appeared to affect R_CONTCT (P = 0.0908), R_TCAMR (P = 0.0203), R_CONTES (P = 0.0126), and VAR_CURR (P = 0.0155). However, the pattern is unclear. The highest value for R_CONTCT (0.35) occurs at the lowest discharge, but the values for R_CONTES are also highest at the lowest discharges (0.29). The two highest values are associated with the two highest discharges although their order is reversed (i.e., 0.14 for 14 kcfs and 0.07 for 16 kcfs). It is consequently difficult to determine the relationship between discharge and the impingement variables, although it seems that contact with escape dominates at lower discharges (12 and 13 kcfs), but contact without escape dominates at higher discharges (14 and 16 kcfs). The bias introduced by the nonrandom occurrence of unitload during the night may be a factor as well as latent effects from previous tests. Judging by the large increase in the imaging rate towards the top of the slot, it may be possible for smolts from a previous discharge condition to still be in the gatewell.

The proportions used to define impingement characteristics are influenced by orifice passage. Thus, if unitload affects orifice passage, then the denominator of the proportions becomes large and will decrease the impingement proportions. Thus, video imaging in the gatewell only will not provide sufficient data for a complete evaluation because proportions of smolts in the gatewell are determined by both the rate that they enter the gatewell and the rate at which they exit the gatewell.

The effect of unitload by camera location is summarized in Table 53 from the third to eighth blocks. Low numbers of observations for unitloads of 12 and 14 kcfs limited the analysis. Consequently, a comparison of results between unitloads 13 and 16 kcfs have the most validity. Unitload appeared to have the largest effect at the bottom camera (Camera 1V has two significant relationships VAR_CURR, P = 0.0078 and R_NOCTRL, P = 0.1465) and particularly the top camera (Camera 5 has five significant relationships) of the MBFVBS. Note that R_NOCTRL is significantly affected by discharge both at camera locations 1B (P = 0.0001) and 1V (0.0078). Fishes having no apparent control over their movement or orientation are probably stunned, dead, or injured. Probably, these fishes were in this condition prior to entry into the bypass system or were damaged on the surface of the bypass screen and transported to these two cameras. Alternatively, high water velocities (up to 11 to 12 fps) at high discharge at camera locations 1B and 1V may provide limited opportunity for smolts to control their position relative to their time spent in the camera imaging zone.

The results presented for the combined analysis at the top of Tables 53 and 56 are probably most influenced by the results from camera 5. Camera 5 results are probably the most robust for three reasons. First, the imaging rate is highest at this camera location so that impingement behavior is most likely to be accurately depicted. Second, the hydraulic conditions at camera 5

appear to be sensitive to unitload and gate setting so that responses of fishes are more likely to be observed here than at other locations. Third, the increased residence time of fishes at this location suggests that detrimental effects caused by stressful hydraulic conditions will be magnified because the same fishes will be exposed to these conditions for potentially long periods of time. Interestingly, unitload affects CURR_ANG at the bottom of the screen, but VAR_CURR at the top of the screen, suggesting that turbulence at the top of the screen is initiated by flow conditions at the bottom of the screen.

a. *Gate setting*. Table 54 summarizes the effects of gate setting on the dependent variables. The top block provides the effects of gate setting for all cameras combined except camera 1B. For the combined setting, gate setting has a statistically significant effect (Table 56) on R_CONTCT (P = 0.0001), R_CONTES (P = 0.0023), R_CONTNO (P = 0.0493), R_TSCRN (P = 0.0057), R_WFLOW (0.0310), and CURR_ANG (0.1202). R_CONTCT has its highest value in the no gate configuration (NG) and its lowest value in the normal gate setting (NO). The greatest proportion of escape after contact (R_CONTES) occurs at the NG setting, and the lowest proportion of escape after contact occurs at the normal gate setting (NO). Thus, smolts are least likely to contact the screen and if they contact the screen, to escape from the screen at the normal gate setting. At the partial gate setting (PR), the response is intermediate. That is, the smolts have an intermediate rate of screen contact and an intermediate rate of escape from the screen. The no gate setting results in the greatest contact and impingement.

Gate setting also has a significant impact on CURR_ANG (P = 0.1202, Table 56). The normal gate storage position provides flows with the least turbulence and most nearly parallel to the screen surface - conditions which usually provide for the least severe hydraulic environment and lowest impingement and screen contact. The no gate setting provides flows with the greatest turbulence and that are least parallel to the surface.

For the combined analysis, the range of values observed for both R_TSCRN and R_WFLOW is only about 10 percent. While statistically significant, these results have too small a range given our probable 5 percent measurement error to assign causality.

Results for individual cameras for the gate setting analysis mirror the results from the analysis of unitload in that results from the bottom MBFVBS camera (1V - 4 significant relationships) and top camera (5 - 4 significant relationships) contain the majority of the significant relationships. For both of these camera positions, the highest contact rate (R_CONTCT) was associated with the no gate position and the lowest contact rate was associated with the normal storage gate position. The pattern for the escape after contact variable (R_CONTCT) for cameras 1V and 5 was similar to the pattern observed for the combined analysis. However, the pattern for the significant impact without escape variable differed between these two cameras. For camera 1V,

a higher proportion of smolts suffered severe impact on the screens (approximately 0.5 - defined as R_CONTNO/R_CONTCT) than at camera 5. This pattern is reflected in the statistically significant relationship between gate setting and R_CONTNO at camera 1V. However, at camera location 5, the opposite was true. While impact was frequent, severe impact was not. For camera 5, the ratio of R_CONTNO to R_CONTCT was generally in the range of 0.10.

Like the results for the effects of unitload, the results of the analysis of storage gate position must also be interpreted with caution because the results are probably influenced by other factors. Conditions on the bypass screen and gap loss can influence results for camera 1V. Similarly, the efficiency of orifice passage can influence the results obtained from cameras 4 and 5.

b. Beginning time. Table 55 presents summaries of results by beginning time. These data are presented for completeness only. The high correlations of beginning time to unitload and gate setting make it impossible to separate out the effects of each independent variable.

Gap Loss

The gap loss evaluation is separated into two sections. The first section presents simple summary statistics (Table 57) and the results of correlation analyses (Table 58) to determine the relationships between independent and dependent variables. The second section provides information summaries by day, unitload, gate setting, beginning time, current angle, and standard deviation of current angle (Table 59). Two summaries of ANOVA results are presented to estimate the influence of different factors on gap loss. The first summary presents the relationship between gap loss and simple hydraulic variables such as current velocity and turbulence. The standard deviation of multiple estimates of current angle was used as a surrogate for turbulence or flow instabilities. The second summary presents the relationship of gap loss to unitload and gate setting.

Summary variable descriptions

A total of 508 smolts were imaged at the gap loss camera over a period of 407.5 min for an imaging rate of 1.25 smolts per min. This rate was consistent with the imaging rate for other bypass screen cameras in the summer. Of these 508 smolts, 188 (37 percent) were observed to pass through the gap. The gap loss determinations were separated into 13 replicates. The lowest percentage of gap loss fish was 0.0 percent (Table 57) based on a total of 9 fishes, the lowest number imaged in one replicate. Nine fishes would seem to be an adequate sample for determining gap loss when the average gap loss

Table 57
Simple Statistics for Dependent and Independent Variables for the Gap Loss Analysis

Variable	N	Mean	Std Dev	Sum	Minimum	Maximum
R_PERMIN	13	1.172931	0.987639	15.248100	0.300000	3.450000
R_TSCRN	13	0.568481	0.121529	7.390259	0.333333	0.789474
R_WFLOW	13	0.798030	0.108181	10.374386	0.680000	1.000000
R_NOCTRL	13	0.026648	0.077188	0.346429	0	0.275000
R_CONTCT	13	0.106976	0.110854	1.390682	0	0.325203
R_GAPLOS	13	0.365360	0.211853	4.749683	0	0.736842
R_CONTES	13	0.025045	0.064785	0.325590	0	0.222222
R_CONTNO	13	0.081930	0.102938	1.065092	0	0.317073
UNITLOAD	13	13.692308	1.377474	178.000000	12.000000	16.000000
GATE	13	2.384615	0.767948	31.000000	1.000000	3.000000
HOURBEG	13	21.769231	1.423250	283.000000	20.000000	24.000000
CURR_ANG	13	130.769231	2.773501	1700.000000	130.000000	140.000000
VAR_CURR	13	0.384615	1.386750	5.000000	0	5.000000

is 37 percent. The maximum gap loss was 0.74 based on a total of 19 imaged smolts. The average current angle of the flow to the screen was 130.8, and the standard deviation in angle was 0.38 (Table 57). However, 12 of the replicates had the same current angle and same standard deviation indicating that the analysis of these two variables was based on only one observation that was different. Consequently, the analysis for current angle and standard deviation of current angle is inadequate and presented in the report only for the sake of completeness.

Correlation analysis of the data show the confounding effects of beginning time on both unitload and gate setting. Consequently, it is impossible to separate the effects of beginning time from these variables. Correlations for CURR_ANG and VAR_CURR should be ignored because they are based on only one observation. Gap loss (R_GAPLOS) is correlated to the variables that describe screen contact including R_TSCRN ($R = 0.74$, $P = 0.0042$), R_CONTES ($R = -0.48$, $P = 0.0970$) and R_CONTNO ($R = 0.63$, $P = 0.0223$).

Effects of operational variables

The effects of CURR_ANG and VAR_CURR are summarized in Table 59. Little information is available other than the normal variance of the data

Table 58
Pearson Correlation Coefficients for Dependent and Independent Variables for Gap Loss Determinations

	R_PERMIN	R_TSCRN	R_WFLOW	R_NOCTRL	R_CONTCT	R_GAPLOS	R_CONTES	R_CONTNO	UNITLOAD	GATE	HOURBEG	CURR_AVG	VAR_CURR
R_PERMIN	1.00000 0.0	0.05037 0.8702	-0.32854 0.2731	-0.01421 0.9632	0.18231 0.5511	-0.06561 0.8314	-0.22915 0.4514	0.34055 0.2549	0.17411 0.5694	0.09542 0.7565	-0.44884 **0.1239**	-0.26557 0.3805	-0.26557 0.3805
R_TSCRN	0.05037 0.8702	1.00000 0.0	-0.07394 0.8103	0.30742 0.3069	-0.02612 0.9325	0.73519 **0.0042**	-0.55426 **0.0493**	0.32070 0.2854	0.28226 0.3501	-0.63208 **0.0205**	-0.53268 **0.0609**	-0.58137 **0.0372**	-0.58137 **0.0372**
R_WFLOW	-0.32854 0.2731	-0.07394 0.8103	1.00000 0.0	-0.17598 0.5652	0.68772 **0.0094**	0.37747 **0.2035**	0.49814 **0.0832**	0.42710 **0.1455**	0.09994 0.7453	-0.16225 0.5964	-0.27813 0.3575	0.56095 **0.0461**	0.56095 **0.0461**
R_NOCTRL	-0.01421 0.9632	0.30742 0.3069	-0.17598 0.5652	1.00000 0.0	-0.21186 0.4872	0.07045 0.8191	-0.14459 0.6374	-0.13715 0.6550	0.02756 0.9288	0.19929 0.5139	0.06064 0.8440	-0.10373 0.7359	-0.10373 0.7359
R_CONTCT	0.18231 0.5511	-0.2612 0.9325	0.68772 **0.0094**	-0.21186 0.4872	1.00000 0.0	0.30011 0.3191	0.41004 **0.1641**	0.81884 **0.0006**	0.35168 0.2387	-0.07074 0.8184	-0.41691 **0.1564**	0.31237 0.2988	0.31237 0.2988
R_GAPLOS	-0.06561 0.8314	0.73519 **0.0042**	0.37747 **0.2035**	0.07045 0.8191	0.30011 0.3191	1.00000 0.0	-0.47992 **0.0970**	0.62523 **0.0223**	0.21922 0.4718	-0.52268 **0.0669**	-0.43629 **0.1361**	-0.51818 **0.0697**	-0.51818 **0.0697**
R_CONTES	-0.22915 0.4514	-0.55426 **0.0493**	0.49814 **0.0832**	-0.14459 0.6374	0.41004 **0.1641**	-0.47992 **0.0970**	1.00000 0.0	-0.18778 0.5390	-0.18772 0.5391	0.17608 0.5650	0.05321 0.8629	0.91448 **0.0001**	0.91448 **0.0001**
R_CONTNO	0.34055 0.249	0.32070 0.2854	0.42710 **0.1455**	-0.13715 0.6550	0.81884 **0.0006**	0.62523 **0.0223**	-0.18778 0.5390	1.00000 0.0	0.49686 **0.0841**	-0.18700 0.5407	-0.48246 **0.0950**	-0.23914 0.4313	-0.23914 0.4313
UNITLOAD	0.17411 0.5694	0.28226 0.3501	0.09994 0.7453	0.02756 0.9288	0.35168 0.2387	0.21922 0.4718	-0.18772 0.5391	0.49686 **0.0841**	1.00000 0.0	-0.03636 0.9061	-0.50681 **0.0771**	-0.15101 0.6224	-0.15101 0.6224
GATE	0.09542 0.7565	-0.63208 **0.0205**	-0.16225 0.5964	0.19929 0.5139	-0.07074 0.8184	-0.52268 **0.0669**	0.17608 0.5650	-0.18700 0.5407	-0.03636 0.9061	1.00000 0.0	0.46919 **0.1058**	0.24077 0.4281	0.24077 0.4281
HOURBEG	-0.44884 **0.1239**	-0.53268 **0.0609**	-0.27813 0.3575	0.06064 0.8440	-0.41691 **0.1564**	-0.43629 **0.1361**	0.05321 0.8629	-0.48246 **0.0950**	-0.50681 **0.0771**	0.46919 **0.1058**	1.00000 0.0	0.04872 0.8744	0.4872 0.8744
CURR_ANG	-0.26557 0.3805	-0.58137 **0.0372**	0.56095 **0.0461**	-0.10373 0.7359	0.31237 0.2988	-0.51818 **0.0697**	0.91448 **0.0001**	-0.23914 0.4313	-0.15101 0.6224	0.24077 0.4281	0.04872 0.8744	1.0000 0.0	1.00000 0.0

Note: For each block of numbers, the top number is the correlation coefficient, and the second number is the probability of obtaining the test statistic (F-value) for the listed correlation coefficient if the null hypothesis (slope = 0.0) is true. Each correlation coefficient is based on 13 observations.

Table 59
Summary Results for Gap Loss Determinations by Day, Unitload, Gate Setting, and Beginning Time

By Day

Day	Freq	Meangapl
1	2	0.37303
2	4	0.26179
3	2	0.34990
4	2	0.63492
5	2	0.49342
7	1	0.00000

By Unitload

Unitload	Freq	Meangapl
12	1	0.42105
13	8	0.32745
14	1	0.32500
16	3	0.46133

By Beginning Time

Hourbeg	Freq	Meangapl
20	4	0.51460
22	6	0.31171
23	1	0.20000
24	2	0.31053

By Current Angle

CURR-ANG	Freq	Meangapl
130	12	0.39581
140	1	0.00000

By St. Dev. of Current Angle

VAR_CURR	Freq	Meangapl
0	12	0.39581
5	1	0.00000

Note: Gap loss rate is defined as the number of smolts observed passing through the gap between the top of the bypass screen and the bottom of the MBFVBS divided by the total number of smolts observed by camera 1B.

because 12 of the 13 observations have the same value for CURR_ANG and VAR_CURR. The effects of unitload and gate setting are also presented in Table 59. Gap loss appears to be weakly associated (Table 60) with gate position (P = 0.1273) and does not appear to be affected by unitload (P = 0.3134) or beginning time (P = 0.6963). The no gate position has the lowest gap loss (0.26) proportion, and both the normal and partial gate positions have the highest gap loss proportion (0.49).

Table 60
Summary Probabilities for Analysis of Effects (P≤0.20 are in bold) of Hydraulic Conditions and Operating/Deployment Conditions on Gap Loss

By Hydraulic Variables	
COMBINED	0.5099
UNITLOAD	0.8149
CURR_ANG	**0.1432**
VAR_CURR	•
N	13
By Oper/Deploy Conditions	
COMBINED	0.3610
UNITLOAD	0.3134
HOURBEG	0.6963
GATESET	**0.1273**
N	13

Note: Probabilities are based on Type I sum of squares for the analysis by hydraulic conditions because of too few degrees of freedom to use Type III sum of squares. Type III sum of squares is used for the operating/deployment conditions analysis.

The relatively weak effect of gate position (P = 0.1273) and lack of significant effect of unitload on gap loss suggest that gap loss is either a consequence of the basic geometry of the MBFVBS and bypass screen or that gap loss is determined by hydraulic conditions on the bypass screen surface not associated with unitload or weakly associated with gate setting. These results are inconsistent with the hydraulic conditions predicted by physical models. Gap loss is affected by hydraulic conditions in the throat area of the screen slot. The conditions in the throat area are affected by the operating gate position. As more flow passes up the screen slot with higher storage gate position there should be a concomitant decrease in gap loss if the path of the smolts is determined by the bulk flow of water across the gap. That is, decreased flow through the gap should result in a reduction in gap loss, and increased flow through the gap should result in an increase in gap loss. The

cause of the weak relationship between gap loss and operating gate storage position is not known. That many of the fishes that are lost in the gap appear to be stunned or injured has been noted. Thus, those conditions that result in fish contact on the screen may also result in proportionately greater gap loss.

The loss of fishes through the gap seems to be high (37 percent). The gap loss can at least be bounded using imaging based estimates of FGE. The imaging rate of the gap loss camera (1.173 smolts/min, Table 57) appears to be approximately equal to the imaging rate of the cameras used for the bypass screen evaluations (0.607 smolts/min, Table 28). During the pilot study (Nestler and Davidson, 1993), estimates of numbers of fishes guided using the depth of vision of two side-by-side cameras were within a factor of about 2 or 3 of estimates obtained using gatewell dipping if the viewing depth were expanded by the width of the screen. Therefore, it is concluded that gap loss is between a maximum of 37 percent (assumes all fishes passing over the bypass screen are imaged) to a minimum of about 12 percent (assumes that approximately 1/3 of the smolts passing over the screen is close enough to the screen surface to be imaged. The pilot study was conducted on a traveling screen, and data from this study suggest that imaging rate is higher for a bar screen than for a traveling screen, possibly because smolts are closer to the screen surface on the bar screen and thus more likely to be imaged. Consequently, for bar screens, imaging rate is expected to be more closely related to FGE than for traveling screens.

5 Discussion

Video Imaging

The results of the study indicate that video imaging of smolts provides information both on the impingement behavior of smolts and flow conditions in the rigorous and complex hydraulic environment of the bypass system. Video imaging may be the only technology that can provide insight into the threshold behavior that results when designs or deployment alternatives are altered. However, video imaging is limited in its range, area of coverage, and ability to discern smolt behavior more than about 30 to 40 cm above the screen surface. Also, imaging data are collected as proportions of smolts meeting a criterion divided by the number observed. Thus, the numerator and denominator can be affected separately. Consequently, interpretation of imaging data must be tempered with an appreciation for the limitations and biases of this technology.

The greatest value of video imaging technology is its ability to provide visual records of conditions on the screen surface that can be used to develop a conceptual framework for bypass systems. Video imaging shows that, from a fish's perspective, the bypass screen system is a complex structural and hydraulic environment that contains at least four critical areas where relatively small changes in design, deployment, or unitload may result in large changes in hydraulic conditions: the toe of the screen, the gap, the top of the MBFVBS, and the bottom of the MBFVBS. Significant changes in the hydraulic field in these zones, potentially caused by relatively small design or operational changes, can have a substantial effect on the effectiveness of the bypass system.

As is always the case for a complex study, this study was limited by several factors that should be addressed during any future video imaging. First, the spring sampling was limited by low numbers of observations that probably influenced results. Future sampling should allow more time for collection of video data in the spring. Second, in many cases the independent variables were correlated to one another rather than being randomly scheduled because of operator convenience or because of schedule requirements not associated with video imaging. Future video imaging efforts must adhere to the experimental protocols established in the study plan. The strength of the

conclusions that could be made in this report were weakened by lack of randomization of experimental conditions. Third, video imaging showed that the presence of the fyke net substantially altered the impingement behavior of smolts. Its effect on the hydraulic environment is unknown, but indirect evidence suggests that the fyke net slows down velocities but does not alter water approach angles. Physical model data suggest that the presence of a fyke net reduces water velocity by about 15 percent. Future video imaging work should be completely separated from FGE work so that the presence of the fyke net does not bias the results of video imaging work. Adjusting study results for the bias introduced by the presence of the fyke net is problematic because of the possibility of threshold responses at critical locations of the hydraulic field of the bypass system. It is recommended that fyke-net based evaluations of bypass systems be interpreted with caution because of the probable significant effect of the presence of the fyke net on the hydraulic field of the bypass system. Fourth, evaluations of the imaging data collected from each of the different areas of the bypass system indicate that effects are not restricted to specific areas of the screen. Conditions on the bypass screen that affect gap loss and orifice passage efficiency probably also affect the findings on the MBFVBS. Therefore, future imaging studies that assess a part of the system must image all parts of the bypass system for an integrated analysis.

ESBS Impingement

While not statistically conclusive because of low numbers of smolts for the SSTS, it seems reasonable to conclude that the ESBS impinges substantially more fishes than the SSTS. The imaging rate for the ESBS is significantly higher than on the SSTS, particularly for camera location 20 where the flow lines are nearly perpendicular to the screen surface. Similar observations of increased impingement and imaging rate were observed for a ESBS compared to a SSTS at The Dalles (Nestler and Davidson, in preparation). This evidence combined with the ability of bar screens to efficiently pass flow (bar screens in flumes produce negligible head losses over a wide range of flows) suggests that bar racks may be relatively undetectable by approaching fishes. In a lightless or at least a very low-light environment, fishes are probably navigating using information transduced by the octavo-lateralis system. A rigid structure, efficient at passing flow (and hence generating relatively little turbulence), would be more difficult for the fishes' octavo-lateralis systems to detect than a flexible mesh. Consequently, smolts would be more likely to strike the unyielding surface of the bar screen than the surface of a traveling screen.

Increased impingement of smolts on the ESBS also may contribute to increased gap loss for several reasons. First, many of the smolts observed to pass through the gap appeared to be stunned or injured (gap loss determinations were made on the ESBS only). Smolts passing over the lip of the screen and between the VBS and bypass screen were even seen surrounded by a halo of scales (Figure 15) suggesting that significant descaling was occurring when smolts contact the screen. Thus, there is a strong possibility that much of the

impingement or descaling damage caused by the ESBS is underestimated by gatewell dipping because the affected fishes are lost through the gap and cannot be recovered or are considered to be fishes not affected by the bypass system. The decreased imaging rate associated with traveling screens suggests that a large proportion of smolts are higher above the screen surface and thus outside the range of imaging. Thus, relatively few smolts would be close enough to the gap in mesh screens for gap loss to be a significant concern.

The bypass screen is slanted relative to the vertical axis of the dam but is not necessarily slanted relative to the flow lines. Imaging data and physical hydraulic models show that the flow lines are nearly perpendicular to the screen at some locations. Smolts are observed to have a significant lateral component to their movement patterns at those locations where flow is observed to be perpendicular to the screen surface. Consequently, smolts may be spending considerable amounts of swimming time above the screen surface until they impinge, exit at the top of the screen, or exit at the toe of the screen. Residence time of smolts on the screen surface may be a significant feature of impingement and guidance.

Increasing Efficacy of Video Imaging

Field and analysis experience have led to the following camera deployment recommendations to increase the efficacy of video imaging. Two cameras should be imaging gap loss and quantifying the proportion of gap loss smolts that seem injured or stunned. Two cameras should be imaging the toe end of the screen to quantify smolts intercepted by the screen by being carried under the screen toe and to quantify the proportion that seem to be injured or stunned. Both of these locations on the screen tend to image higher proportions of injured fishes, and the hydraulics on the screen would suggest that injured or damaged fishes would more likely be pushed close to the screen surface at these points. Presently, these fishes are not considered to be guided, although the bypass screen is having a definite effect on their conditions. Evaluations of the screens cannot be performed without this information. Four additional single-mount cameras can be located on different parts of the screen to characterize smolt impingement characteristics.

Based on summer evaluations, four cameras probably are adequate to characterize the impingement characteristics of smolts on the MBFVBS. Analysis of the data indicates that most significant relationships between deployment configuration and screen performance occurs at camera locations 1V, 4, and 5. It is recommended that cameras be deployed at these locations and at a location intermediate between locations 2 and 3.

It is suspected that certain screen designs or operational conditions may result in increased contact of smolts to the screen because a greater proportion of the population is close to the screen surface. This may be an important variable to fully evaluate the performance of a particular screen design or

deployment configuration. Consequently, it is important to have estimates of total guidance that can be compared to individual camera imaging rate to obtain an indirect estimate of the numbers of smolts passing above the field of vision of the cameras. Gatewell dipping is hindered by the presence of the cameras on the MBFVBS. It is recommend that an imaging system be developed to quantify orifice passage so that orifice passage can be compared to imaging rates on the MBFVBS.

The camera configuration outlined above will result in approximately 13 to 14 cameras being employed across one bypass system. Possibly, one camera could be eliminated from the MBFVBS, and another camera could be eliminated from the screen surface leaving a minimum number of 11 to 12 cameras to completely characterize a single design/deployment alternative. Imaging only parts of the bypass system is inadequate because of the undocumented effects of other parts of the system.

One of the difficulties of using cameras on the bypass screens is the unknown and sometimes variable depth of vision of the cameras. It is not possible to obtain imaging rates and impingement data that can be used to compare effects of location or time if the depth of vision is changing. It is recommended that in future imaging work, a known field of imaging would be physically marked on the screen surface to aid in expanding results to the total screen width.

One of the unanticipated benefits of the underwater video cameras was their ability to provide information about the hydraulic environment on the screen surface. It is recommended that future imaging studies use "telltales" as an aid to estimate water current angle and that consideration be given to the development of a method to estimate water velocity from video imaging. These additional data could help substantially in providing a direct and accurate measure of the hydraulic environment at each camera location, help in identifying unit or bay effects, and provide a means of certifying the accuracy of the physical model predictions to the prototype.

Optimizing Bypass System Efficiency

Bypass system efficiency can be optimized using the camera configuration outlined above. The major sources of smolt injury (impingement and screen contact) and gaps in the present recovery system of fyke nets and gatewell dipping (gap loss and loss under the toe of the screen) can be quantified and minimized. A bypass system performance evaluation system based on the following metrics could be developed. First, MBFVBS performance is its ability to guide fishes from the gap to the orifice which is determined by the slope of imaging rate on the MBFVBS from the gap to the orifice. For example, if imaging rate is constant (flat slope) across the MBFVBS cameras, then smolts are leaving the gatewell at about the same rate that they are entering the gatewell. Conversely, if the imaging rate increases towards the top of the gatewell slot (steeper slope), then smolts are experiencing difficulty in

locating and exiting the orifice. The flatter this slope then the more efficiently smolts are passing up the MBFVBS. The steeper this slope, the more smolts are "piling up" in the MBFVBS. Second, screen performance (ability to benignly intercept and guide smolts to the MBFVBS) is determined at two levels. Passage loss level is determined by the ratio of smolts imaged at the gap loss and toe loss cameras (both expanded by appropriate factors to estimate totals) to corrected passage estimate obtained from the MBFVBS. Screen impingement/damage level is determined by the ratio of injured/stunned fishes observed by the gap and toe loss cameras and MBFVBS cameras (all expanded by appropriate factors). The goal of this imaging is to develop design or deployment characteristics that optimize the hydraulics (laminar flows, low velocity, parallel to screen) and passage (minimize passage loss and screen impingement/damage ratios). FGE could be estimated if supplemental data were available from netting or fixed aspect hydroacoustic sampling to quantify the passage of smolts through the turbine. Bay and unit effects also must be controlled during these evaluations.

Recommended Follow-up Studies

In addition to the general recommendations made above to improve the efficacy of imaging, it is also recommend that the following specific evaluations be performed.

a. Compare gap loss between a traveling screen and bar screen.

b. Repeat the ESBS/SSTS evaluation because of limited numbers of replicates available for the SSTS.

c. Determine light bias on the bar screen because the bar screen is more reflective than the traveling screen.

d. Quantify hydraulic effects resulting in differences in bays or units.

e. Compare similar screen/deployment alternatives at other projects or other years to determine the consistency of the results.

6 Conclusions

In order of perceived significance, the following conclusions are presented based upon the results of imaging studies at McNary Dam.

a. The presence of the fyke net does not affect the angle of the flow; however, the fyke net reduces the proportion of smolts impinged on the screen (from 12 to 3 percent) and reduces the impingement index (from 0.42 to 0.34).

b. Increasing the screen angle from 55 to 62 deg increases the impingement proportion and impingement index. This result is counterintuitive and no explanation is presently offered.

c. Increasing unitload increases impingement proportion and impingement index and increases the rate at which fishes are imaged, but at a rate greater than simple volumetric increases would suggest. It is inferred that increased unitload tends to force smolts closer to the screens. Presently, the images are being reprocessed to increase the precision with which hydraulic variables are obtained. Extensive viewing of the images suggests that variation in water angle may also be an important variable.

d. Analysis of gate setting and screen position is limited by low sample size.

The video imaging provided insight into the hydraulic and impingement characteristics of the different screen designs and configurations and also provides a technology to describe changes in hydraulic patterns and impingement characteristics in relation to intake design and powerhouse and dam configuration. In the future, video imaging should not be performed concurrently with fyke netting nor should it be relegated to time periods significantly outside the periods of maximum smolt passage, since both affect imaging rate and impingement variables.

a. It is possible to use existing technology to successfully image smolts as they approach and are intercepted by bypass screens and guided up VBSs.

b. Impingement behavior of smolts on the screens is highly dependent on local hydraulic conditions on the bypass screen and VBS. The results demonstrate that impingement behavior of smolts on the screen must be described and evaluated in terms of the spatially variable hydraulic environment of the screen because camera location was a statistically significant variable describing the impingement of smolts.

c. More smolts impinged on the ESBS than on the SSTS.

d. Over the range of hydraulic variables available in the spring, local current angle had a larger effect than local velocity.

e. Increased impingement was observed with the 62 deg versus 55 deg screen angle.

f. Gap loss is a significant feature of the ESBS.

Results indicate that more smolts impinged on the ESBS than on the SSTS. However, there are insufficient data to conclusively relate our findings to differences in screen type only. Differences in impingement charcteristics of screens may also be affected by differences in screen length (40 ft versus 20 ft) which substantially alter the percentage of the intake that is blocked (22 versus 47 percent). Additionally, individual and synergistic effects mediated by the deployment or configuration of the screen, slot, and VBS may influence the results. Recent improvements to certain design details of bar screens may reduce the impingement rates from those observed in this study. A more complete understanding of hydraulic patterns and associated response of smolts will require additional testing, particularly to describe effects on impingement rates resulting from alterations in bar screen design from those investigated in this study.

References

Nestler, J. M., and Davidson, R. A. (1993). "Imaging smolt behavior on extended-length traveling screens, McNary Dam: 1991 Pilot study," Technical Report EL-93-24, U.S. Army Engineer Waterways Experiment Station, Vicksburg, MS.

_____. "Imaging smolt behavior on an extended-length submerged traveling screen at The Dalles Dam in 1993," Technical Report (in preparation), U.S. Army Engineer Waterways Experiment Station, Vicksburg, MS.

Peterman, R. M. (1990). "Statistical power analysis can improve fisheries research and management." *Can. J. Fish. Aquat. Sci.* 47, 2-14.

Pucket, K. J., and Anderson, J. J. (1987). "Conditions under which light attracts juvenile salmon." *Conference on Fish Protection at Steam and Hydro Power Plants*. San Francisco Hilton and Towers, San Francisco, California, October 28-30, 1987. Sponsored by EPRI, Electric Power Research Institute.

SAS/STAT User's Guide, Release 6.03 Edition. (1988). SAS Institute, Inc., Cary, NC.

Appendix A
Specifications for Video Cameras

1. Underwater CCD Monochrome Television Camera OE 1359

   a. Sensitivity: 0.03 lux on the sensor
   b. Lens: 3.7 mm, f/1.6 - f/300 Auto Iris
   c. Power: 16-24 V d.c. at 200 mA maximum
   d. Size: 152 mm length - 53 mm diam
   e. Weight: in air 0.59 kg - in water 0.27 kg
   f. Cost: $10,500.00

2. DeepSea Power & Light Micro-SeaCam Underwater Video Camera

   a. Sensitivity: 1 lux
   b. Lens: 60 deg angular field of view in water
   c. Power: 12 VDC at 140 mA maximum
   d. Size: 122 mm length - 36 mm diam
   e. Weight: in air 0.4 kg - in water 0.3 kg
   f. Cost: $5,200.00

3. Silicon-Intensified-Target (SIT) TV Camera SL-99

   a. Sensitivity: 1,000 times greater than a standard vidicon
   b. Lens: 12.5 mm, f/1.4
   c. Power: 12.7 VDC at 850 mA $\pm$ 50 mA
   d. Size: 14 in. length X 3.75 in diam
   e. Weight: 9 lbs (4.0 kg) in air, 4 lbs (1.8 kg) in water
   f. Cost: $10,500.00

Appendix B
Detailed Data Encoding Procedures for Bypass Screens

After the tape consolidation process is complete, the consolidation tapes are reviewed and data are recorded onto the code forms. The code forms consist of a series of blocks and variables corresponding to those blocks. These variables are given codes that identify fish behavior patterns relative to the screens. The coding variables are abbreviated in order to fit into the blocks specified for the particular variables. The code form is divided into two parts: the header card, and the individual fish-screen interaction table that contains each fish sampling.

Header Cards

The header card serves to categorize the fish sampling into groups having the same testing conditions or testing environment. Table B1 lists the blocks, variable names, and code names to be entered as the header card.

Data Cards

The second portion of the coding form consists of the coding variables used to describe each individual sampling of data for the specified header card. Each fish (sample) has a specific approach to and retreat from the screen, an orientation relative to the screen, and can exhibit one of several different impingement behaviors ranging from entrainment without screen contact to complete impingement with no escape.

Several possible behavioral patterns associated with fish impingement are recorded in blocks on the code form. The coding form for each particular fish corresponding to a particular group (header card) is similar to the header card coding. The following table (Table B2) describes the variables, codes, and blocks used in coding individual fish impingement events.

Table B1
Description of Header Card Variables for Bypass Screens Used to Describe General Testing Conditions for Groups of Fishes

Block	Var. Name	Description
1	Card Code	Identifies the data as being a header card. Code: A
2-3	Dam Name	Identifies the dam being tested. Code: MC-McNary
4-5	Year	Year in which imaging test occurs. Code: 92-1992
6-7	Month	Month in which imaging test occurs. Code: 05-spring, 07-summer
8-9	Day	Day in which testing occurred. Code: 01-30
10-11	Unit Load	Discharge through the turbine in kcfs. Code: 12, 13, 14, 15, 16
12-13	Unit Number	Turbine number Code: 1-30
14-15	Bay Number	One of three bays in each intake. Code: A, B, or C.
16-19	Hour Begin	Time at which imaging test began. Code: Military time
20-23	Hour End	Time at which imaging test ended. Code: Military time
24	Turbidity Code	Turbidity measurement. Code: S-Secchi disk, N-NTU, J-JTU, E-Estimated visibility in inches
25-26	Turbidity	Scalable turbidity measurement. Code: 00-99
27-28	Water Temp.	Temperature (C) of the water at imaging test time. Code: 00-99
29	Screen Type	Type of bypass screen being tested. Code: T-Standard-length Traveling Screen, B-Standard-length Bar Screen, X-Extended-length Bar Screen, E-Extended-length Traveling Screen, S-Stream-Lined Traveling Screen
30-31	Screen Length	The length (feet) of the screen being tested. Code: 20-Traveling Screens, 40-Bar Screens
32-33	Screen Angle	The angle at which the screen being tested is adjusted. Code: 55, 62
34-35	Screen Porosity	The percentage of the porosity plate. Code: 20, 30
36-39	Camera Type	Type of camera used in the imaging test. Code: The first 2 blocks contain the first 2 letters of the camera manufacturer, and the last 2 blocks contain the first 2 letter/characters of the model number.
40-41	Camera Location	The distance (feet) of the camera measured from the top of the screen being tested. Code: (see Table 2)
42-45	Light System	The lighting system used in the imaging testing. Code: The first 2 blocks contain the first 2 letters of the lighting manufacturer, and the last 2 blocks contain the first 2 letter/characters of the model number.
46-48	Maximum Source Level	The maximum source level of the lighting system measured in watts. Code: 000-999 Usu. 100
49-51	Light Source Setting	The dial setting for the light source. Code: 000-999 Usu. 60
52-53	Distance from Camera	The distance (in.) of the light source from the cameras. Code: 00-99
54-55	Field Crew Chief	The crew chief in charge of the data collection. Code: BD-Bob Davidson
56-58	Original Tape Number	The original tape in which this particular sampling is taken. Code: 000-999
59-60	Gate Position	The gate setting used during this particular sampling. Code: NG-no operating gate, PR-partially raised operating gate, NO-normal or stored operating gate
61-62	Fyke Net	Is the fyke net in place? Code: NF-no fyke net, FK-fyke net in place
63	Camera Number	The camera number which was used to record this particular sampling. Code: 1, 2, 3, 4, 5, 6

Table B2
Description of Data Card Variables for Bypass Screens Used to Describe Each Impingement Event

Block	Var. Name	Description
1	Card Code	Identifies on the code form that this is impingement information of a particular sample. Code: B
2-3	Specification Code	Identifies the species of the fish. All smolts were assumed to be chinooks. Code: CH
4-5	Life Stage	Identifies the life stage of the sample. Code: YR-yearling (spring) or SY-subyearling (summer)
6-7	Size	Size of the fish in millimeters (mm). Code: 000-999
8-10	Tape Number	Consolidation tape number from which the sample is viewed. Code: 000-999
11-13	Fish Number	Sequence number in which the fish is viewed from the consolidation tape. Code: 001-999
14	Cycling Status	Is the screen cycling when the fish approach it? Note: Only occurs on traveling screens. Code: Y-yes, N-no
15	Impingement Type	Defines whether the fish touched the screen along with its approach to and its retreat from the screen. Code: E-Entrainment, no impingement; P-Entrainment, impingement, with no escape; G-Entrainment, impingement, with escape; I-Impingement, no entrainment observed; T-Impingement, retreat, no approach observed; N-Approach, Impingement, no retreat observed; A-Impingement probable, given velocity and approach angle
16-17	Approach Position	The position at which fish approach the screen. Code: 11-head first, back up; 12-head first, back down; 21-tail first, back up; 22-tail first, back down; 15-parallel to the screen
18-20	Approach Vert. Angle	The angle at which the fish approach the screen. Code: 0-180 deg (Toe of screen = 0, Head = 180)
21-23	Approach Horiz. Angle	Direction in which fish approach the screen relative to the camera. Code: (+)-toward screen, (-)-away from screen
24-25	Retreat Position	The position at which the fish retreat from the screen. Note: This code is not filled in if the fish is entrained only. Code: Same codes as Approach Position codes.
26-28	Retreat Vert. Angle	The angle at which the fish retreat from the screen. Note: This code is not filled in if the fish is entrained only. Code: Same codes as Approach Vertical Angle codes.
29-31	Retreat Horiz. Angle	Direction in which fish retreat from the screen relative to the camera. Note: This code is not filled in if the fish is entrained only. Code: Same as Approach Horizontal Angle
32-33	Escape Behavior	The position at which the fish escapes entrainment. Code: Same as the Approach and Retreat Position codes
34-36	Escape Angle	The angle in which the fish escapes entrainment. Code: 0-180
37	Life Sign	Is the fish dead? Code: Y-yes, N-no
38	Operculum Damage	Is the operculum of the fish damaged? Code: Y-yes, N-no
39	No. of Hits	Number of times the fish hit the screen. Code: 0-9
40-41	Impingement Location Hit-1 Code	Location on the screen where the fish touched on the first hit. Code: MO-mesh only, TO-tie bar only, MB-slide from mesh to tie bar, TM-tie bar to mesh
42-43	Impingement Location Hit-2 Code	Location on the screen where the fish touched on the second hit. Code: Same as the impingement location hit-1 Code
44-46	Water Current Angle	Measure of the instantaneous water current angle relative to the screen at the time of the fish-screen interaction with an accuracy of 5 deg. Code: 0-180 deg

Appendix C
Detailed Data Encoding Procedures for Vertical Barrier Screen and Gap Loss Determinations

Code forms are divided into two parts: the header card and the individual fish-screen interaction table that contains each fish sampling. The code forms consist of a series of blocks and variables corresponding to those blocks. These variables are given codes that identify fish behavior patterns relative to the screens. The coding variables are abbreviated in order to fit into the specified blocks.

Header Cards

The header card serves to categorize the fish sampling into groups having the same testing conditions or testing environment. Table C1 lists the blocks, variable names, and code names to be entered in the header card.

Data Cards

The second portion of the coding form consists of the coding variables used to describe each impingement rate and category and gap loss for the specified header card. Each group of smolts is separated into a variety passage category. Table C2 describes the variables, codes, and blocks used in coding MBFVBS fish interactions. A laboratory counter is used to tally the number of smolts in each of the categories.

Table C1
Description of Header Card Variables for VBS and Gap Loss Used to Describe Testing Conditions for Groups of Fishes

Block	Var. Name	Description
1	Card Code	Identifies the data as being a Header Card. Code: A
2-3	Dam Name	Identifies the dam being tested. Code: MC-McNary
4-5	Year	Year in which imaging test occurs. Code: 92-1992
6-7	Month	Month in which imaging test occurs. Code: 07 summer
8-9	Day	Day in which testing occurred. Code: 01-30
10-11	Unit Load	Discharge through the turbine in kcfs. Code: 12, 13, 14, 15, 16
12-15	Hour Begin	Time at which imaging test began. Code: Military time
16-19	Hour End	Time at which imaging test ended. Code: Military time
20	Screen Type	Type of bypass screen being tested. Code: T-Standard-length Traveling Screen, B-Standard-length Bar Screen, X-Extended-length Bar Screen, E-Extended-length Traveling Screen, S-Stream-Lined Traveling Screen
21-22	Screen Porosity	The percentage of the porosity plate. Code: 20, 30
23-24	Field Crew Chief	Individual in charge of collection of field data
25-27	Original Tape Number	Tape number of original tape on which camera images are located
28-29	Gate Position	Closure gate position
30-32	Duration	Duration of imaging
33-34	Camera Number	Number of camera

Table C2
Description of Data Card Variables for Bypass Screens Used to Describe Each Impingement Event

Block	Var. Name	Description
1	Card Code	Identifies on the code form that this is impingement information of a particular sample. Code: B
2	Block	Identifies which time block is being used for subsampling
3-5	No. moving away from screen	The number of smolts definitely moving away from the screen with the screen being defined as a plane
6-8	No. moving toward screen	The number of smolts definitely moving toward the camera. The camera location is defined as a point. This variable and the next can be evaluated for camera or light bias
9-11	No. moving away from camera	The number of smolts definitely moving away from the camera with the camera being defined as a point
12-14	Empty	
15-17	No. in direction of flow	Number of smolts definitely moving in the direction of the flow
18-20	No. against direction of flow	Number of smolts definitely moving against the direction of the flow
21-23	No. with no swimming control	Number of smolts unable to actively and effectively maintain control of their position or orientation in the flow field
24-26	No. scraping with escape	Number of smolts contacting or scraping the screen surface and escaping
27-29	No. scraping without escape	No. of smolts contacting or scraping the screen but that are unable to escape the screen surface through their own activity
30-32		
16-17	Approach Position	The position at which fish approach the screen. Code: 11-head first, back up; 12-head first, back down; 21-tail first, back up; 22-tail first, back down; 15-parallel to the screen
18-20	Approach Vert. Angle	The angle at which the fish approach the screen. Code: 0-180 deg (toe of screen=0, head=180)
21-23	Approach Horiz. Angle	Direction in which fish approach the screen relative to the camera. Code: (+)- toward screen, (-)-away from screen
24-25	Retreat Position	The position at which the fish retreat from the screen. Note: This code is not filled in if the fish is entrained only. Code: Same codes as Approach Position codes
26-28	Retreat Vert. Angle	The angle at which the fish retreat from the screen. Note: This code is not filled in if the fish is entrained only. Code: Same codes as Approach Vertical Angle codes

(Continued)

Table C2 (Concluded)

Block	Var. Name	Description
29-31	Retreat Horiz. Angle	Direction in which fish retreat from the screen relative to the camera. Note: This code is not filled in if the fish is entrained only. Code: Same as Approach Horizontal Angle
32-33	Escape Behavior	The position at which the fish escapes entrainment. Code: Same as the Approach and Retreat Position codes
34-36	Escape Angle	The angle in which the fish escapes entrainment. Code: 0-180
37	Life Sign	Does the smolt exhibit any evidence that it is alive? Code: Y-yes, N-no
38	Operculum Damage	Is the operculum of the fish damaged? Code: Y-yes, N-no
39	No. of Hits	No. of times the fish hit the screen. Code: 0-9
40-41	Impingement Location Hit-1 Code	Location on the screen where the fish touched on the first hit. Code: MO-mesh only, TO-tie bar only, MB-slide from mesh to tie bar, TM-tie bar to mesh
42-43	Impingement Location Hit-2 Code	Location on the screen where the fish touched on the second hit. Code: Same as the Impingement Location Hit-1 Code
44-46	Water Current Angle	Measure of the instantaneous water current angle relative to the screen at the time of the fish-screen interaction with an accuracy of 5 deg. Code: 0-180 deg

REPORT DOCUMENTATION PAGE

Form Approved
OMB No. 0704-0188

1. AGENCY USE ONLY *(Leave blank)*

2. REPORT DATE
July 1995

3. REPORT TYPE AND DATES COVERED
Final report

4. TITLE AND SUBTITLE
Imaging Smolt Behavior on Bypass Screens and a Vertical Barrier Screen at McNary Dam in 1992

5. FUNDING NUMBERS

6. AUTHOR(S)
John M. Nestler, Robert A. Davidson

7. PERFORMING ORGANIZATION NAME(S) AND ADDRESS(ES)
U.S. Army Engineer Waterways Experiment Station
3909 Halls Ferry Road, Vicksburg, MS 39180-6199

8. PERFORMING ORGANIZATION REPORT NUMBER
Technical Report EL-95-21

9. SPONSORING/MONITORING AGENCY NAME(S) AND ADDRESS(ES)
U.S. Army Engineer District, Walla Walla
Building 602, City-County Airport
Walla Walla, WA 99362-9265

10. SPONSORING/MONITORING AGENCY REPORT NUMBER

11. SUPPLEMENTARY NOTES
Available from National Technical Information Service, 5285 Port Royal Road, Springfield, VA 22161.

12a. DISTRIBUTION/AVAILABILITY STATEMENT
Approved for public release; distribution is unlimited.

12b. DISTRIBUTION CODE

13. ABSTRACT *(Maximum 200 words)*

During the spring and summer of 1992, video imaging of smolt bypass systems at McNary Dam on the Columbia River was conducted using low-light sensitive underwater video cameras to record smolt behavior and impingement characteristics on a modified balanced flow vertical barrier screen (MBFVBS), a standard-length submerged traveling screen (SSTS), and an extended-length submerged bar screen (ESBS). The cameras on the ESBS recorded smolt behavior to three closure gate settings, two screen positions, three discharges, two screen angles, and presence/absence of a fyke net. The cameras on the SSTS recorded smolt behavior only at the standard deployment settings. A total of 3,684 smolts representing 458 conditions were imaged, processed, and analyzed. Five cameras were located on the MBFVBS and imaged the passage of smolts up the gate slot. During imaging of the MBFVBS, one additional camera was located on top of the bypass screen to document gap loss and smolt passage over the top of the bypass screeen. The cameras on the MBFVBS recorded smolt behavior to four unitloads (12,000, 13,000, 14,000, and 16,000 cfs) and three closure gate settings (normal gate setting, partial gate setting, and no gate). A variety of hydraulic and behavioral data were collected from each recorded image for the bypass screens. Data from physical model studies were used to supplement imaging data for some design or deployment configurations. For the bypass screens, hydraulic data included direct measurements of water approach angle relative to the screen surface.

(Continued)

14. SUBJECT TERMS
Bar screens
Bypass screens
Fish protection
McNary Dam
Salmon
Smolts
Video imaging

15. NUMBER OF PAGES
175

16. PRICE CODE

17. SECURITY CLASSIFICATION OF REPORT	18. SECURITY CLASSIFICATION OF THIS PAGE	19. SECURITY CLASSIFICATION OF ABSTRACT	20. LIMITATION OF ABSTRACT
UNCLASSIFIED	UNCLASSIFIED		

13. (Concluded).

Behavioral data collected included descriptions of the approach of the smolt to the screen (i.e., angle of approach, angle of retreat after a strike, orientation of the fish in the water) and descriptions of entrainment and impingement of smolts on the screen (e.g., entrainment without strike or impingement, strike with escape, impingement without escape, head-first approach without strike or impingement, and head-first approach with impingement). The video imaging demonstrated that direct imaging of smolt behavior in the different parts of a bypass system can provide valuable information on the effects of different screen designs or deployment configurations. Video imaging within the bypass screen system should be used to supplement fish guidance efficiency studies to determine localized effects of the bypass system.